WT-1405

Military Category: 14

OPERATION PLUMBBOB

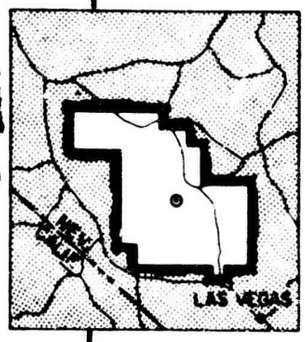

NEVADA TEST SITE
MAY-OCTOBER 1957

Project 1.5

GROUND MOTION STUDIES at HIGH INCIDENT OVERPRESSURE

Issuance Date: June 20, 1960

HEADQUARTERS FIELD COMMAND
DEFENSE ATOMIC SUPPORT AGENCY
SANDIA BASE, ALBUQUERQUE, NEW MEXICO

Inquiries relative to this report may be made to

Chief, Defense Atomic Support Agency
Washington 25, D. C.

DO NOT RETURN THIS DOCUMENT

ABC Technical Information Service Extension
Oak Ridge, Tennessee

WT-1405

OPERATION PLUMBBOB—PROJECT 1.5

GROUND MOTION STUDIES at HIGH INCIDENT OVERPRESSURE

William R. Perret

Sandia Corporation
Albuquerque, New Mexico

FOREWORD

This report presents the final results of one of the 46 projects comprising the military-effect program of Operation Plumbbob, which included 24 test detonations at the Nevada Test Site in 1957.

For overall Plumbbob military-effects information, the reader is referred to the "Summary Report of the Director, DOD Test Group (Programs 1–9)," ITR–1445, which includes: (1) a description of each detonation, including yield, zero-point location and environment, type of device, ambient atmospheric conditions, etc.; (2) a discussion of project results; (3) a summary of the objectives and results of each project; and (4) a listing of project reports for the military-effect program.

ABSTRACT

Project 1.5 observed vertical and radial accelerations and vertical displacements produced in the ground by air shock from Shot Priscilla, which had an estimated yield of 37 kt, and a burst height of approximately 700 feet. Instrumentation was included to measure vertical acceleration at two depths in the vicinity of ground zero and both radial and vertical acceleration at the surface and at depths of 10, 30, 60, and 100 feet for pressure ranges of 270, 187, 120, and 59 psi. Vertical acceleration was observed at a depth of 200 feet at the 300-psi station. Relative displacements were measured between the surface and points roughly 10, 30, 60, 100, and 200 feet deep at each pressure range. Motion of three reinforced, cast-in-place, concrete piles extending from the surface to a depth of 100 feet, adjacent to the 187- and 120-psi free-field instrument stations, was studied by accelerometers near the top and bottom of each pile. Permanent ground displacement was observed by preshot and postshot first-order surveys of a series of monuments.

Data from the station near ground zero was lost, because of temporary adverse effects of ionizing radiation on cable insulation. Seven additional channels of accelerometer data were lost, because of carrier failure after a zero-time short circuit in one amplifier. A total of 64 of 73 readable records were recovered by Project 1.5.

Ground-baffle air-pressure gages recorded overpressures roughly in the predicted range.

Precision of ground-acceleration data was adversely affected by low ratios of signal to set range. Accelerations were attenuated as the inverse 0.75 power of depth except at the station of highest incident overpressure, where the exponent was 1.4. Peak radial accelerations were generally similar to peak vertical accelerations except at surface gages.

Peak transient vertical displacements decreased exponentially with depth to a point below 100 feet. No definitely measurable transient displacement occurred below 100 feet. At all stations the absolute vertical displacement maxima δ decreased exponentially according to $\delta = \delta_0 e^{-0.017D}$, where D is depth in feet and the zero subscript denotes surface displacement.

PREFACE

Projects 1.4 and 1.5 of Operation Plumbbob were concerned with similar aspects of the same phenomena, air-shock-induced underground motion and stress. Project 1.4 observed and analyzed accelerations, stresses, and strains (relative displacement over 5-foot or 10-foot spans) in a range of depths down to 50 feet, with emphasis on the region down to 10 feet. Project 1.5, the subject of this report, concentrated more specifically on observation and analysis of accelerations and displacements over depths ranging to 200 feet.

These projects represented the separate but parallel thinking of two organizations, Stanford Research Institute (Project 1.4) and Sandia Corporation (Project 1.5). The planning for both involved close cooperation, and it is anticipated that the final analysis and usefulness of each project's results will complement the other.

Project 1.5 was planned and executed as a part of Program 1 of Operation Plumbbob. Lt. Col. H. T. Bingham, Director of Program 1 during planning and execution of the project, contributed materially to its success, as did Lt. Col. John Kodis who succeeded Col. Bingham im midoperation.

Field instrumentation and data recording were performed by Division 5231 of Sandia Laboratory under the Project Officer, Joe W. Wistor, who was assisted by Harry E. Bell, Ross R. French, W. Kieth McCoy, John H. Morrison, Clarence R. Pickens, and Ryan Pierson. Data reduction was accomplished in Division 5240 of Sandia Laboratory by Robert J. Beyatte.

The author served as scientific advisor to the project.

CONTENTS

TABLES

Chapter 1
INTRODUCTION

1.1 OBJECTIVE

Project 1.5 was concerned with free-field motion in soil subjected to air-blast loading in peak-overpressure ranges greater than 50 psi and through depths greater than have previously been studied. This study was intended to furnish basic data from Shot Priscilla in terms of both acceleration and displacement versus time for use in protective-construction design. In addition to displacement-time data, observation of permanent displacement on a diameter through ground zero serves to indicate the residual compression of the soil. A third part of the study, observations of acceleration in buried vertical reinforced concrete structural elements, was included to provide information that could be correlated with free-field results. Data from this project serves also for correlation with pertinent design information derived from related studies of Program 3.

1.2 BACKGROUND

The philosophy of design for underground protective construction has changed radically in recent years as a consequence of new requirements and categories of protection and new and greater magnitudes of damaging phenomena. It is no longer considered adequate to provide personnel shelters safe for short periods against an overpressure of a few pounds per square inch and general fragmentation shelters for dispersed aircraft and supply depots. Protective construction must now provide long-period safety for vital personnel and strategic retaliatory weapons and weapon vehicles. Such protection must be effective against the high peak overpressures of long duration associated with multimegaton weapons, as well as against accompanying radiological hazards.

Knowledge of reaction of ground to air-blast loading has never been complete and has rarely kept pace with requirements of designers of underground structures. The problem is ultimately one of developing an understanding not only of the reaction of soils to air-blast loading and the reaction of structures to the resultant soil loading, but also the interaction of the structure response and soil and the effect of these factors on the structure.

The first of these pertinent areas of study, i.e., reaction of ground to air-blast loading, includes the objectives of this experiment. It has previously been investigated for high-explosive charges ranging from a few pounds to several hundred pounds burst above ground (Reference 1) and during several nuclear explosions. The high-explosive studies have included peak overpressures up to about 100 psi, involving positive-phase duration of the order of 10 msec. Some observations of earth accelerations, vertical and radial components, and a few of earth stress and strain components have been made for air-blast loading resulting from air or surface bursts of nuclear devices at the Nevada Test Site yielding radiochemical energies of the order of tens of kilotons TNT equivalent (References 2, 3, 4).

Further, some observations have been made of three components of ground acceleration induced by surface bursts of kiloton-range and megaton-range devices at the Eniwetok Proving Ground (References 5 and 6). Essentially all ground-motion data from surface or air bursts of nuclear devices have been made at peak incident overpressures ranging downward from 100 psi, the greater part having been below 60 psi, and at depths less than 20 feet. A few observations of vertical acceleration have been made as deep as 50 feet, and two of these were made

at very-high overpressures, 100 feet in ground range, for a nuclear explosion (Reference 7). Positive-phase duration of incident overpressure for this data was of the order of 100 to 1,000 msec. This acceleration data has, in many cases, been satisfactorily analyzed for velocity and displacement information.

The general pattern of previous studies has not been comprehensive. Data derived from a multiplicity of air-blast sources is naturally complex, and heterogeneity of soil conditions and nonlinearity of soil parameters have made their correlation difficult and extrapolation from them extremely hazardous. Present knowledge of ground motion to be anticipated from air-blast loading of the ground surface is at best sketchy; it is confined to relatively shallow depths, and its variation with depth has been established by only a meager amount of data. In particular, knowledge of the magnitude and variation of ground-motion parameters at incident overpressures in the higher ranges (above 50 or 100 psi), of critical interest in protective structural design, is conspicuously inadequate or nonexistent.

Following Operation Redwing, one significant and highly encouraging piece of information became available (Reference 6). Air-blast-induced ground accelerations were observed with shallow instrumentation installed for Shot Lacrosse to give information on close-in telemeter-package motion. Peak accelerations from incident overpressure peaks up to about 425 psi correlated well with corresponding data from Operation Ivy (Reference 5) and showed similar exponential relationships between pressure and accelerations, but different coefficients, probably because the instruments were much shallower on Operation Redwing.

No previous studies of the reaction of long, vertical, underground structural elements to air-blast loading are known to have been undertaken. Several studies of reaction of reinforced-concrete piles to driving are documented in the literature, but these were concerned with reaction of the pile to repeated driving impacts and did not involve reaction of the piles and soil to simultaneous shock loads.

1.3 THEORY

A satisfactory theory for ground motion induced by air-blast loading has not been established, because the mathematics necessary for proper formulation of equations of motion for soil are still in a developmental stage and because the real nature of variations of soil parameters, such as stress-strain relationships under dynamic loads, is not well understood. Some estimates of a reasonably intelligent nature can be made concerning these problems and their solution. Reference 8 discusses some aspects of this problem helpfully. Work on the nonlinear mathematics of elastoplastic materials has been in progress for several years and should eventually be helpful toward understanding the dynamic loading problems in soil. The problem has been studied in the Mathematics Department, University of California, Berkeley, under Office of Naval Research and DASA sponsorship and has yielded some useful theoretical understanding, only to be restricted by lack of basic knowledge of soil-parameter relationships applicable to dynamic loading. Several other promising theoretical approaches are being studied, but there is currently no sound theoretical basis for solving many of the problems posed by underground construction. Approximate methods and empirical correlation of experimental data must presently provide the entire basis for design.

Chapter 2
THE EXPERIMENT

2.1 DESIGN OF THE EXPERIMENT

Project 1.5 was planned to observe relative motion of a series of points in the ground as a function of depth and peak air-blast overpressure loading. Primarily, vertical-component acceleration and relative displacement were observed as a function of time. End instruments placed at various depths and ground ranges furnished a pattern of data including the full range of interest for current and near-future design requirements. Observations of horizontal radial acceleration were included at several depths to indicate lateral motion of the ground.

Acceleration-time data may be integrated to furnish velocity-time and displacement-time information. As a cross check and backup measurement, a number of relative-displacement gages of new design were included to provide displacement-time data between each accelerometer station and a surface-anchoring pad. Actually, the longest-span displacement gage, between the surface pad and a 200-foot-deep anchor, was expected to provide information concerning absolute displacement of the surface for a period of 0.1 second, or longer, following incidence of air blast at the surface pad, because of finite transit time between the surface and gage anchor.

Project 1.5 instrument array consisted of five stations (Figure 2.1 and Table 2.1), one located 75 feet from ground zero and the remainder located at predicted peak-overpressure ranges for 400, 200, 100, and 50 psi. Figure 2.1 includes for correlation F-1.3 and F-1.4 station locations of Stanford Research Institute parallel Projects 1.3 and 1.4 (References 9 and 10). At the ground-zero station (F-1.5-9010) instrumentation to indicate vertical accelerations was installed at depths of 60 and 100 feet. Primary instrumentation at the four F-1.5-9012 stations included a concrete pad 3 feet thick and 7 feet in diameter (Figure 2.2), which contained vertical and radial component accelerometers, an air-pressure gage, and transducer elements of five relative-displacement gages. Beneath the pad at each station were four vertical accelerometers, one each at depths of 10, 30, 60, and 100 feet, and radial-component accelerometers at the same depths with a few exceptions (Table 2.1). Four relative displacement gages were installed with lower ends anchored to the accelerometer canister; the fifth was anchored 200 feet deep to an accelerometer housing at one station and to concrete deadmen at the other three.

Additional instrumentation included at several of the stations comprised: (1) a vertical accelerometer 200 feet deep at the 400-psi station (F-1.5-9012.01); (2) radial accelerometers 10 feet deep at the 200- and 50-psi stations (F-1.5-9012.02 and -9012.04); (3) vertical accelerometers 10 feet deep and offset about 10 feet laterally from the pads at both the 400- and 100-psi stations (F-1.5-9013.01 and -9013.02).

Three reinforced-concrete piles, uncased and nominally 16 inches in diameter by 100 feet long, were cast in place adjacent to the free-field stations of Project 1.5 at the 200-psi (Station F-1.5-9054.01) and 100-psi (Station F-1.5-9054.02) ground ranges for Shot Priscilla. One pile (Station F-1.5-9054.03) was offset 50 feet north of the 100-psi station as a backup facility.

The piles, topped flush with the ground surface, represent elements of long vertical structures. Each was instrumented 1 foot above the lower end and 1 foot below the top with vertical component accelerometers. An additional accelerometer oriented to indicate radial motion was included at the lower end of the Station F-1.5-9054.02 pile.

In addition to transient-displacement measurements, permanent displacement of the ground surface at 18 points (Figure 2.1) in the high overpressure region was derived from preshot and

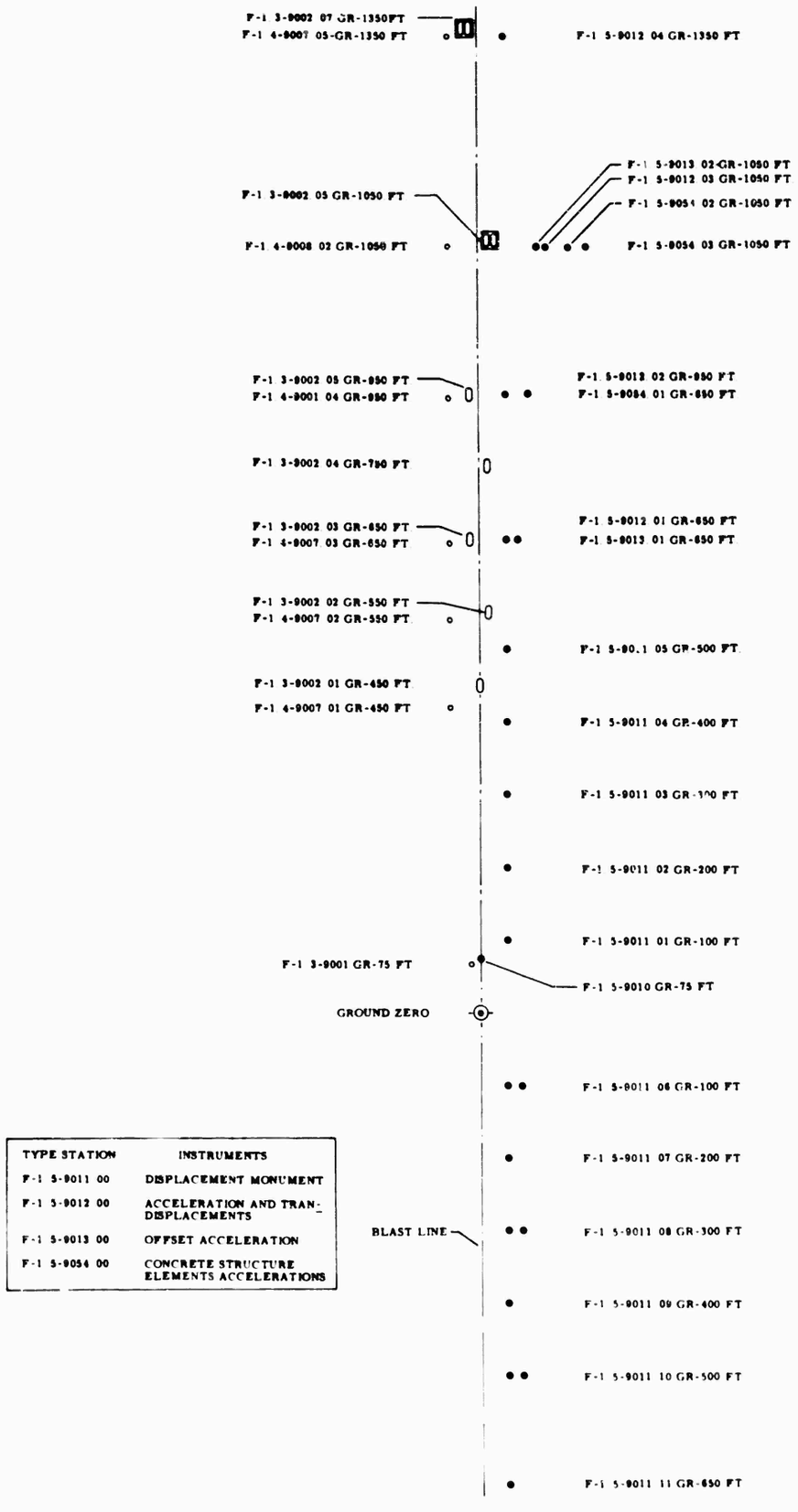

Figure 2.1 Ground motion blast line, Shot Priscilla.

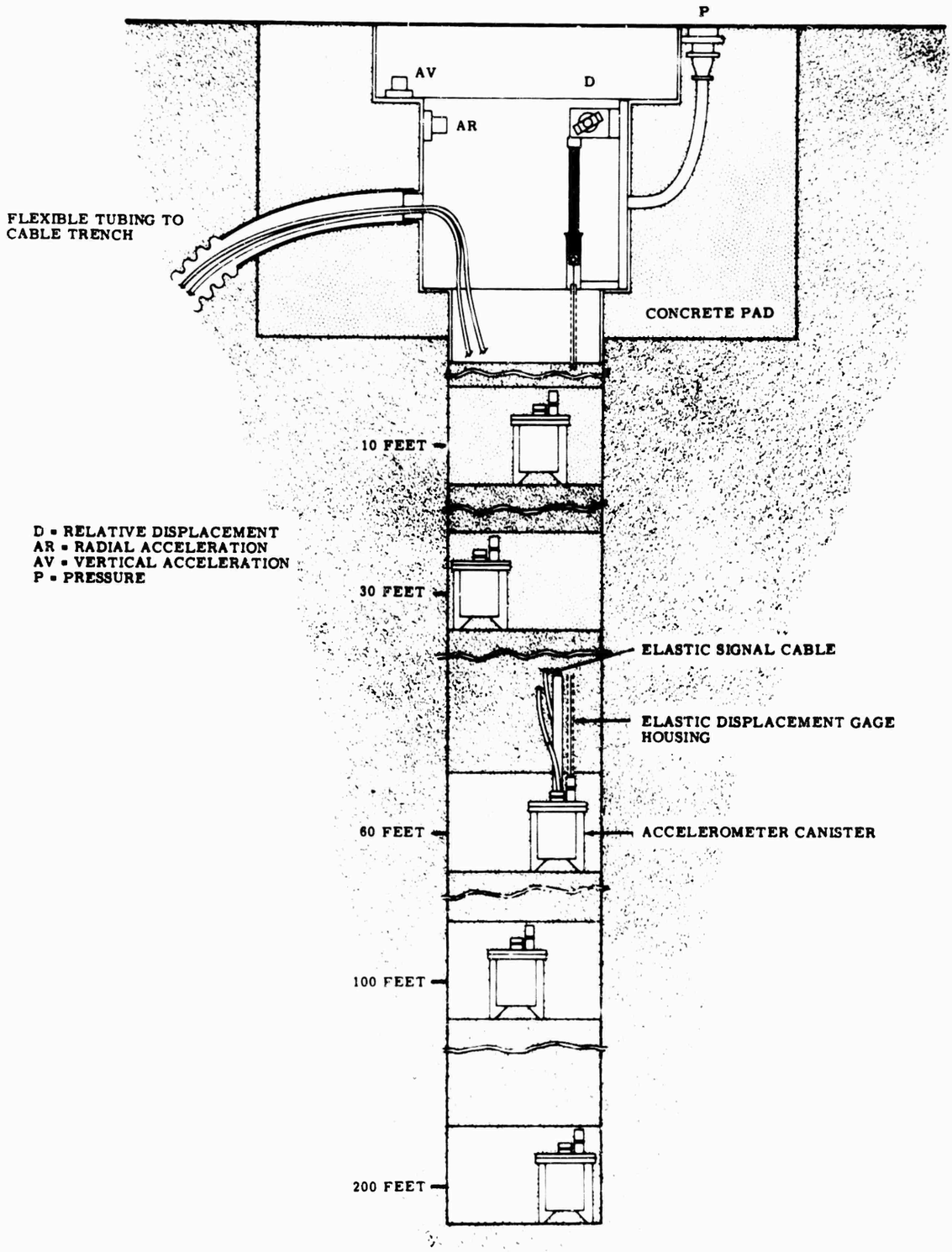

Figure 2.2 Schematic elevation of typical F-1.5-9012 station.

postshot first-order[1] surveys of an array of monuments (Station F-1.5-9011.01 through F-1.5-9011.14) located on a diameter through ground zero and including the instrument pads of Project 1.5. Additional permanent-displacement data from the vicinity of ground zero was derived from similar surveys on a grid in that area.

2.2 SET-RANGE DERIVATION

Set ranges for three types of instruments used in Project 1.5 were derived either by scaling or through analytical procedures. Set ranges for ground-baffle pressure gages at the four F-1.5-9012 stations were determined by location of these stations at specific overpressure ranges.

Accelerometer set ranges were scaled from existing data for Shot 4 of Operation Tumbler-Snapper (References 2 and 3) and data derived from Shot Lacrosse of Operation Redwing (Reference 6). The first determination of set ranges for acceleration was made by extrapolating the Tumbler-Snapper Shot 4 data to pressure ranges as high as 500 psi. However, information from Redwing Shot Lacrosse provided data for shallow earth acceleration at incident overpressures as high as 400 psi. These latter data formed the basis for final set ranges in Project 1.5.

TABLE 2.1 INSTRUMENTATION

P = overpressure, D = relative displacement, AV = vertical acceleration, and AR = radial acceleration.

Station	F-1.5-9010	F-1.5-9012.01	F-1.5-9013.01	F-1.5-9012.02	F-1.5-9064.01	F-1.5-9012.03	F-1.5-9013.02	F-1.5-9064.02, 03	F-1.5-9012.04
Ground Range, ft	75	650	650	650	850	1,050	1,050	1,050	1,350
Nominal Overpressure, psi	Unspecified	600	400	200	200	100	100	100	50
Depths, ft									
0	—	P, AV, AR	—	P, AV, AR	AV*	P, AV, AR	—	AV*	P, AV, AR
10	—	AV, D	AV	AV, AR, D	—	AV, D	AV	—	AV, AR, D
30	—	AV, AR, D	—	AV, AR, D	—	AV, AR, D	—	—	AV, D
60	AV	AV, AR, D	—	AV, AR, D	—	AV, AR, D	—	—	AV, AR, D
100	AV	AV, AR, D	—	AV, AR, D	AV†	AV, AR, D	—	AV†	AV, AR, D
200	—	AV, D	—	D	—	D	—	—	D

*Actual depth, 1 foot
†Actual depth, 99 feet.

Set ranges for relative-displacement gages were derived by an approximate analytical treatment, since no measurements of this type were known to have been made previously. The procedure followed assumed an idealized incident overpressure wave acting on a purely elastic medium. Integration of an approximate form of Hooke's law, between limits determined by distance between end points of the gages, gave a value for relative displacement. Assumed idealized overpressure Δp_i in the ground was used in the alternative forms:

$$\Delta p_i = \Delta p_m \left[1 - \beta (x - ct) \right] e^{-\beta (x - ct)}$$

or

$$\Delta p_i = \Delta p_m \left[1 - \alpha \left(t - \frac{x}{c} \right) \right] e^{-\alpha \left(t - \frac{x}{c} \right)} \qquad (2.1)$$

Where: Δp_m = peak overpressure

$\left(t - \frac{x}{c} \right)$ = retarded time for the wave traveling through a depth x in soil of seismic velocity c

$(x - ct)$ = retarded distance

α = logarithmic time constant for the shock wave decay

β = logarithmic range factor

The shock was assumed to travel through the ground as a plane wave roughly parallel to the surface without viscous or frictional attenuation of Δp_m in depth. Either form of Equation

[1] A first-order survey is one in which precision of 1 part in 25,000 is maintained.

2.1 is applicable, and it follows that $\beta = -\alpha/c$. The upper end of each relative-displacement gage was anchored at the ground surface. Displacement to be measured was consequently approximated by relative displacement of the ground surface and a parallel plane at the depth of the lower gage anchor.

Assumed linear elastic behavior of the soil under dynamic loading suggests use of the approximation for Hooke's law:

$$\frac{du}{dx} = \frac{\Delta p_i}{E} \tag{2.2}$$

Where: u = transient vertical displacement at x
E = the dynamic modulus of the soil.

Over the range of depth from 0 (at the surface) to x, displacement is given by:

$$u = \frac{\Delta p_m}{E} \int_x^0 \left[1 - \beta(x - ct)\right] e^{-\beta(x - ct)} dx \tag{2.3}$$

whence

$$u = \frac{\Delta p_m}{E} e^{-\alpha t} \left[(ct - x) e^{-\beta x} - ct \right] \tag{2.4}$$

The result is a rough first approximation that ignores several dynamic characteristics of soils, such as effects of loading history and energy absorption for which no simple adequate analytical expression is presently available. Evaluation of Equation 2.4 should, however, provide reasonable set ranges for gages of the type used. Suitable values were chosen for the parameters: t, travel time for the seismic pulse through soil to the depth x; c, seismic velocity in the soil; E, a computed or observed dynamic soil modulus; and α, a time constant for the incident shock wave which defines positive-phase duration so that $1 - \alpha t$ vanishes.

Certain further assumptions were made in deriving set ranges for the relative-displacement gages. In general, these assumptions were that: (1) average seismic velocities varied with depth from 1,200 ft/sec between the surface and 10 feet to 3,000 ft/sec between the surface and 200 feet; (2) the dynamic modulus E was related to the seismic velocity by the one dimensional approximation

$$c = \sqrt{E/\rho} \tag{2.5}$$

where the density ρ was taken as 90 lb/ft^3; and (3) the positive-phase duration from which alpha was determined varied from 50 msec at 400 psi to 500 msec at 50 psi. These assumptions are admittedly crude and were used subject to some adjustment, particularly in derived values of E, but they proved adequate for use in approximating set ranges.

Chapter 3
INSTRUMENTATION

3.1 INSTRUMENTS

End instruments employed in the dynamic measurements included variable-reluctance air-pressure gages and accelerometers manufactured by Wiancko Engineering Company (Reference 11), and relative-displacement gages developed by Sandia Corporation from a basic design used by Ballistic Research Laboratory (References 1 and 12). Air-pressure gages and displacement gages were used only in F-1.5-9012 stations, illustrated schematically in Figure 2.2.

Accelerometers were mounted in canisters (Figure 3.1) at all stations including F-1.5-9010, -9012, and -9013. These canisters included a cast-aluminum pot to which the cover was attached through a flange sealed by an O ring. The cover plate carried a rigid frame machined to accommodate accelerometers oriented to respond to motion both parallel and normal to the axis of the canister (vertical).

Signal cables from each accelerometer passed through compression bushings in the cover. These cables were spiraled on $\frac{3}{8}$-inch bungee elastic shock cord, and the whole was enveloped loosely in a flexible plastic sheath. This assembly, stretched about 10 percent at installation, permitted large latitude for tensile or compressive displacements between the buried canister and surface pad with minimum cable strains.

A section of square aluminum tubing was welded to the canister cover at its center and oriented with one side normal to the response axis of the radial accelerometer. An index for radial orientation was provided by an external directional arrow on the cover. Provision was made in canister covers for anchoring the lower end of relative-displacement gage wires and protective tubing.

Relative-displacement-gage transducer units (Figure 3.2) consisted of a ten-turn helical potentiometer driven by a length of fine piano wire wrapped over a light aluminum drum. A helical tension spring attached at one end to the transducer housing carried an anchor plug at its far end. One end of the 0.015-inch piano wire was fastened to the spring anchor plugs and its inner end was secured to the aluminum drum wheel. Tension in the light piano wire, adjusted to about 20 pounds, was derived from a clock spring, which loaded the axle between drum and potentiometer.

Relative-displacement-gage transducers were mounted on large steel cylinder mounts (Figure 3.3), cast into concrete surface-anchoring pads. Lengths of 0.060-inch piano wire extended from fastenings at the free ends of the helical springs to collet fittings on accelerometer canisters or deadman anchors. These wires were enclosed in suitable lengths of $\frac{1}{2}$-inch-outside-diameter, flexible, bronze bellows tubing (not shown in Figure 3.1) attached at its lower end to the wire anchor and at its upper end to the surface pad. The bellows tubing was sufficiently flexible to follow locally any displacement of the soil but permitted the wire to move freely, independent of local soil forces.

Signals from end instruments were amplified and recorded by a system similar to that used by Sandia Corporation on previous full-scale operations. This system included Consolidated Engineering System D, consisting of 3-kc carrier supplies and multiple-channel amplifier-demodulator equipment. Output of each System D unit was converted to a frequency-modulated signal, which was recorded on magnetic tape in a multichannel Ampex Model 3439 recorder.

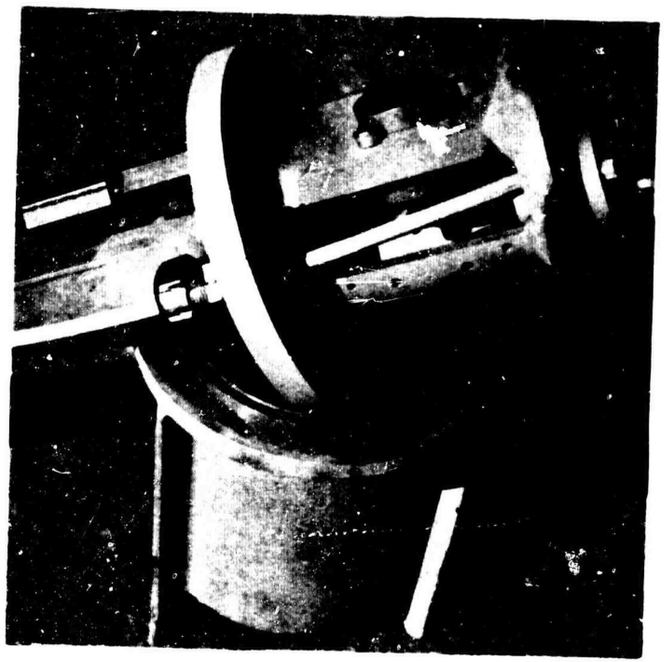

Figure 3.1 Two-component accelerometer canister, gages in place.

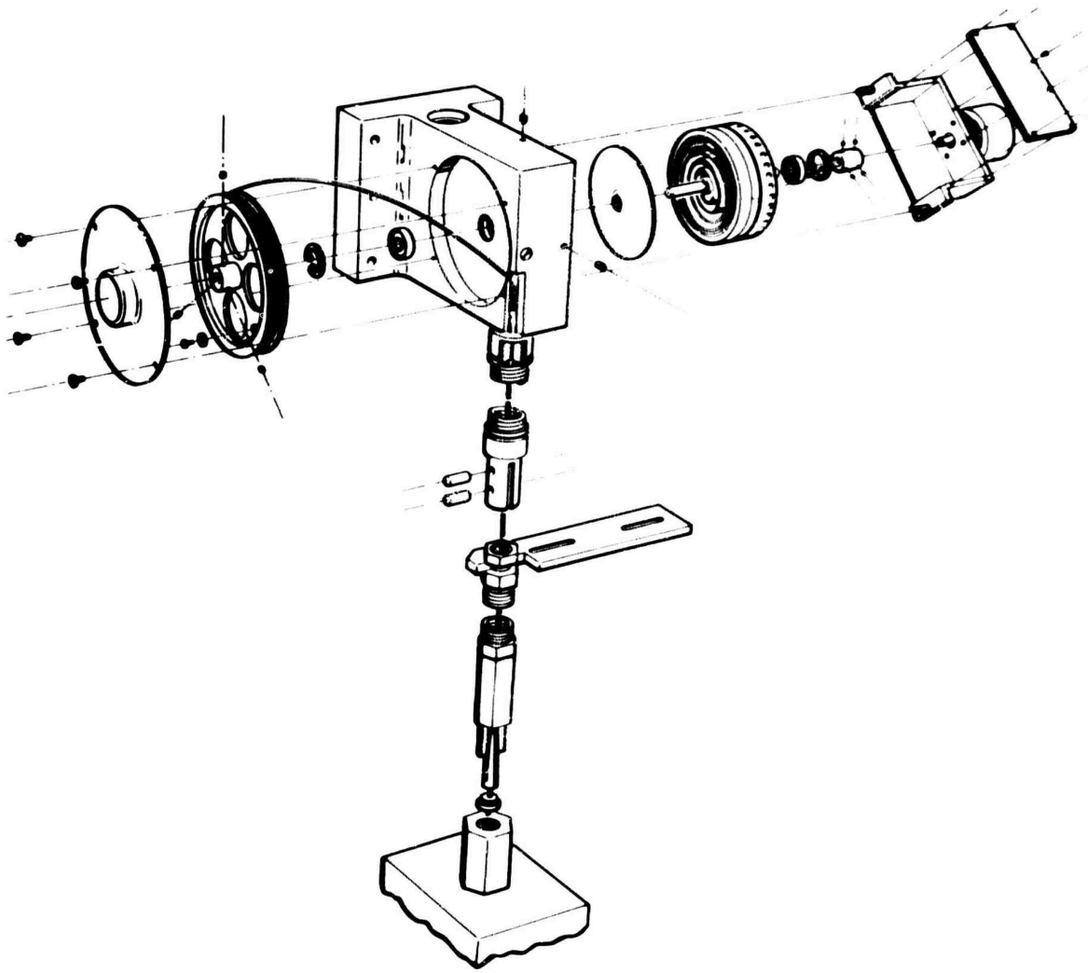

Figure 3.2 Relative displacement gage, exploded view.

Records were converted after recovery to oscillograph traces on a special playback system that compensated for wow and flutter introduced by recorder tape transports. Both time and amplitude scales of the photographic records were adjusted to give optimum legibility.

3.2 CALIBRATION

Calibration of gages followed procedures developed during previous full-scale operations, with the exception of requirements for the new relative-displacement gages. All gages were

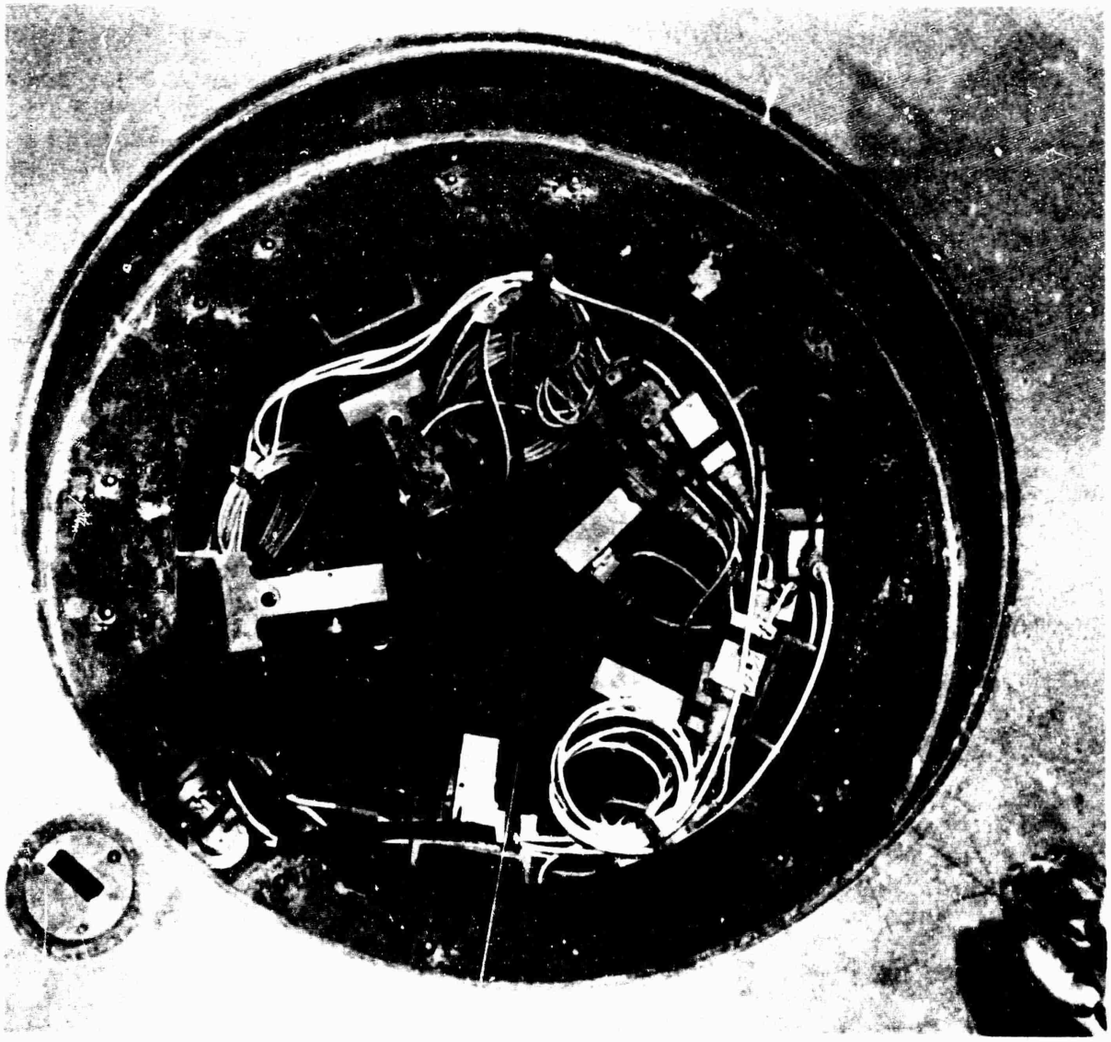

Figure 3.3 Interior of surface pad showing displacement and mounted acceleration transducers.

calibrated to about 133 percent of set range in four steps, including set range. Direct application of metered air pressure to the air-pressure gages in place gave a static calibration signal through the designated signal cable and recorder channel. Flat response of the gage from static through dynamic frequencies above 500 cps permitted use of a static calibration procedure.

Accelerometers were calibrated on a precisely controlled spin table through assigned signal cables and recorder channels. Static calibration was again adequate, because of linearity of gage response over the range of frequencies anticipated and for which the recording system was considered effective.

Calibration of relative-displacement gages was performed after installation was complete. Transducer units were attached to a precise screw, and the potentiometers were approximately centered. Static displacements of the unit along the screw through prescribed positive- and negative-displacement set ranges gave calibration signal over assigned cables and amplifier channels.

3.3 INSTALLATION

Accelerometers for Station F-1.5-9010 and for the two shallow offset observations at Station F-1.5-9013 and F-1.5-9013.02 were to respond to vertical accelerations only and required no azimuthal orientation. At Station F-1.5-9010, one acceleration canister was placed in an open hole 100 feet deep. The canister was lowered by means of a sectional orienting rod. The rod

Figure 3.4 Typical F-1.5-9012 station ready for sealing.

consisted of 18-foot lengths of 1-inch-square aluminum tubing, bolted together with snug-fitting sleeves and attached to the square tubing on the canister cover by a remotely controlled release mechanism. The canister was grouted with high-early cement slurry placed around the gage by means of a 2-ft^3 bail bucket. The canister was covered with grout to a height of about 6 inches. The placement rod was detached after the grout had set, and backfill of dry sand was rodded in 2-foot lifts to the proper elevation for the 60-foot instrument canister. Grouting and backfill procedures were repeated for this gage position, and the bungee-cord signal-cable assemblies for each canister were stretched about 2 feet and anchored to a steel bar on the floor of the cable trench adjacent to the hole. Similar procedures were used in placing shallow offset accelerometers.

The F-1.5-9012 stations, which combined acceleration, relative-displacement, and incident-overpressure observations, included a concrete surface-anchoring pad (Figure 3.4) to accommodate transducers for these measurements (Figure 3.3).

Each of these stations included a 12-inch-diameter hole, 200 feet deep, for instrument placement. These holes were drilled by an oilfield-type rotary drill using bentonitic drilling

mud. This situation was not desirable, since the column of moist soil surrounding each installation could introduce a perturbation in the free field. All borings were bailed after completion and were nearly dry when gages were placed. Drilling with air flow rather than mud would have provided the preferably dry holes.

Placement of gages in the F-1.5-9012 stations followed the pattern described for the F-1.5-9010 installation, with the exception of azimuthal orientation of the canisters that contained

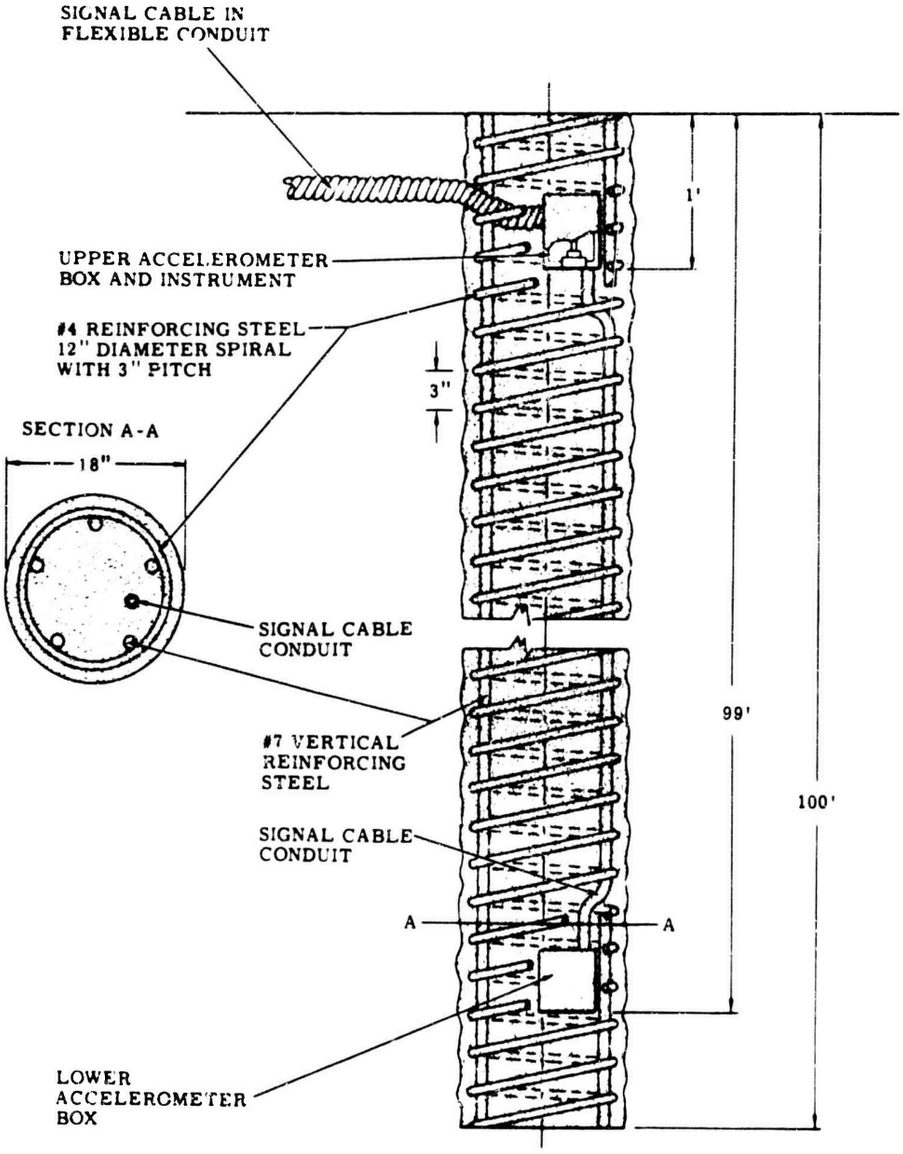

Figure 3.5 Schematic section of reinforced concrete pile, Station F-1.5-9054.

radial accelerometers and the use of deadman anchors for 200-foot displacement gages at all stations except F-1.5-9012.01. Azimuthal orientation of canisters was accomplished by means of the sectional square tubing. Care was taken during assembly of the rod as the canister was lowered to ensure matching of the marked side of each length of tubing. A small-diameter sight tube attached to the top of the rod when the canister was in place permitted orientation of the gage to within 5 degrees of the line through ground zero.

Displacement-gage transducer units were attached to the cylindrical steel mount. Upper ends of the bellows-tube housing which surrounded the gage wires were anchored (Figure 3.3)

before grout and backfill were placed around the canister. Bungee cords were stretched and fastened to hooks in the wall of the transducer mount only after grout had set and 3 to 6 feet of dry sand backfill had been compacted above it.

Instrument holes were backfilled to the bottom of gage-mount cylinders (Figure 3.3). Displacement gages and air-pressure gages were calibrated after backfilling was completed and the station cleaned up. Following calibration, each station was closed by a reinforced aluminum cover plate (Figure 3.4).

Concrete piles at Stations F-1.5-9054.01 through F-1.5-9054.03 were cast in place in open holes and reinforced with vertical and spiral steel. Five Number 7 vertical steel bars were

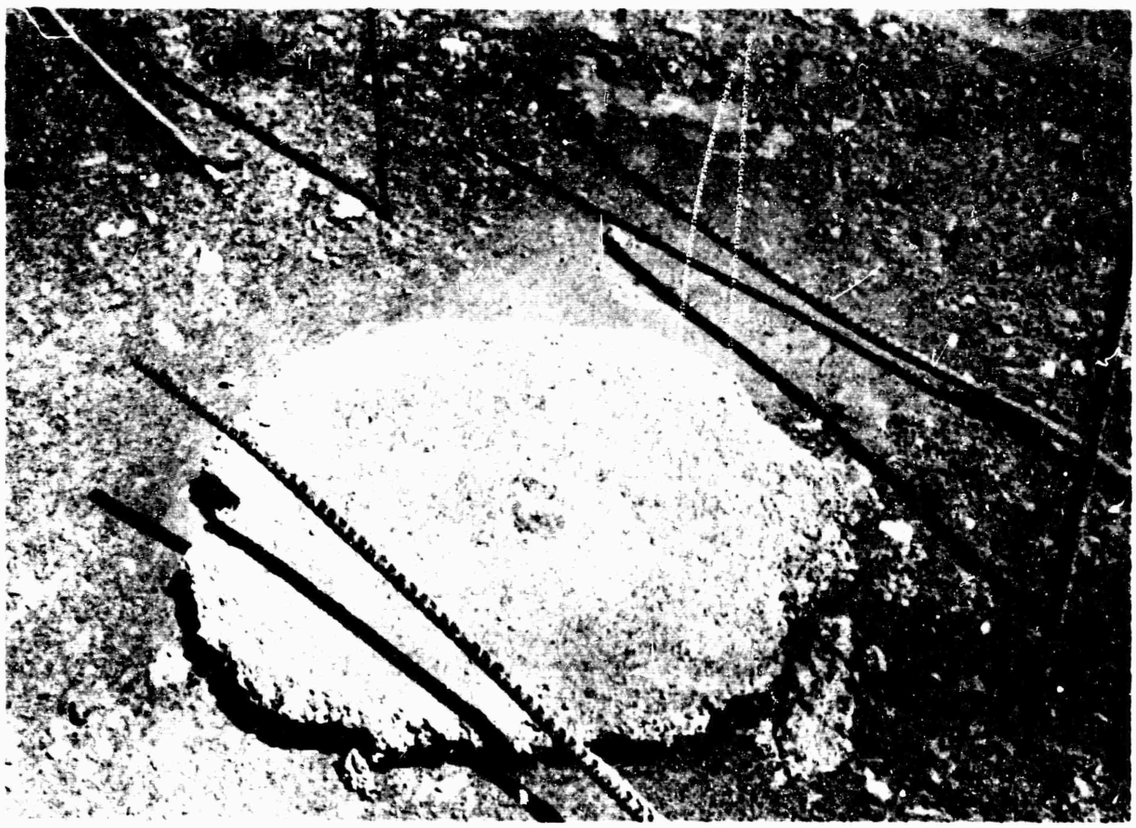

Figure 3.6 Postshot view of survey monument, Station F-1.5-9011.02.

spaced around the spiral steel, lapped four feet at the joints and welded. The spiral steel, made of Number 4 bar, was wrapped into a 12-inch-diameter spiral of 3-inch pitch on the vertical bar. Small steel boxes designed to contain accelerometers were welded to the steel of each pile at appropriate levels (Figure 3.5).

Accelerometers for the piles were calibrated and installed in the steel boxes before the reinforcing steel was placed. Signal cables were run through $\frac{3}{4}$-inch conduit within the steel cage and through flexible conduit from the cage to the adjacent cable trench.

Concrete designed for about 3,000-psi strength using high-early cement was mixed at the site and tremied into the holes after all reinforcing was in place.

Permanent displacement was measured by a preshot and postshot first-order survey on a series of monuments (F-1.5-9011 stations) located at ground ranges of 100, 200, 300, 400, 500, 650, 850, 1,050, and 1,350 feet along the blast line eastward from ground zero and a symmetrical array westward, including the concrete surface pads of the F-1.5-9012 stations (Figure 2.1). Each survey monument (Figure 3.6) was a cast-in-place concrete pillar, 2 feet in diameter and 3 feet deep, flush with the ground surface, and each contained a bronze survey marker. The addition of 2 to 4 feet of gravel and silt fill over an area extending roughly

200 to 300 feet surrounding ground zero made questionable the meaning of displacements measured on monuments only 3 feet deep. Consequently, three concrete columns, 8 feet deep and approximately 7 inches in diameter, were offset about 10 feet from Stations F-1.5-9011.06, -9011.08, and -9011.10 at 100, 300, and 500 feet east of ground zero. Each surface pad of the F-1.5-9012 stations contained three survey markers at 120-degree intervals on a 5.5-foot circle (Figure 3.4) to provide information on tilt as well as elevation changes. A detailed preshot survey on a rectangular grid of 50-foot spacing was made over an area 1,000 feet on a side surrounding ground zero. A postshot survey was made on the same grid about 2 weeks after the shot.

Chapter 4
RESULTS

4.1 RECOVERY AND LOSSES

All recorders operated satisfactorily during Shot Priscilla with 100-percent tape recovery. However, playback showed loss of both channels at Station F-1.5-9010 (75 feet from ground zero), six of the eight channels in one Consolidated amplifier bank and one channel that showed no calibration or acceleration signal. Thus, there were 64 of 73 information channels from which data were derivable. The gage identification code used for Project 1.5 is described in Table 4.1.

Postshot circuit checkout showed all end instruments, cable insulation, and circuits to be normal. One amplifier channel had shorted out at time zero. This overloaded the 3-kc carrier supply for one eight-channel amplifier bank and dropped carrier voltage to about 20 percent of normal.

Examination of the records and circuits for Station F-1.5-9010 showed loss of signal within 1 msec of time zero with a typical pattern for a short circuit. However, postshot circuit checks showed good insulation to ground for all conductors and normal circuit resistance through transducer coils. It is concluded from this information that the high radiation flux to which the ground-zero region was subjected probably made the cable insulation conductive during most of the 3-minute record run. Cables for Station F-1.5-9010 gages were carried in an 8-foot-deep trench from 1,000 feet in ground range to within 100 feet of ground zero. From the ground-zero end of the 8-foot trench to Station F-1.5-9010, a distance of about 20 feet, cables ran through a trench that, after final grading, was about 3 feet deep. It is not specifically evident from the results that failure at this station was caused by inadequate radiation shielding in the shallow section of the cable trench, but it seems reasonable to assume that the difficulty occurred there. Whether or not the deeper cover (8 feet) would have been adequate is a matter for conjecture.

4.2 RECORDS

Magnetic-tape records recovered for all information channels produced playback that indicated normal performance through time zero. In addition to the records lost by probable radiation damage and by a short circuit in one amplifier bank, there were observable changes in the center frequency of the FM oscillators for nine channels at about time zero. This frequency change altered zeros for the records and affected the postshot calibration signal, but in most cases it did not seriously restrict usefulness of the records.

Most accelerometers were calibrated and installed for set ranges considerably above maximum observed accelerations; in a few cases maximum signals were only 5 percent of set range and taxed the playback facility severely. However, careful and diligent effort on the part of the playback operators produced legible, useful records from all but the nine acceleration channels that were lost through circuit malfunction. Time scales are good on all records, and the extent to which it has been possible to push amplitude scales beyond normal performance ranges for recording and playback systems is remarkable.

4.3 INCIDENT OVERPRESSURE

Incident overpressure observed at the four F-1.5-9012 stations are presented as functions of time in Figure 4.1. Pertinent data derived from this set of curves are included in Table

4.2. A developing precursor is shown in the overpressure curves. No significant rounding or turbulence degradation of the main shock peak is evident with the possible exception of 4-P-0.

Peak overpressures were less than predicted at the two closer stations by about a third at the 4-P-0 gage, but by only 7 percent at the 2-P-0 gage. On the other hand, peaks derived

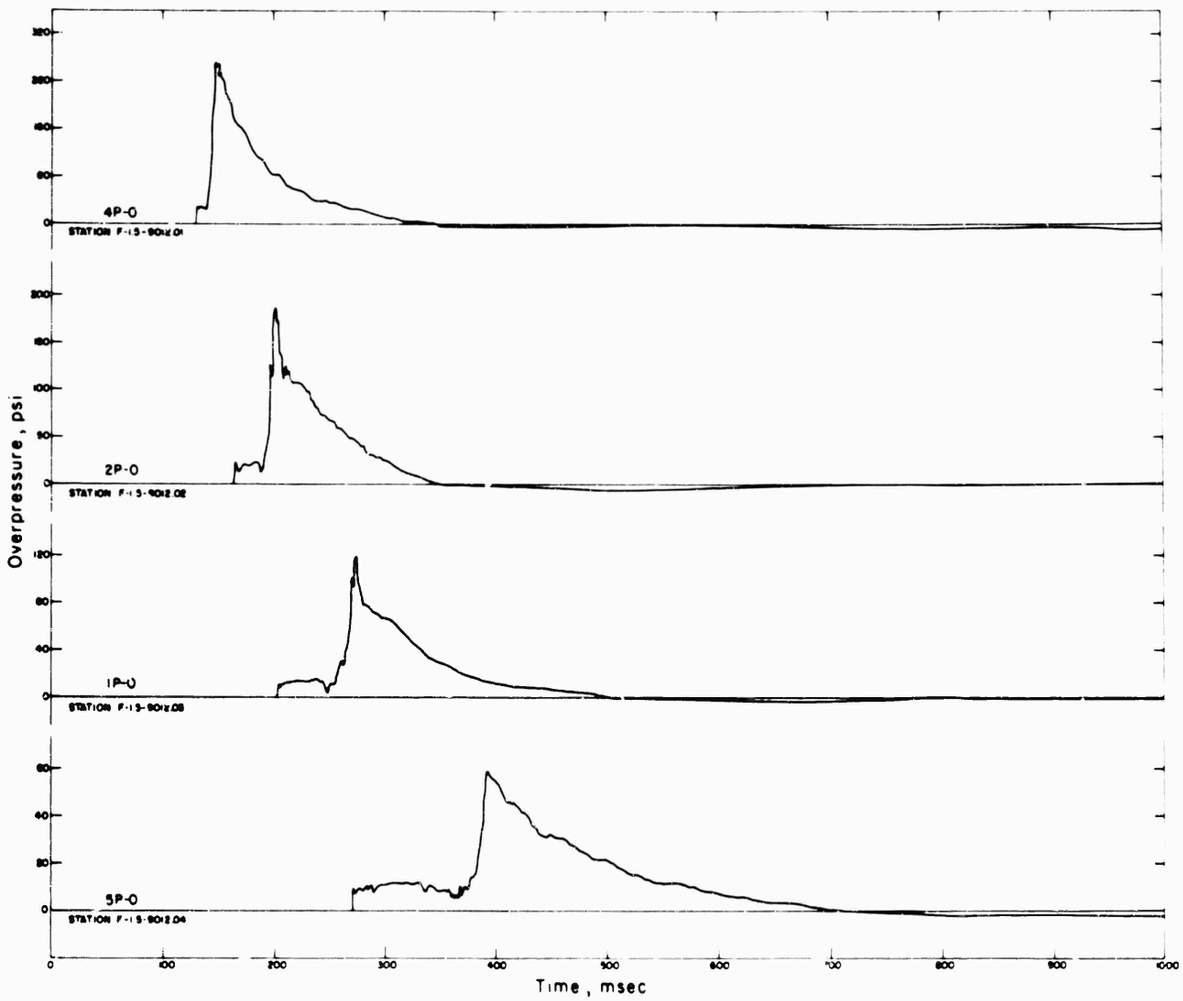

Figure 4.1 Overpressure incident on ground surface, F-1.5-9012 Stations.

from the 1-P-0 and 5-P-0 gages were both about 20 percent above prediction. These departures from the Shot Priscilla prediction are illustrated in Figure 4.2, which shows the prediction curve and the assumed range of error in the prediction. All data, with the exception of 4-P-0 peak overpressure, falls within the ranges of the estimate.

Precursor and main-shock propagation velocities derived from arrival times are given in Table 4.3. These velocities are all above acoustic values for ambient conditions, as would be expected within the ground ranges of the F-1.5-9012 stations.

Overpressure-time data was integrated to give impulse intensity data as a function of time. The results of this integration are shown in Figure 4.3, and maximum impulses are included in Table 4.2.

4.4 FREE-FIELD ACCELERATIONS

Legible records were derived from all free-field accelerometers, except the eight that were served by channels affected by oscillator circuit malfunction, and a ninth, 4 AV-0, for which playback showed complete absence of calibration and accelerometer signals suggesting amplifier

TABLE 4.1 GAGE IDENTIFICATION

Letters designate parameter:

P = overpressure
D = relative displacement
AV = vertical acceleration
AR = radial acceleration

Prefix numbers designate predicted overpressure range:

4 = 400 psi predicted at Station F-1.5-9012.01
2 = 200 psi predicted at Station F-1.5-9012.02
1 = 100 psi predicted at Station F-1.5-9012.03
5 = 50 psi predicted at Station F-1.5-9012.04

Suffix numbers designate nominal depths:

0 = surface
10 = 10 feet deep, etc.

Suffix numbers not separated from parameter letters by dash designate offset distance from an F-1.5-9012 station.

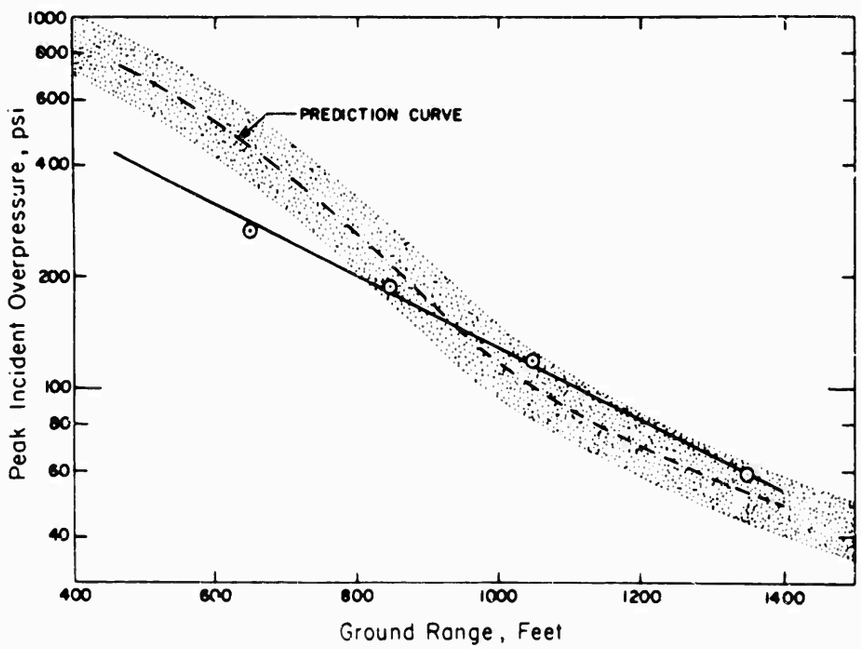

Figure 4.2 Overpressure versus range and prediction curve.

TABLE 4.2 INCIDENT OVERPRESSURE AND IMPULSE

Gage	Station	Ground Range	Precursor		Main Shock		Positive Phase Duration	Peak Impulse Intensity
			Arrival	Overpressure	Arrival	Overpressure		
		ft	msec	psi	msec	psi	msec	(lb-sec)/in^2
4-P-0*	F-1.5-9012.01†	650	130	31	141	270	211	14.2
2-P-0	F-1.5-9012.02	850	164	23	194	187	245	9.7
1-P-0	F-1.5-9012.03	1,050	203	17.5	255	120	307	7.8
5-P-0	F-1.5-9012.04	1,350	270	12.1	380	59.1	442	6.5

* See Table 4.1.
† See Table 2.1 and Figure 2.1

failure. Much of the acceleration data, other than peaks, is of low precision, since signal-to-set range ratios were generally in the range of 10 to 20 percent. Only the surface-level accelerometers gave signals as high as 40 to 50 percent of set range, and these were adversely affected by ringing of the gage mount. Evidently, use of EPG data without correction for soil differences is not suitable for estimating set ranges for underground accelerometers at NTS.

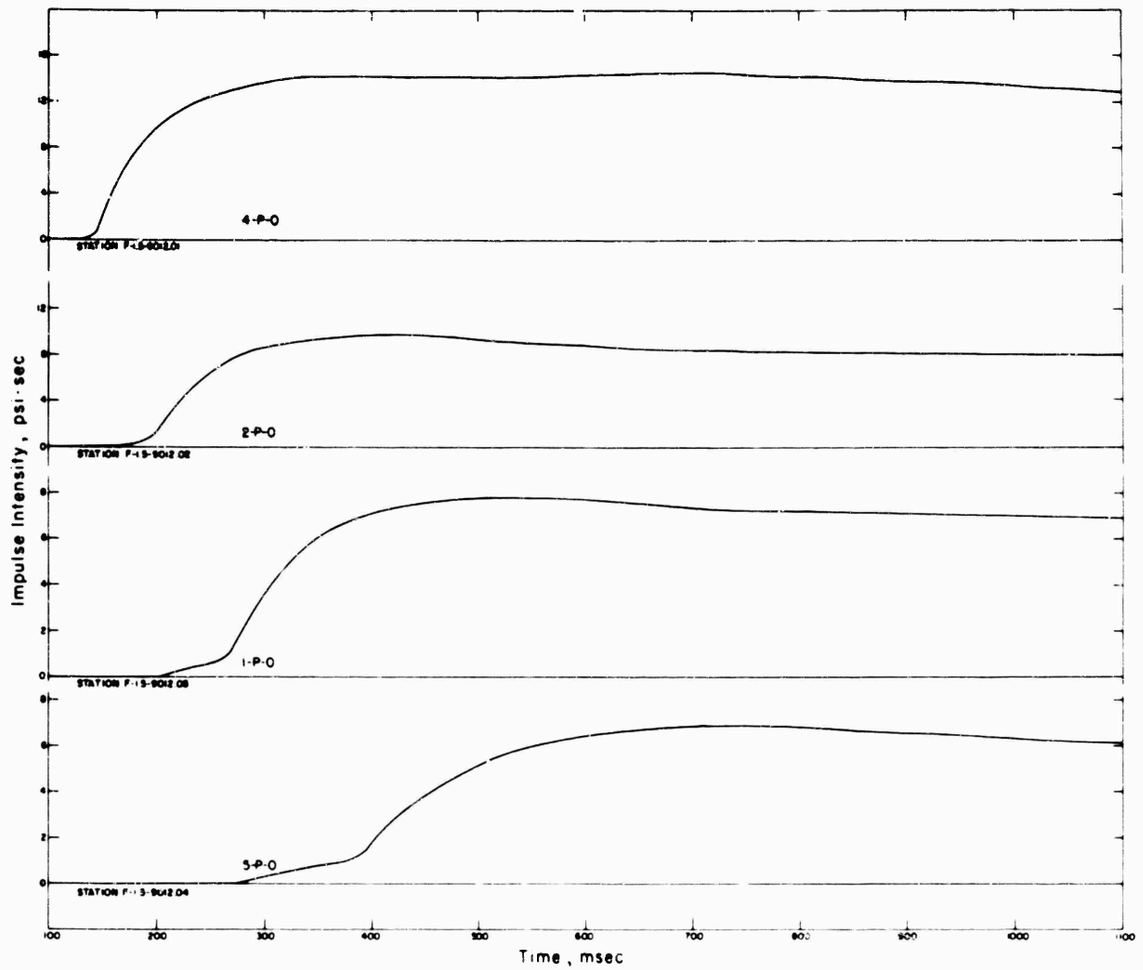

Figure 4.3 Impulse intensity incident on ground surface, F-1.5-9012 Stations.

Acceleration data from nearly all free-field gages were integrated to give velocity-time records to which corrections were applied to show return to rest at reasonable times. Integration found to give irrelevant results for four surface gages, because of the strong ringing of gage mounts.

TABLE 4.3 SHOCK PROPAGATION VELOCITIES IN AIR

Ground Range	Propagation Velocity	
	Precursor	Main Shock
ft	ft/sec	ft/sec
650 to 850	5,880	3,770
850 to 1,050	5,130	3,280
1,050 to 1,350	4,480	2,400

Corrected velocity data was integrated to give displacement-time data. Curves of acceleration, velocity, and displacement versus time for each F-1.5-9012 station are presented in Figures 4.4 through 4.23. Dashed lines shown on most velocity curves represent the initial

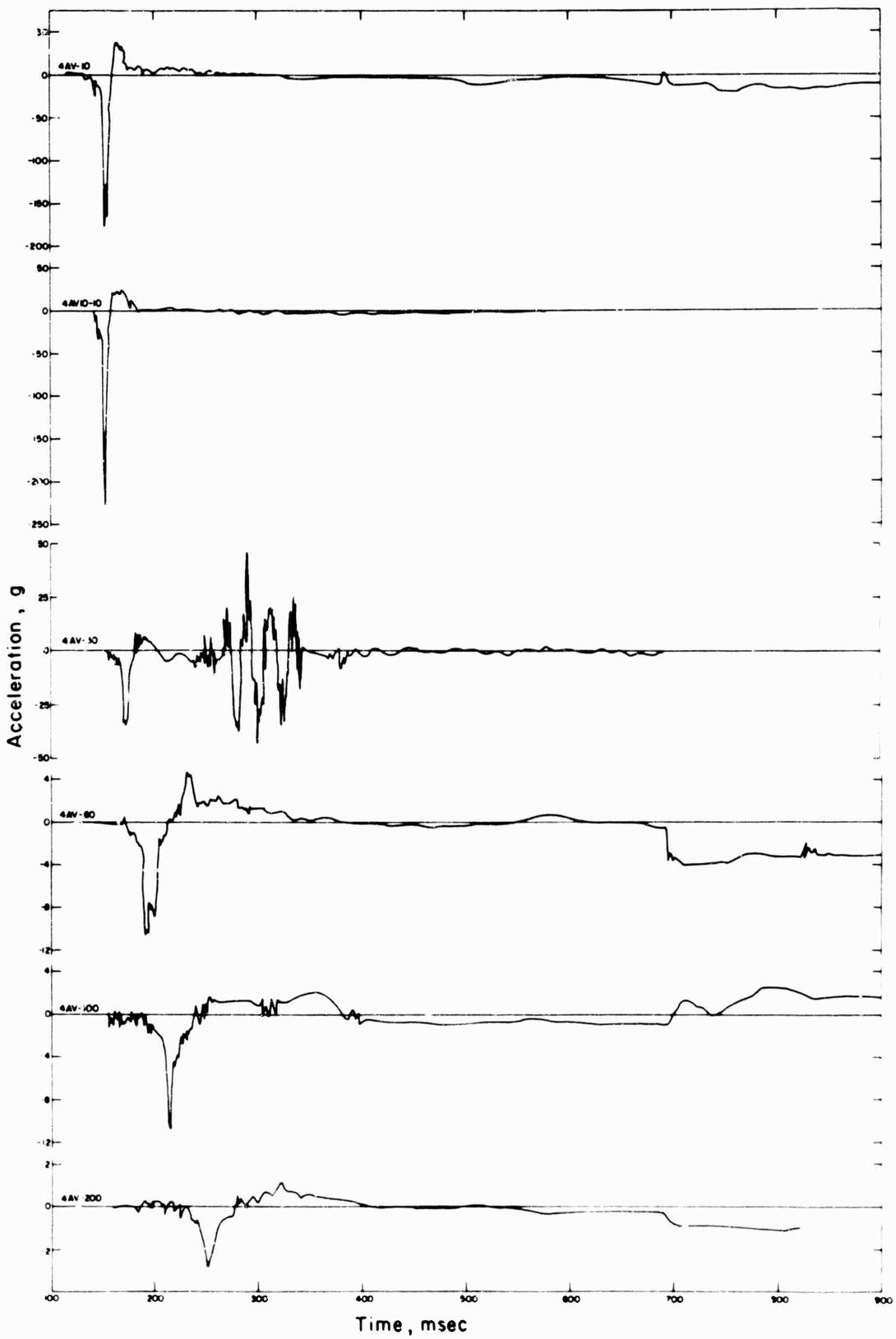

Figure 4.4 Vertical acceleration, Station F-1.5-9012.01.

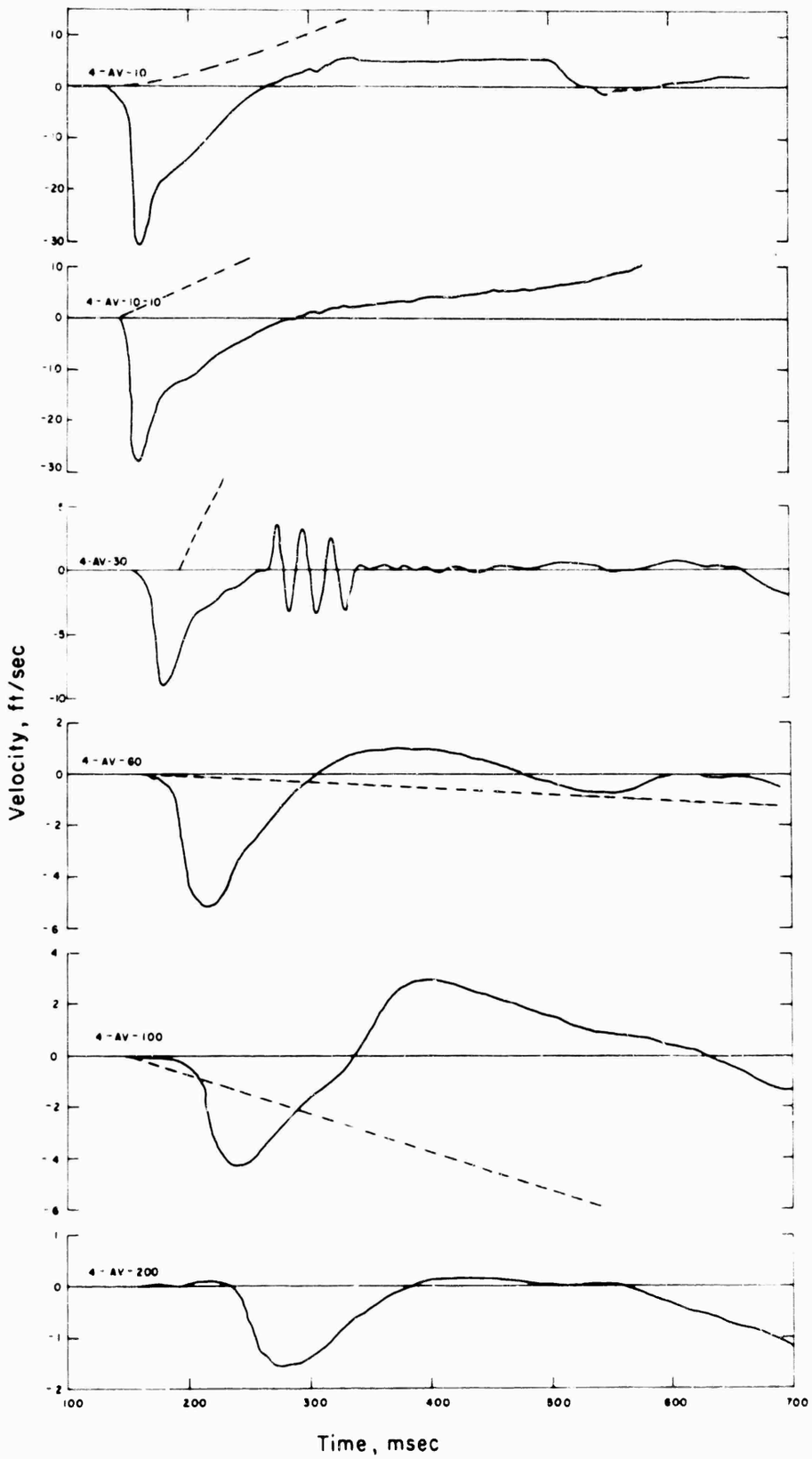

Figure 4.5 Vertical velocity, Station F-1.5-9012.01.

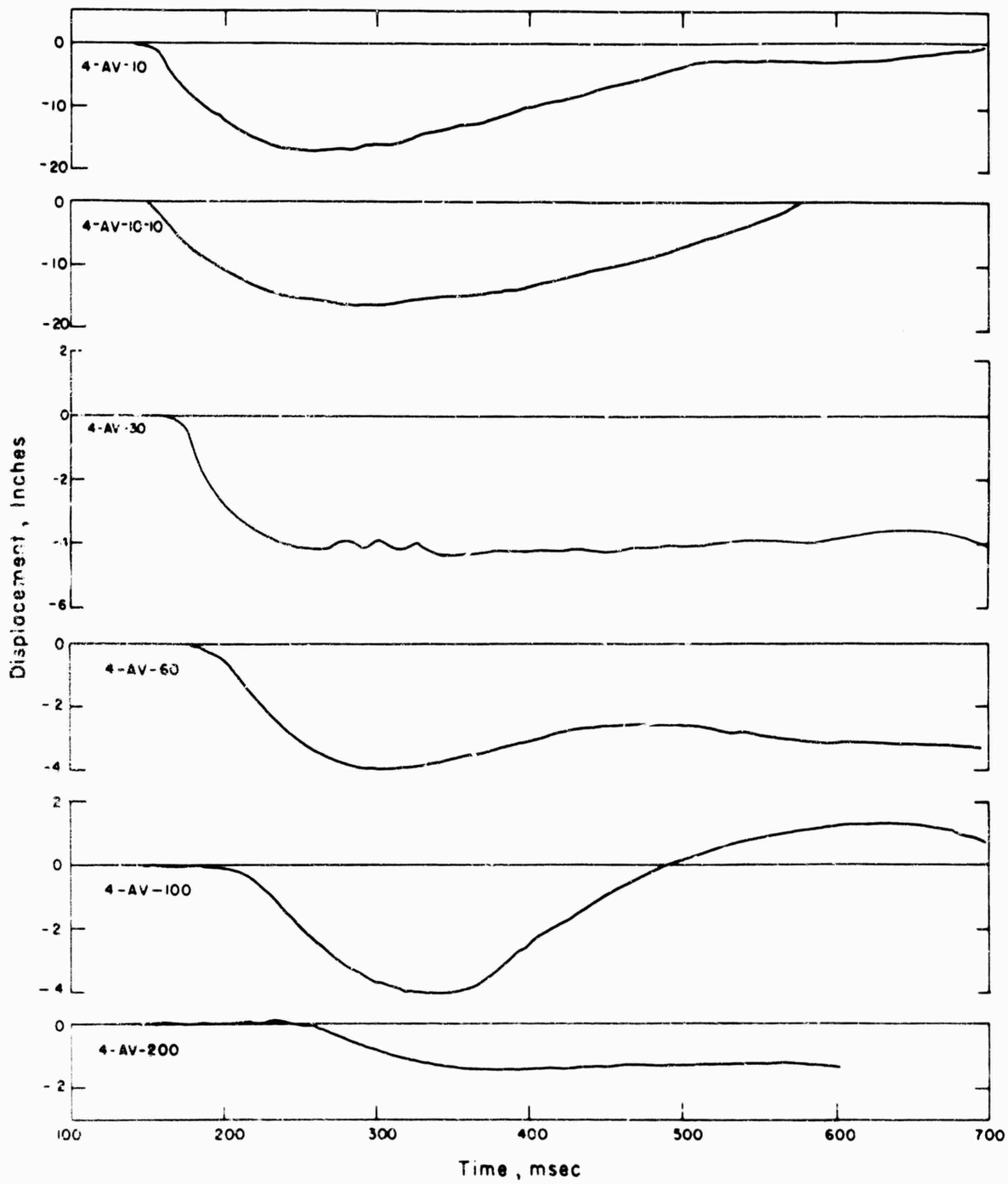

Figure 4.6 Vertical displacement, Station F-1.5-9012.01.

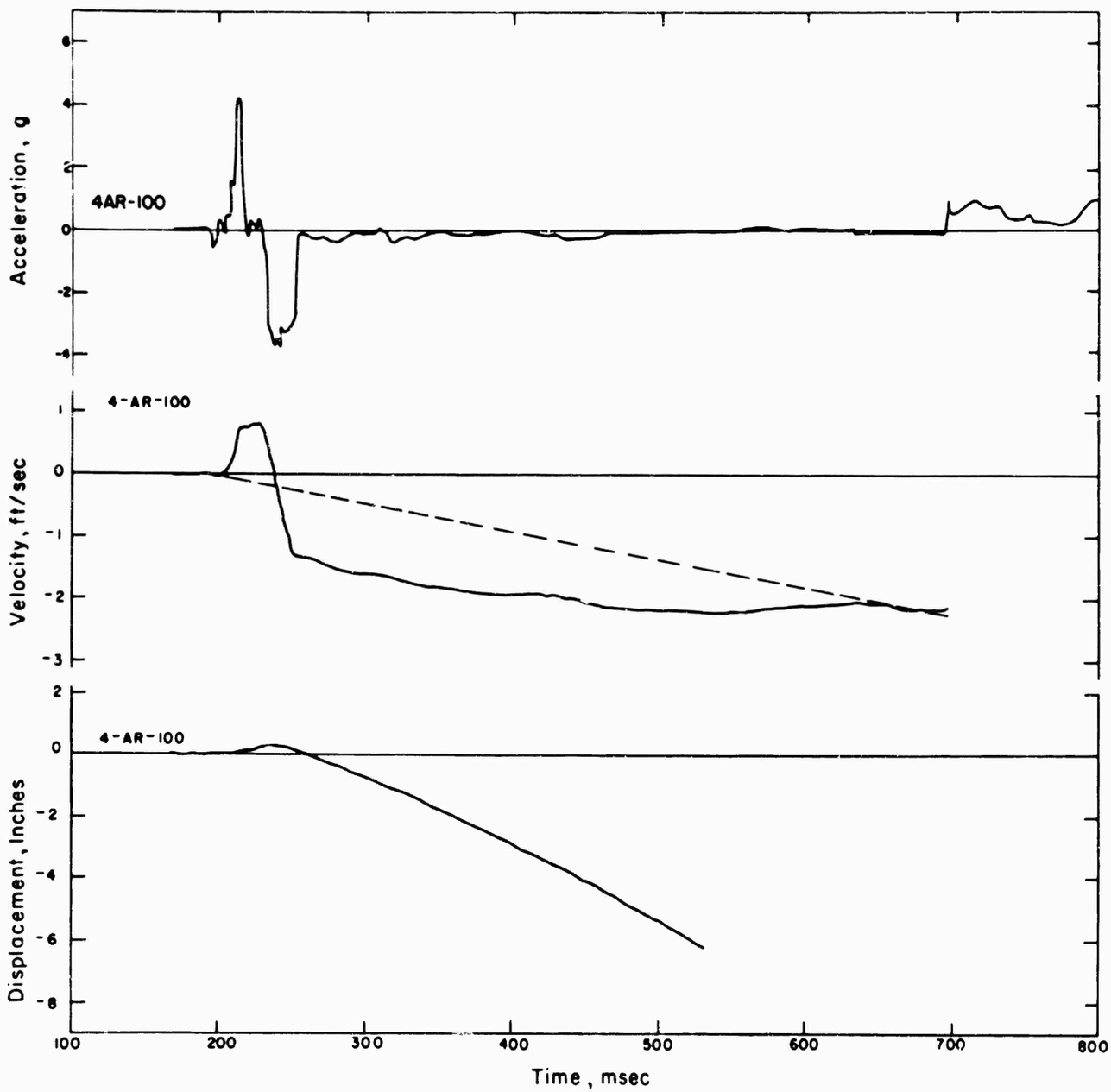

Figure 4.7 Radial acceleration, velocity, and displacement, Station F-1.5-9012.01.

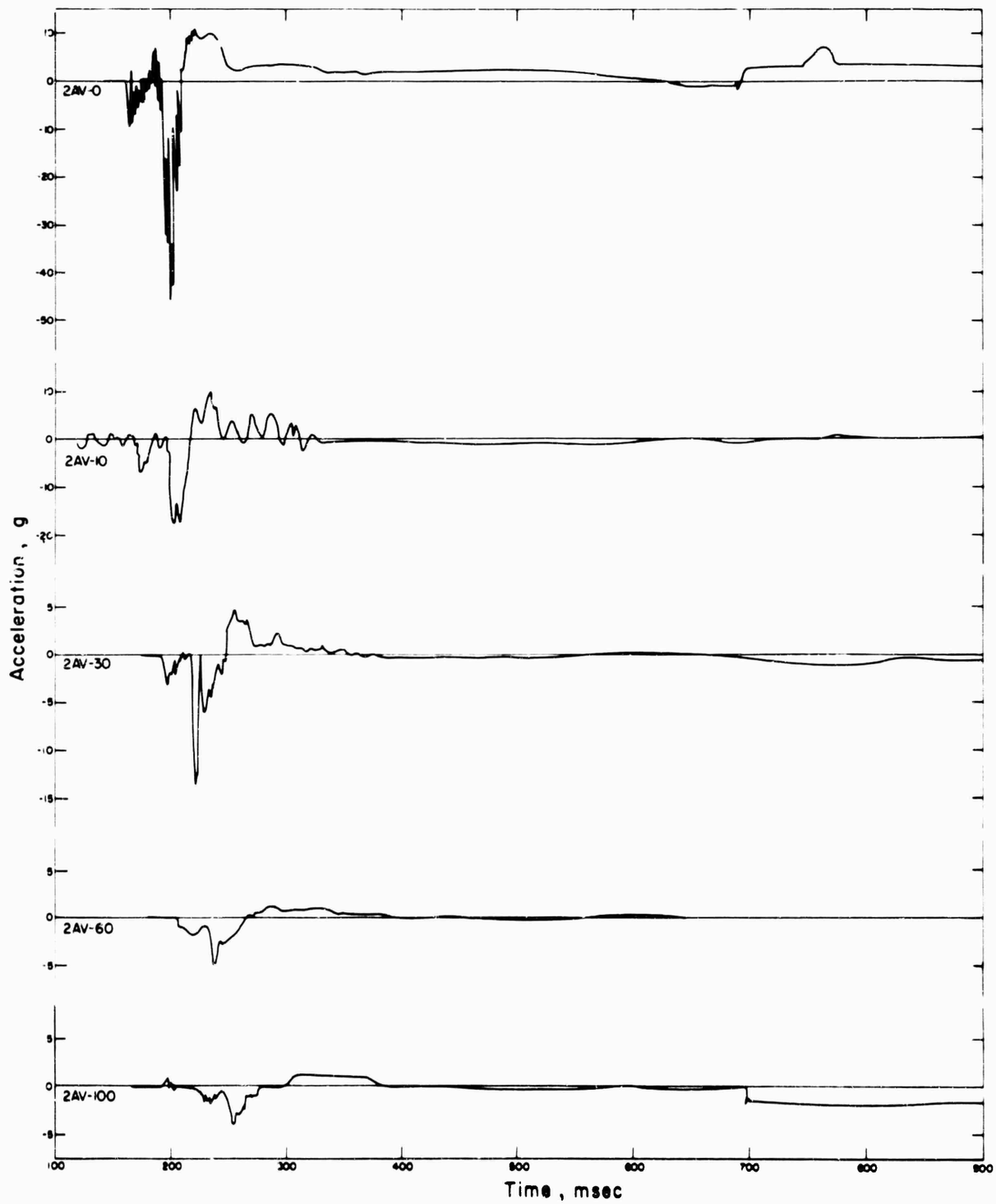

Figure 4.8 Vertical acceleration, Station F-1.5-9012.02.

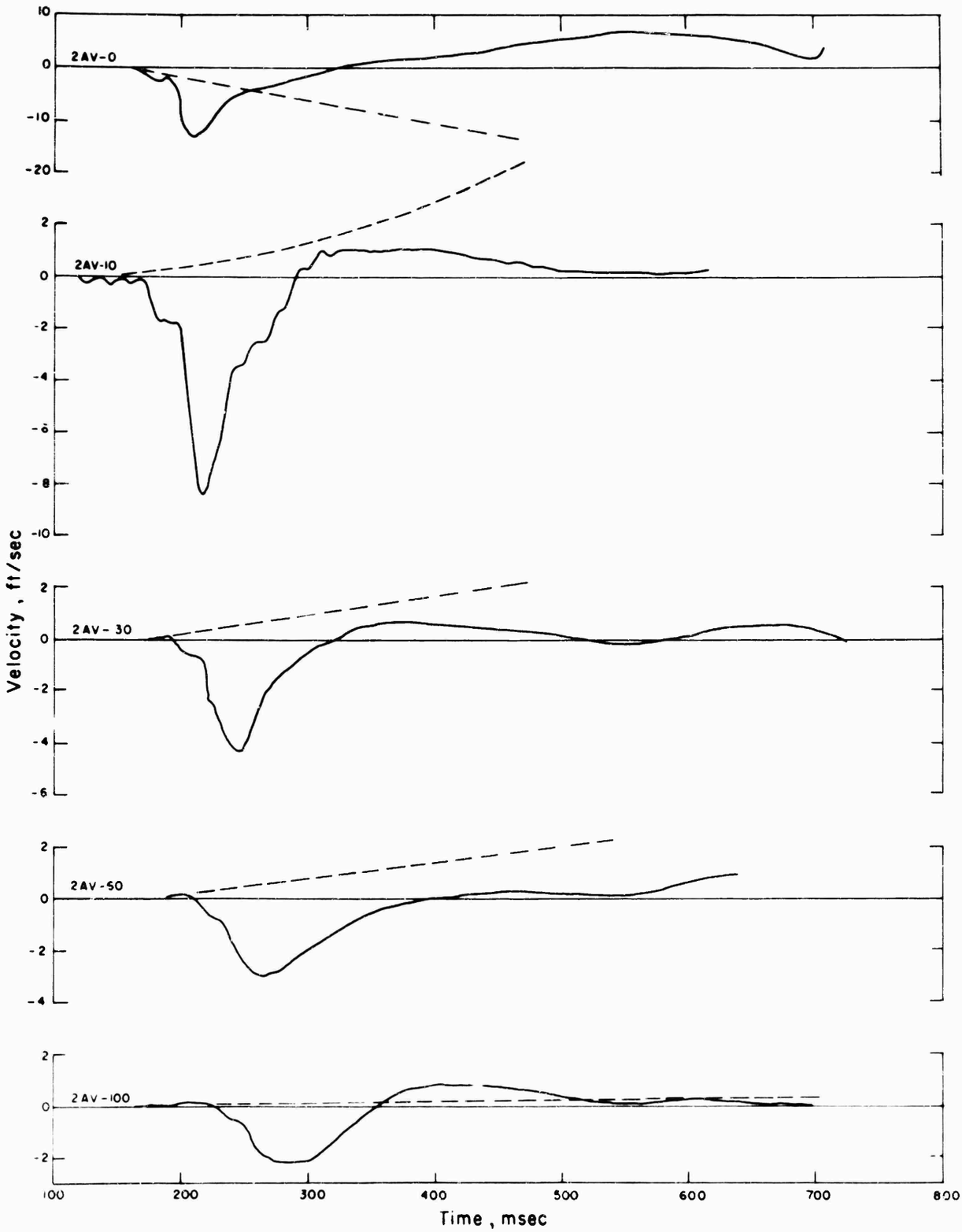

Figure 4.9 Vertical velocity, Station F-1.5-9012.02.

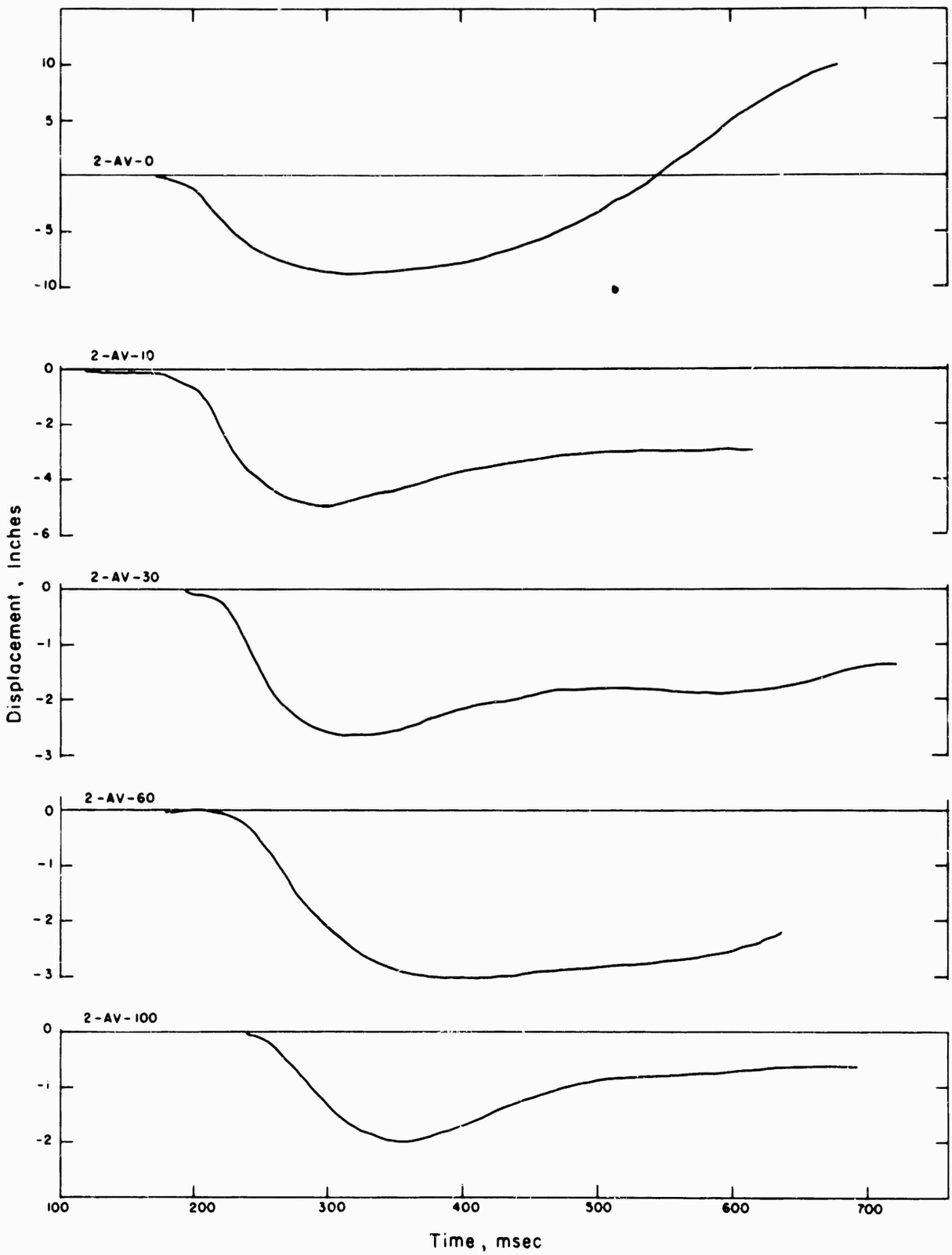

Figure 4.10 Vertical displacement, Station F-1.5-9012.02.

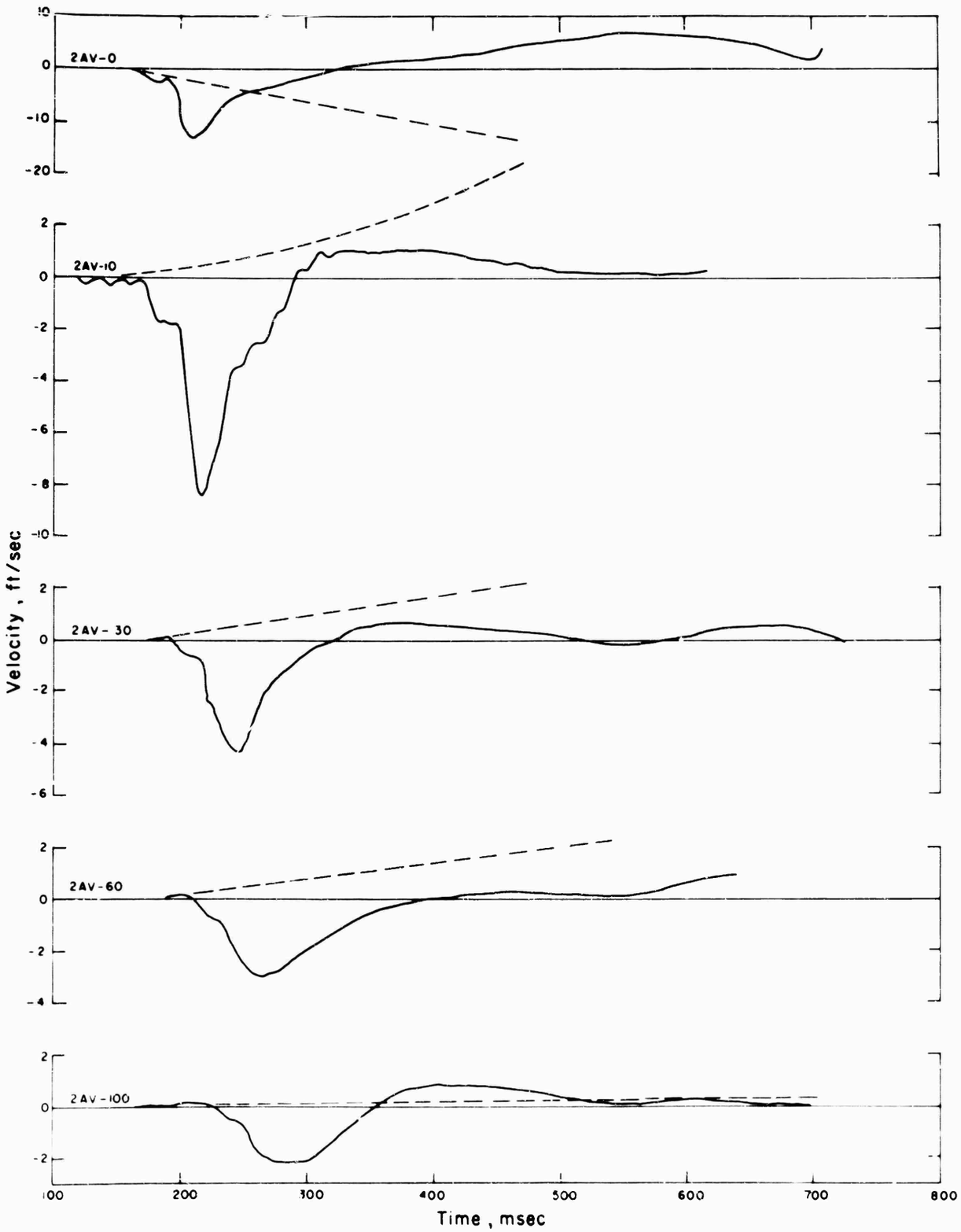

Figure 4.9 Vertical velocity, Station F-1.5-9012.02.

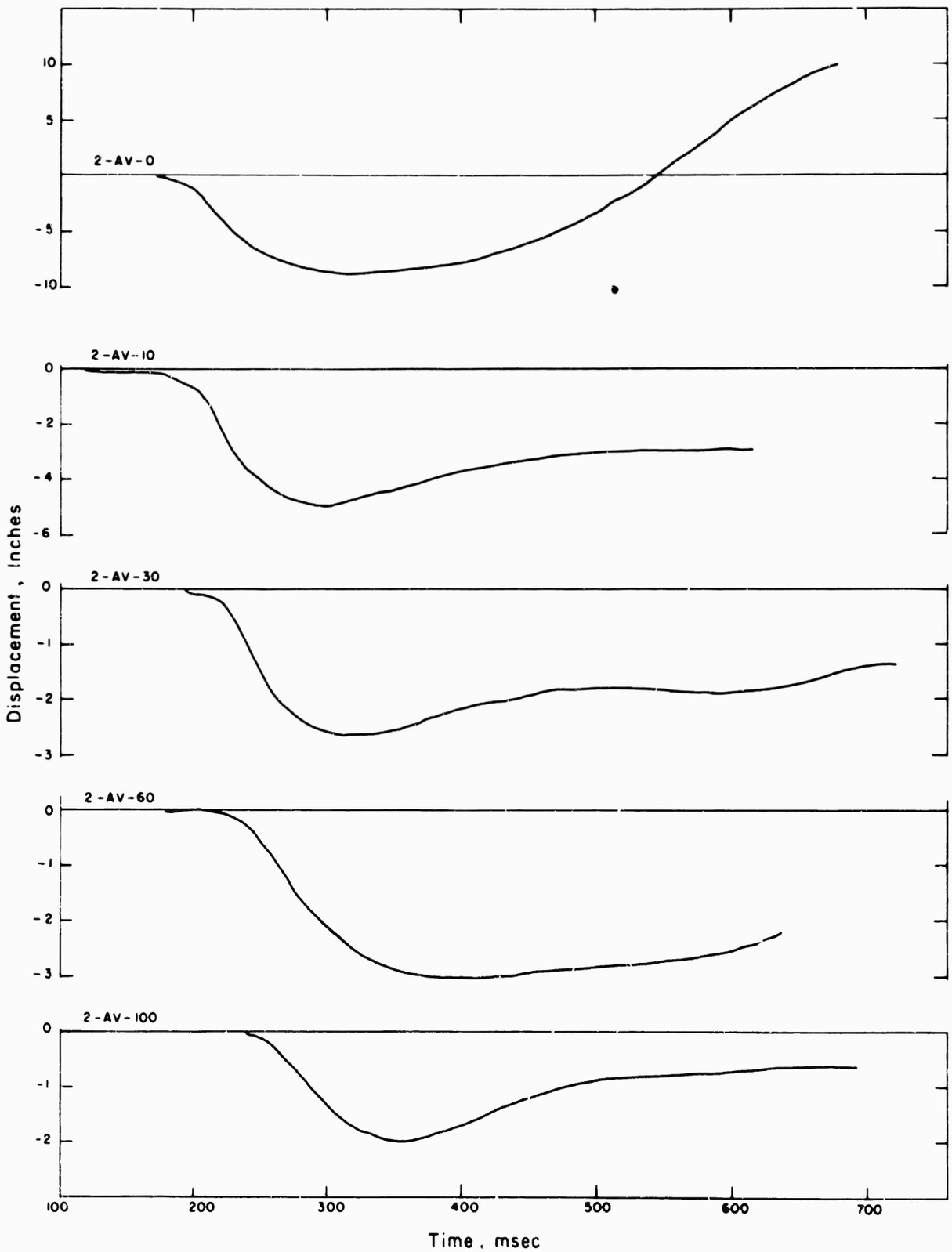

Figure 4.10 Vertical displacement, Station F-1.5-9012.02.

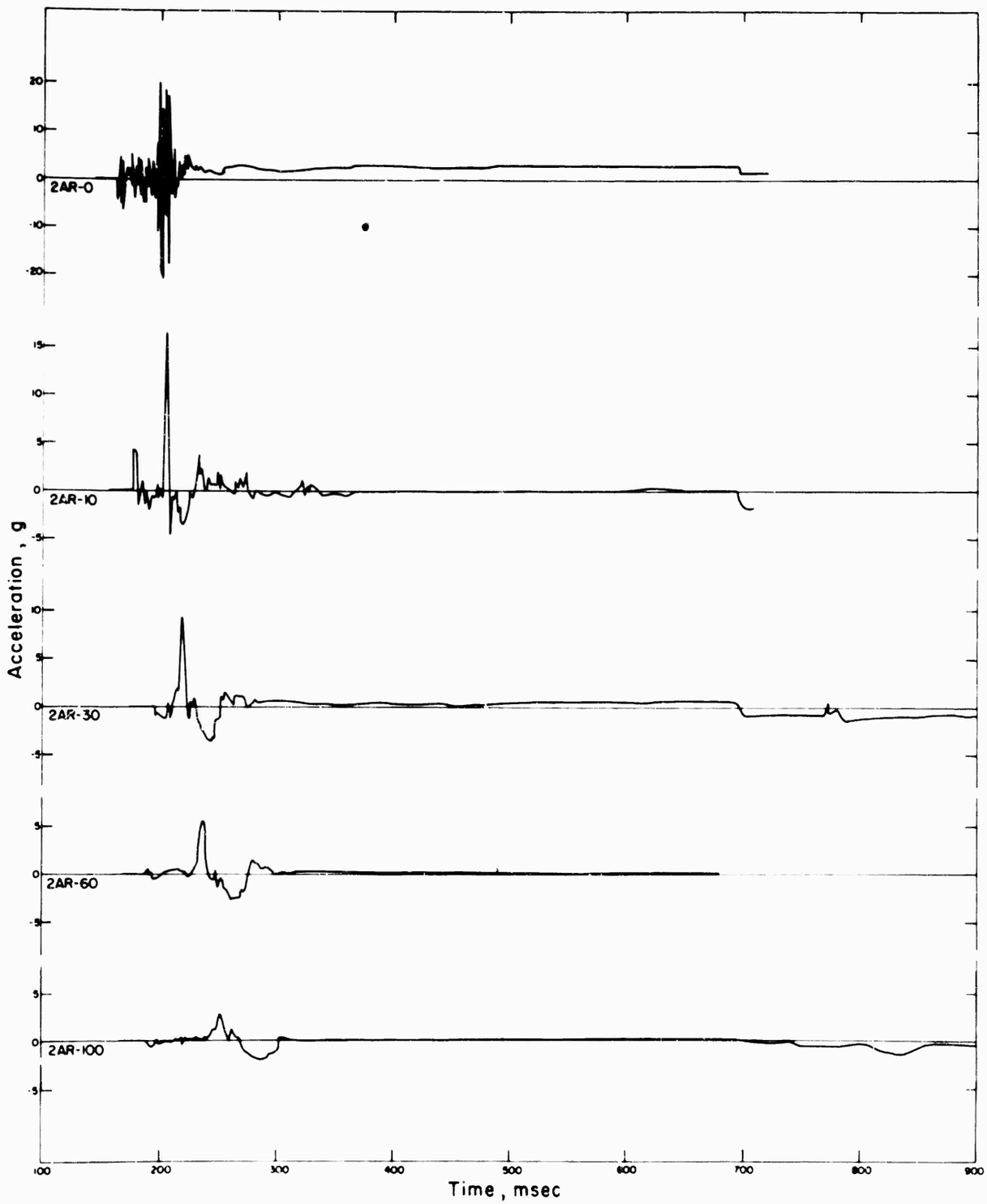

Figure 4.11 Radial acceleration, Station F-1.5-9012.02.

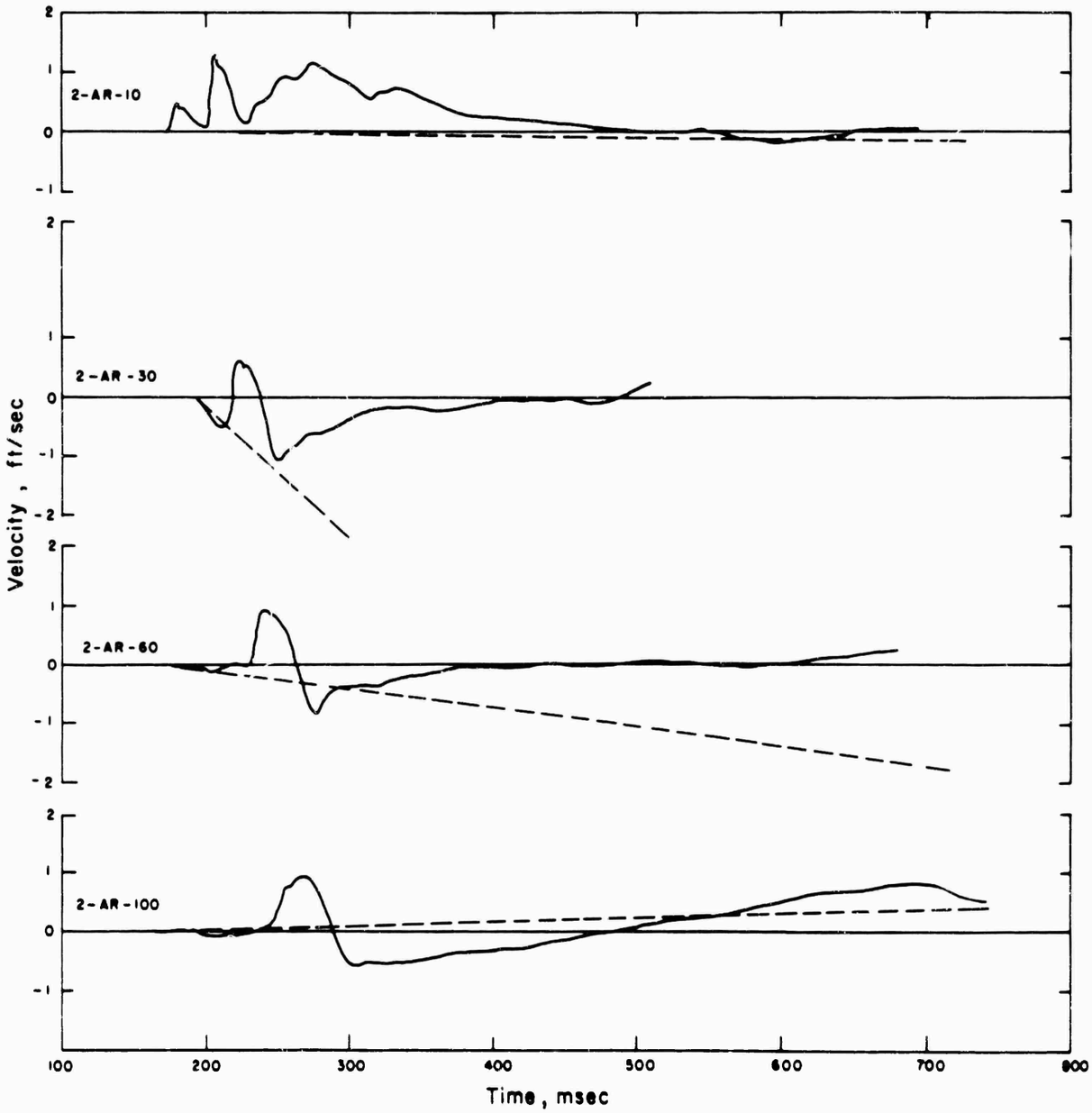

Figure 4.12 Radial velocity, Station F-1.5-9012.0%.

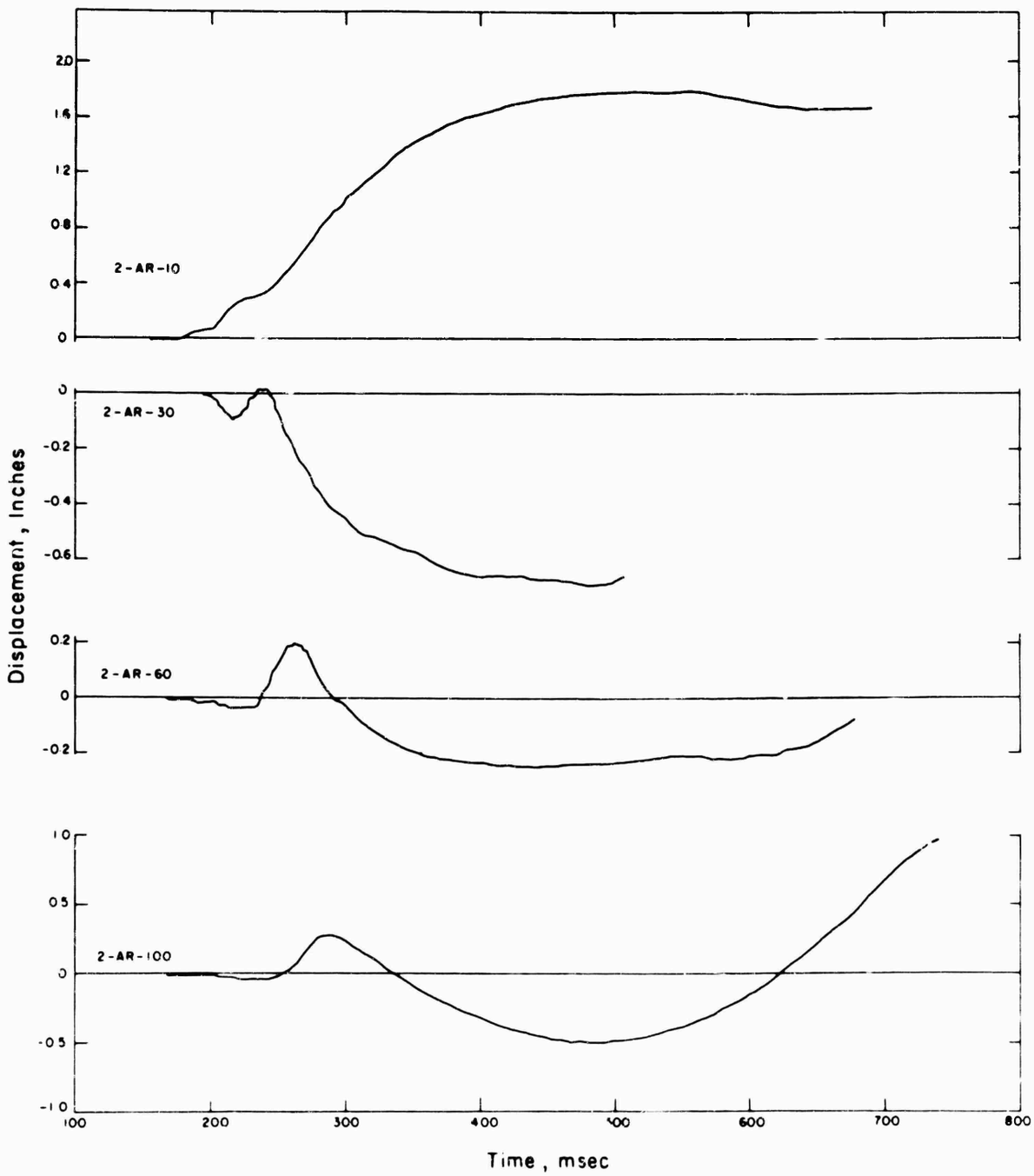

Figure 4.13 Radial displacement, Station F-1.5-9012.02.

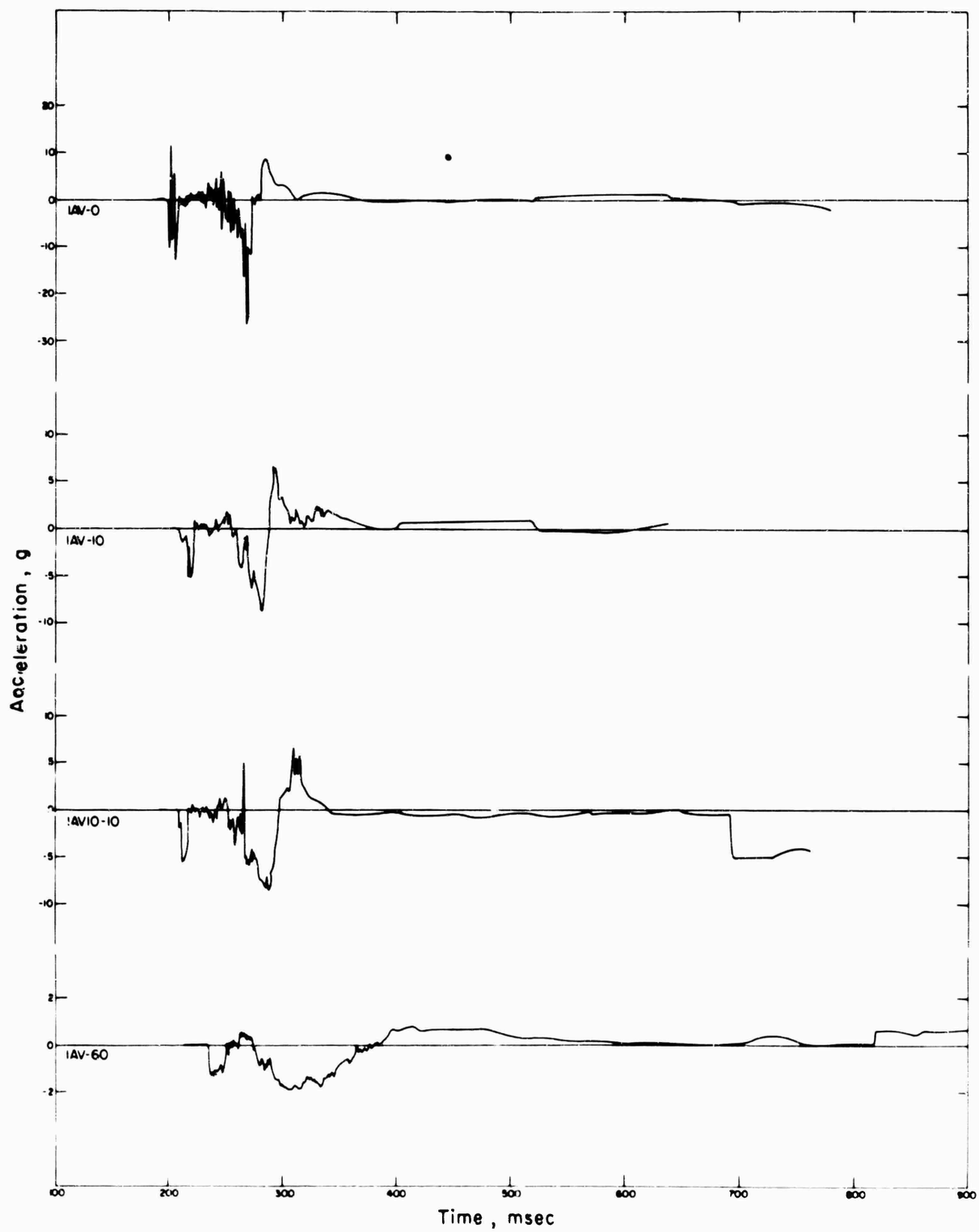

Figure 4.14 Vertical acceleration, Station F-1.5-9012.03.

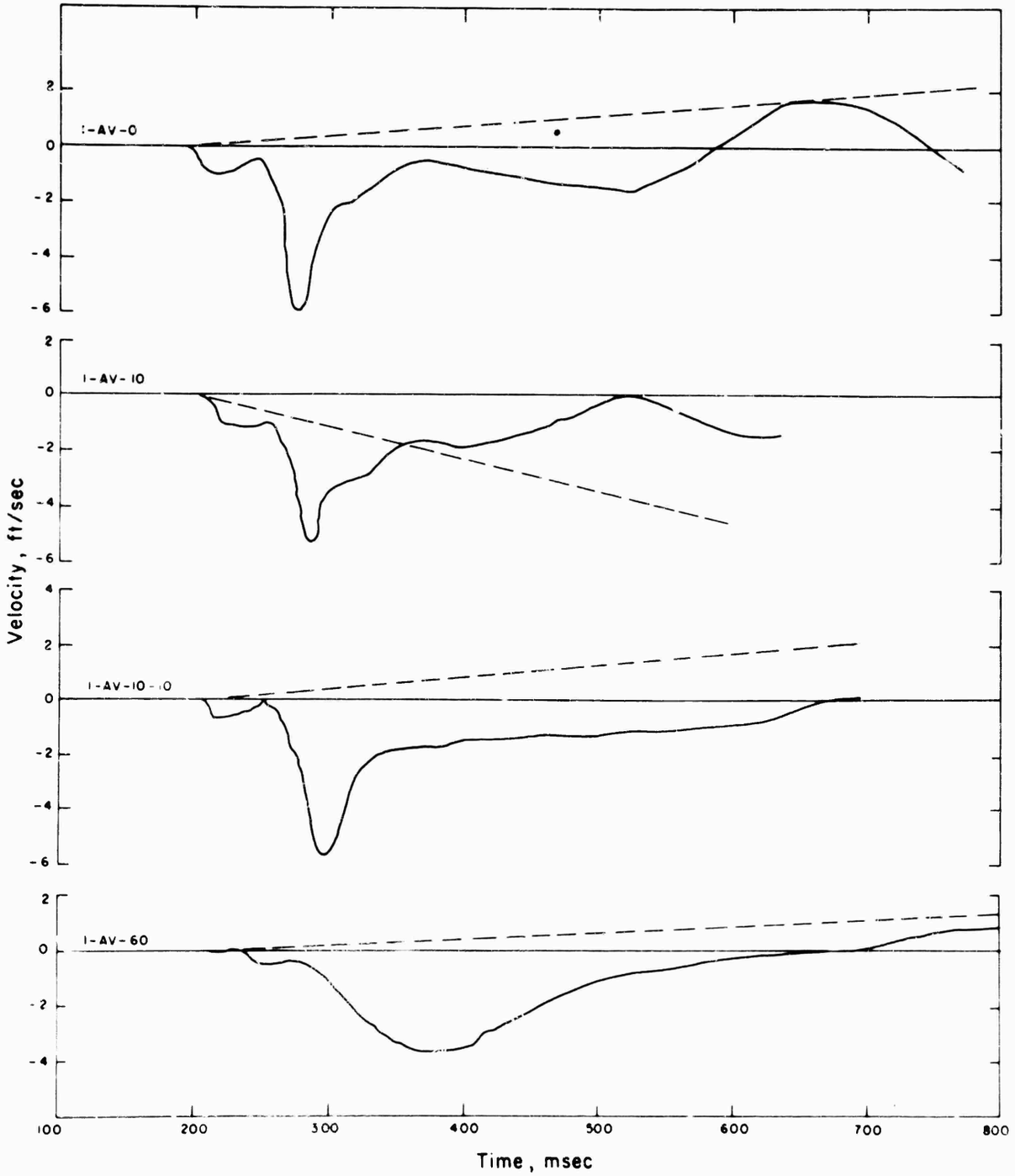

Figure 4.15 Vertical velocity, Station F-1.5-9012.03.

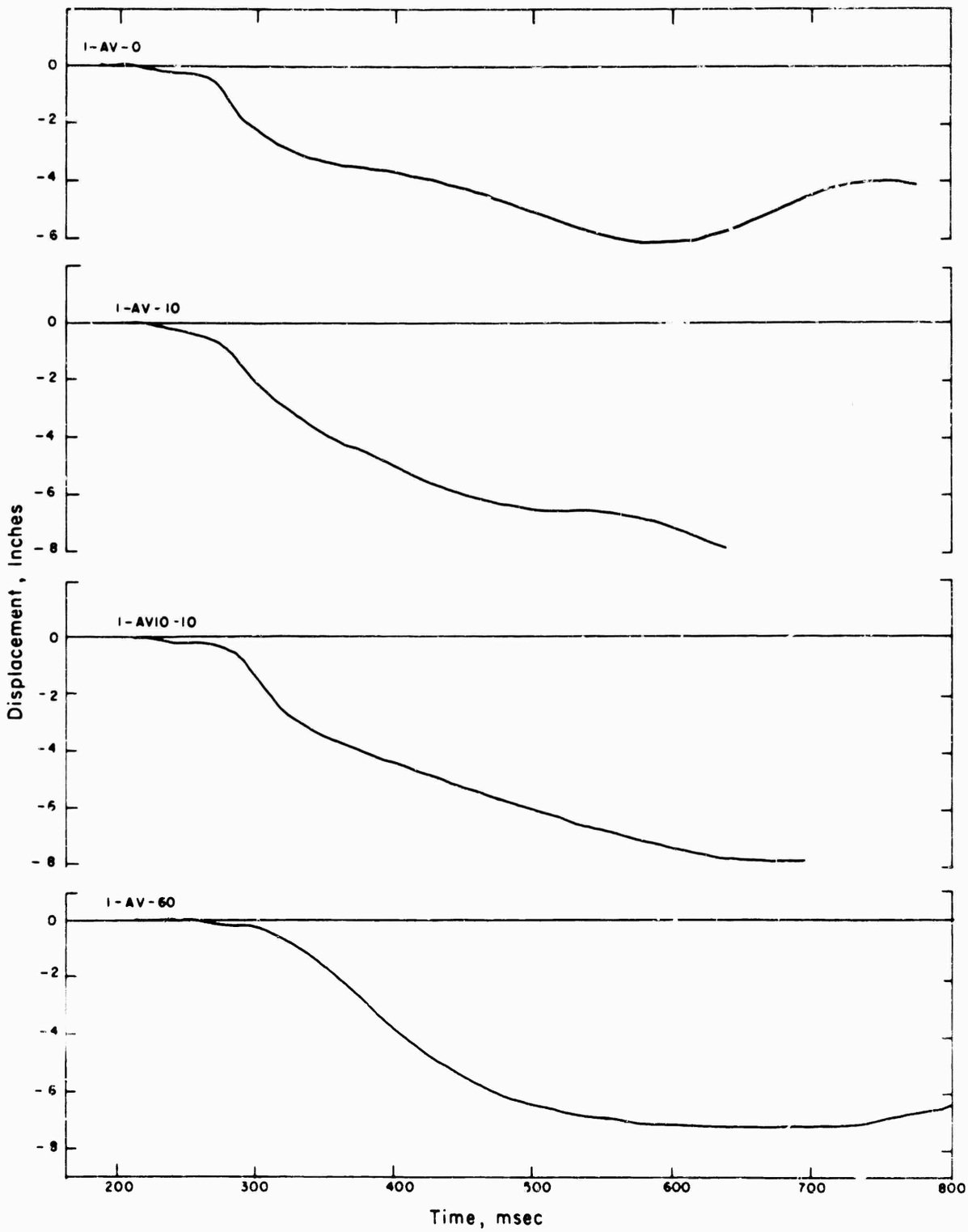

Figure 4.16 Vertical displacement, Station F-1.5-9012.03.

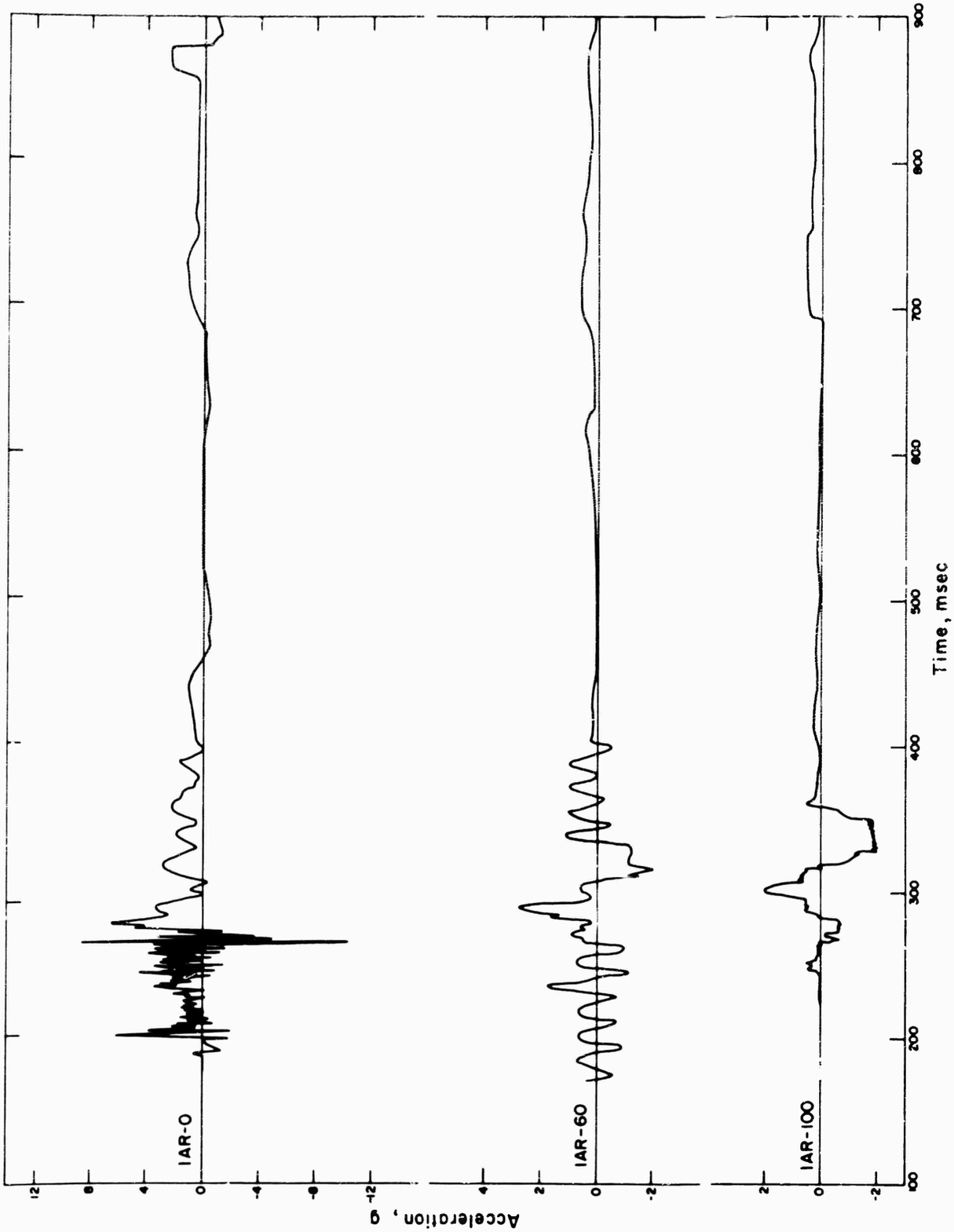

Figure 4.17 Radial acceleration, Station F-1.5-9012.03.

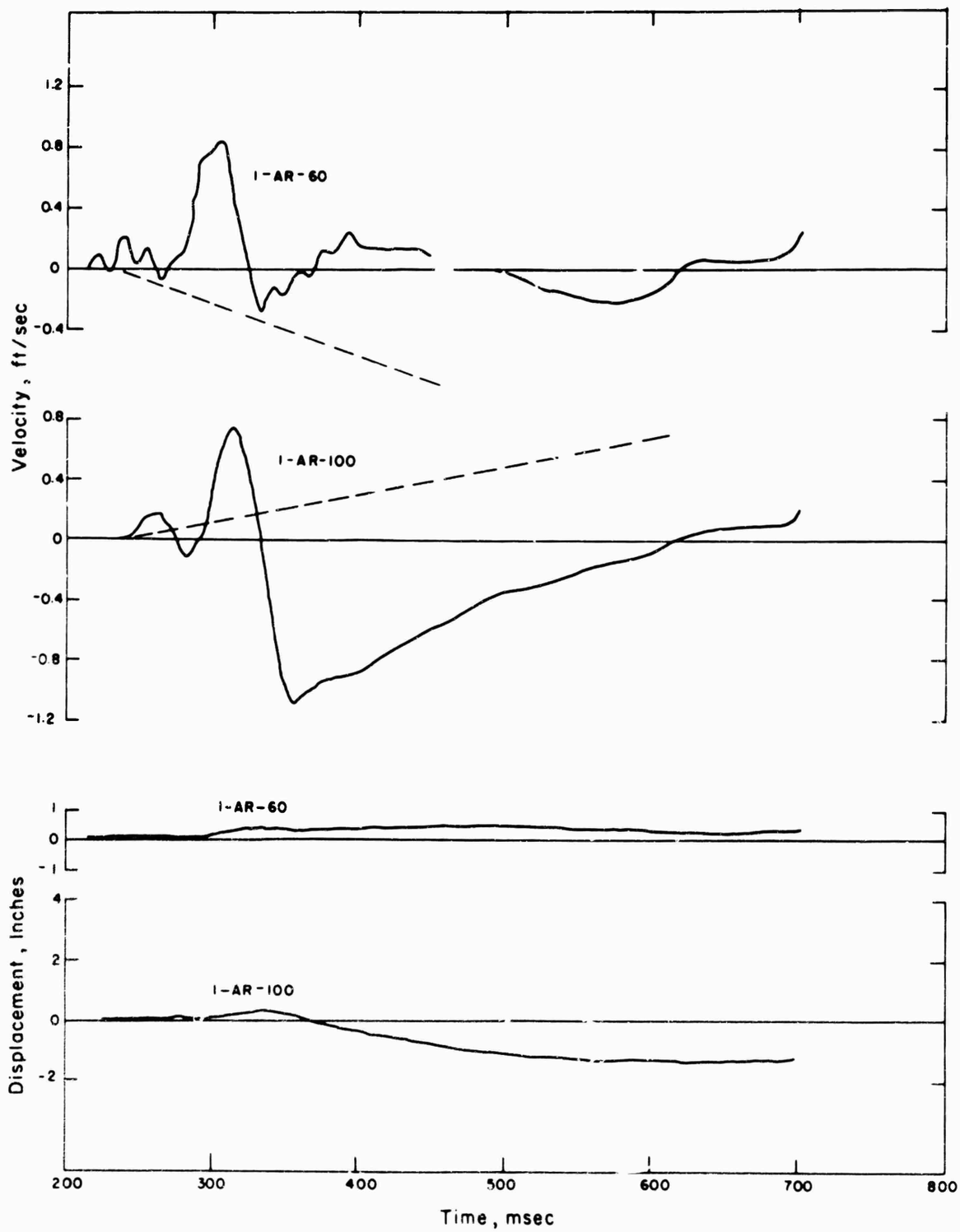

Figure 4.18 Radial velocity and displacement, Station F-1.5-9012.03.

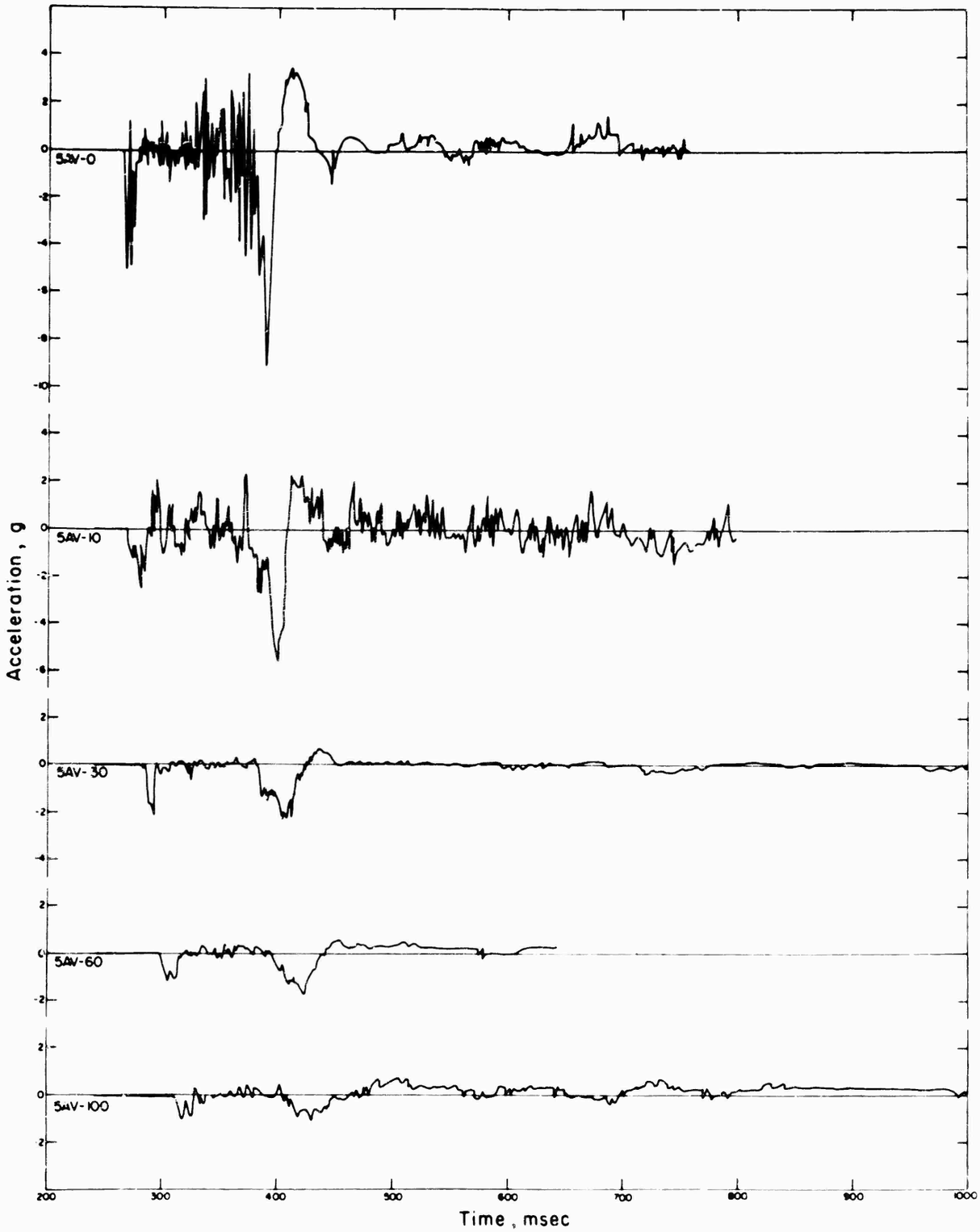

Figure 4.19 Vertical acceleration, Station F-1.5-9012.04.

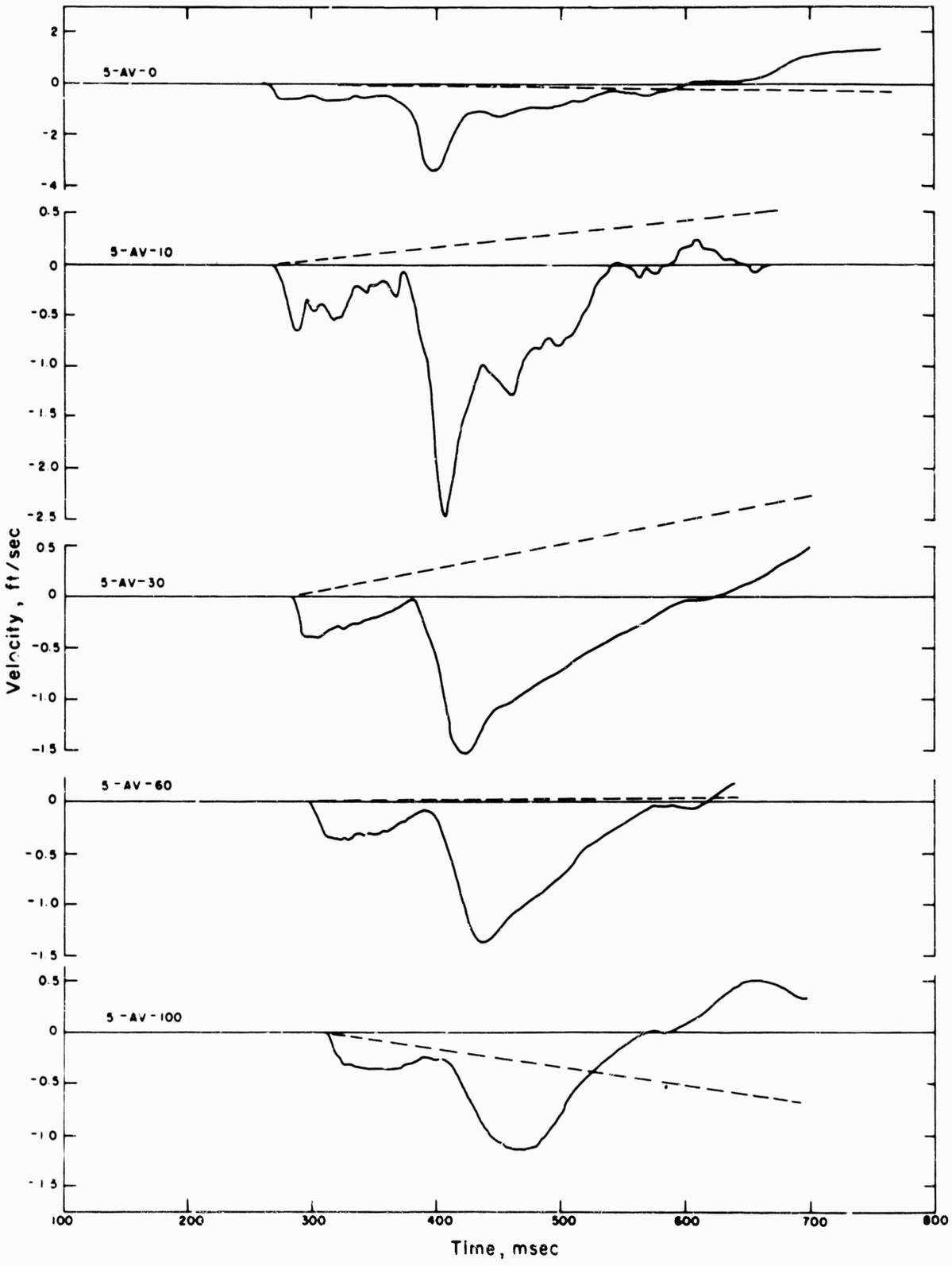

Figure 4.20 Vertical velocity, Station F-1.5-9012.04.

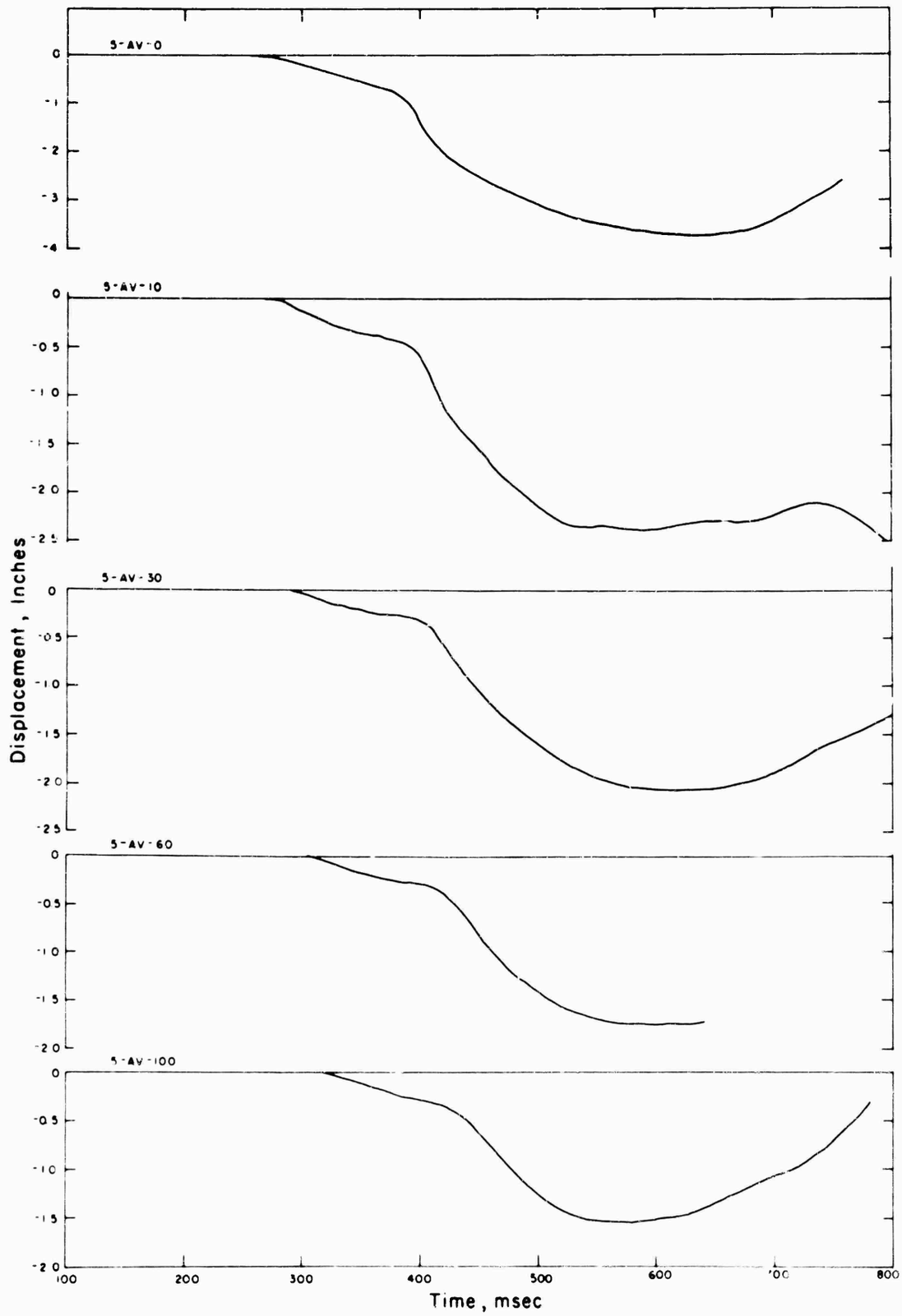

Figure 4.21 Vertical displacement, Station F-1.5-9012.04.

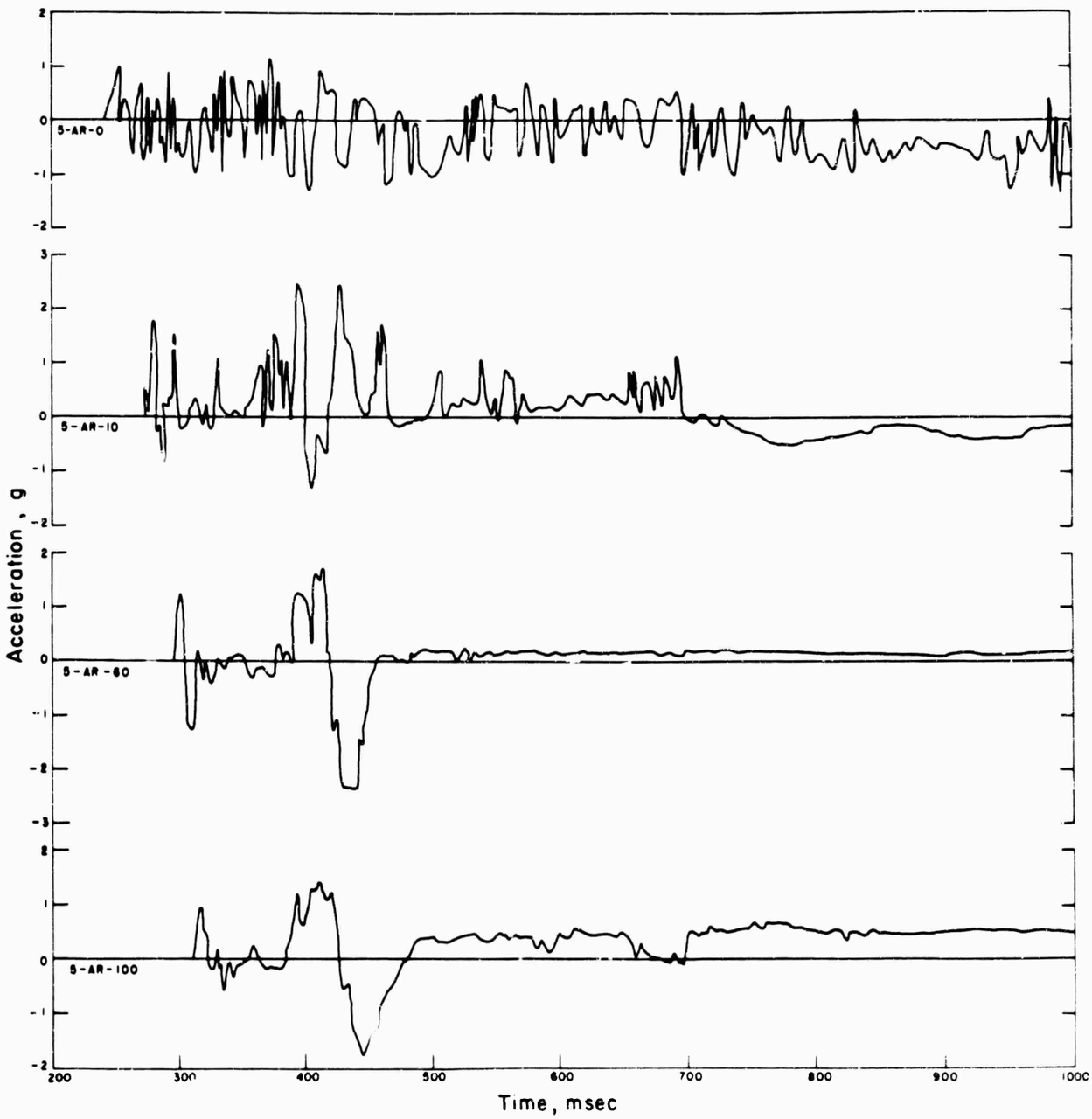

Figure 4.22 Radial acceleration, Station F-1 5-9012.04.

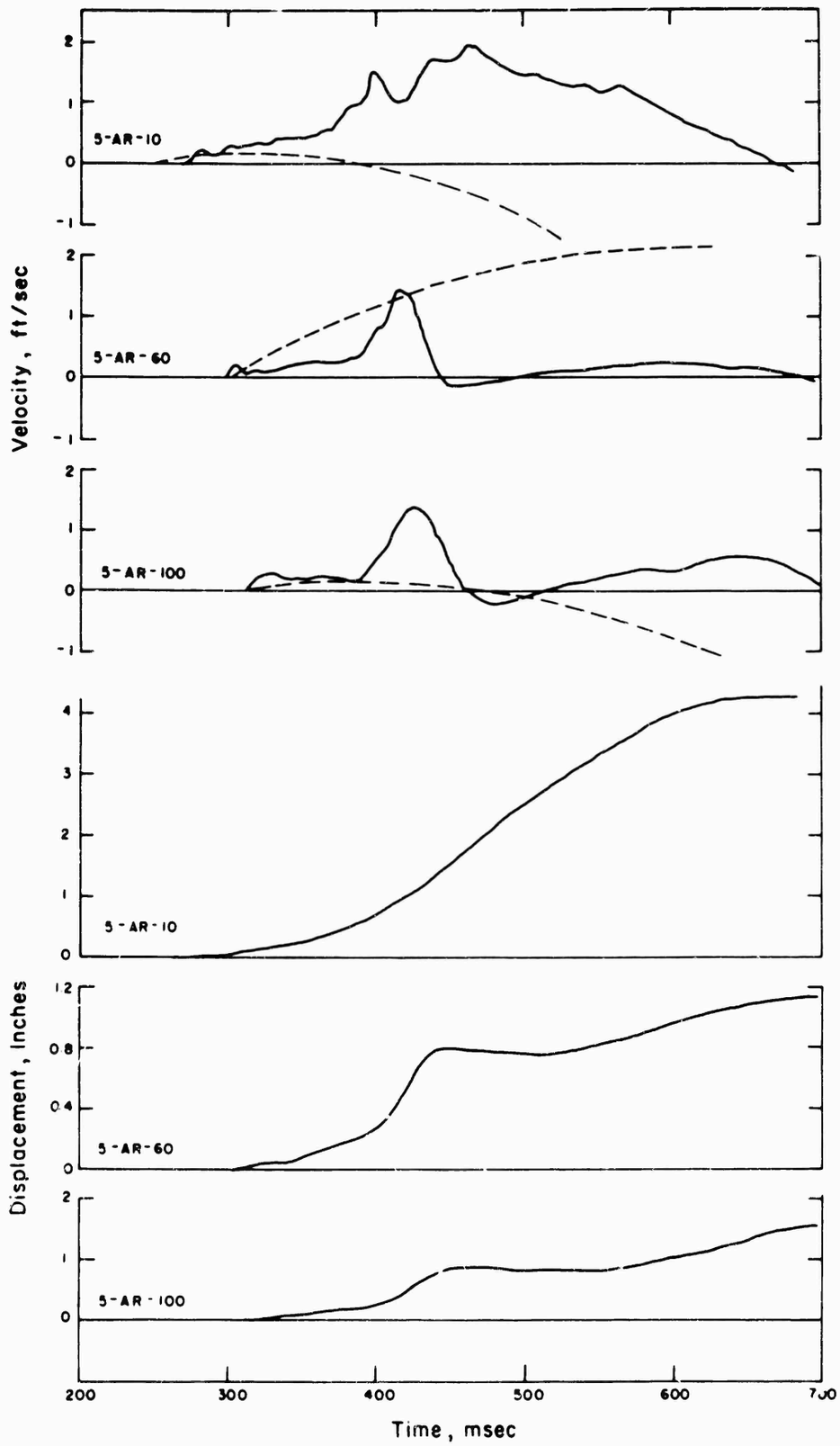

Figure 4.23 Radial velocity and displacement, Station F-1.5-9012.04.

zero line and indicate the degree of correction applied. These corrections result in either an upward or downward shift of the acceleration record zero, or in a linear drift in that zero. In all cases, the magnitude of the shift or drift represents only a small portion of the gage set range.

Pertinent data derived from the free-field accelerometers is compiled in Table 4.4. Velocity and displacement data is introduced in Chapter 5.

TABLE 4.4 GROUND ACCELERATIONS

Gage Number	Ground Range	Depth	Arrival Time	Peak Acceleration		Set Range	Maximum Acceleration as Percent of Set Range
				Positive *	Negative		
	ft	ft	msec	g	g	g	pct
4AV-10	650	10	132	35.1	177	300	59
4AV10-10	650	10	141	23.8	228	300	76
4AV-30	650	30	155	8.7	34.8	150	23
4AV-60	650	60	173	4.7	10.6	99	11
4AV-100	650	100	188	2.2	10.8	75	14
4AR-100	650	100	192	4.2	3.7	75	5
4AV-200	650	200	230	1.1	2.8	24	12
2AV-0	850	0	163	10.5	45.6	150	30
2AR-0	850	0	162	19.9	18.4	150	13
2AV-10	850	10	170	10.0	17.9	150	12
2AR-10	850	10	175	16.4	3.5	150	11
2AV-30	850	30	190	4.6	13.6	75	18
2AR-30	850	30	195	9.3	3.7	75	13
2AV-60	850	60	199	1.0	4.9	45	11
2AR-60	850	60	199	5.6	2.5	45	12
2AV-100	850	100	214	1.3	3.9	36	11
2AR-100	850	100	214	2.9	2.0	36	8
1AV-0	1,050	0	197	8.2	27.0	99	27
1AR-0	1,050	0	191	6.2	2.1	99	6
1AV-10	1,050	10	210	6.7	8.8	99	9
1AV10-10	1,050	10	209	6.5	8.4	99	8
1AV-60	1,050	60	233	0.8	1.9	36	5
1AR-60	1,050	60	233	2.7	2.0	36	8
1AR-100	1,050	100	246	1.9	2.1	21	10
5AV-0	1,350	0	268	3.5	9.1	75	12
5AR-0	1,350	0	—	1.1	1.3	75	2
5AV-10	1,350	10	271	2.3	5.4	75	7
5AR-10	1,350	10	273	2.5	1.4	75	3
5AV-30	1,350	30	284	0.7	2.2	36	6
5AV-60	1,350	60	298	0.6	1.8	21	9
5AR-60	1,350	60	298	1.7	2.4	21	11
5AV-100	1,350	100	312	0.8	1.0	15	7
5AR-100	1,350	100	312	1.4	1.8	15	12

* Positive vertical accelerations are upward, positive radial accelerations are outward.

4.5 DISPLACEMENTS

Data was obtained from all relative displacement gages, but it was not clear initially that meaningful information would derive from three of the records. Relative displacements were converted to absolute displacements of the surface slab and gage anchors on the assumption that the deepest gage anchors were not displaced. A plot of peak relative displacements for each station (Figure 4.24) indicates that the assumption is a realistic approximation. Thus, gages spanning the depth from the surface to the anchor at 200 feet represented absolute motion of the surface. Relative displacement-time curves are shown in Figures 4.25 through 4.28.

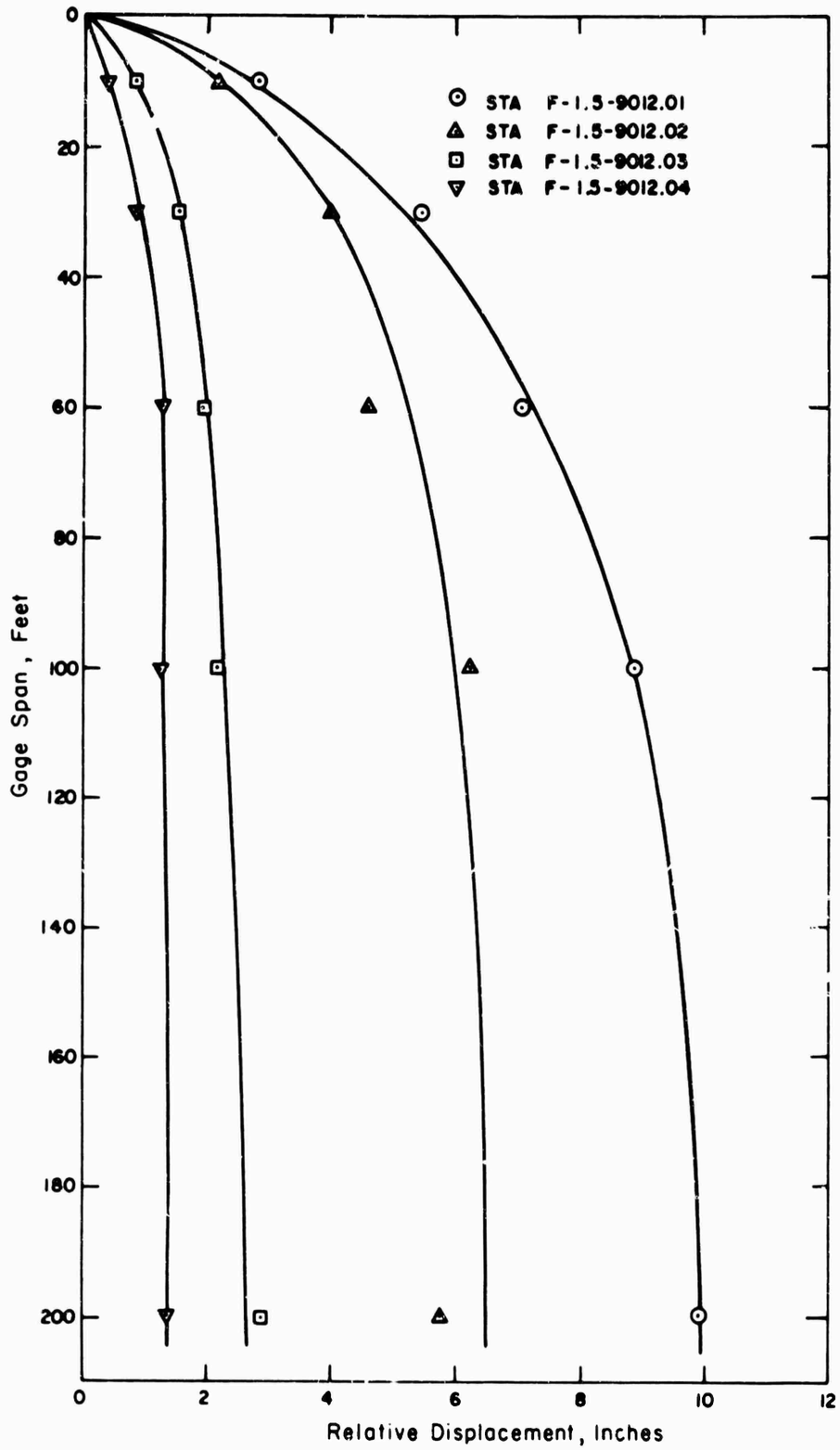

Figure 4.24 Peak relative displacement versus gage span.

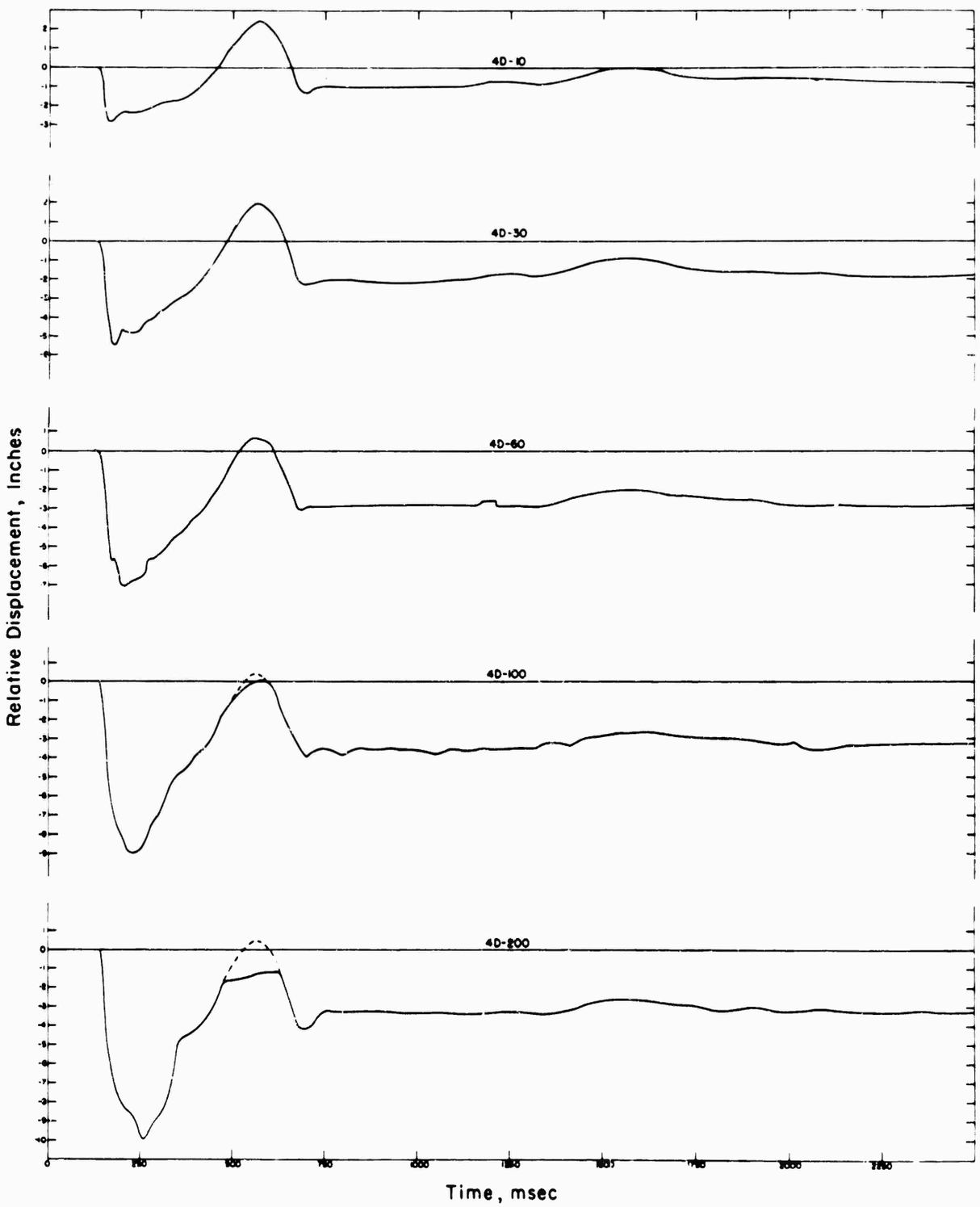

Figure 4.25 Relative displacement, Station F-1.5-9012.01.

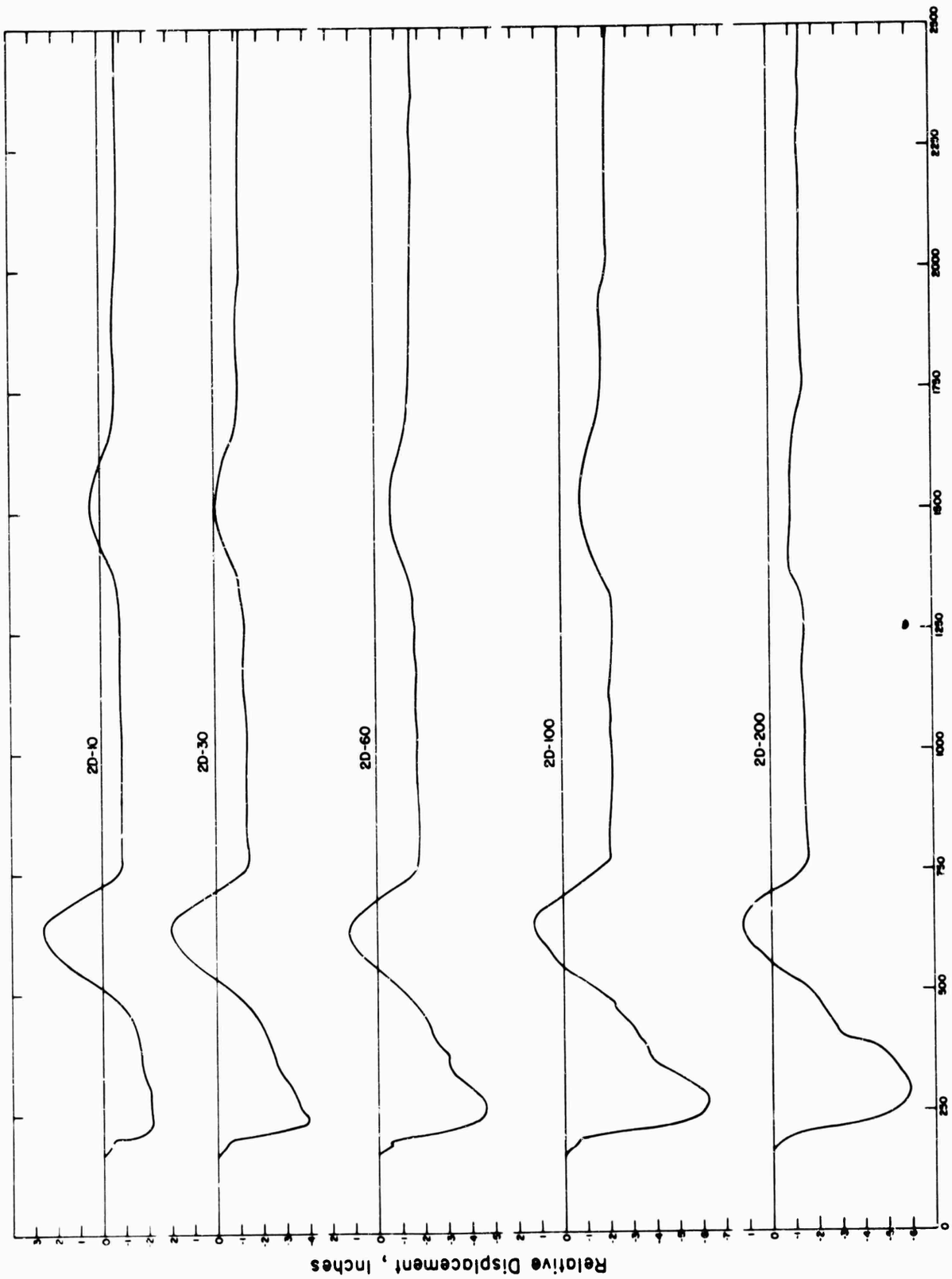

Figure 4.26 Relative displacement, Station F-1.5-9012.02.

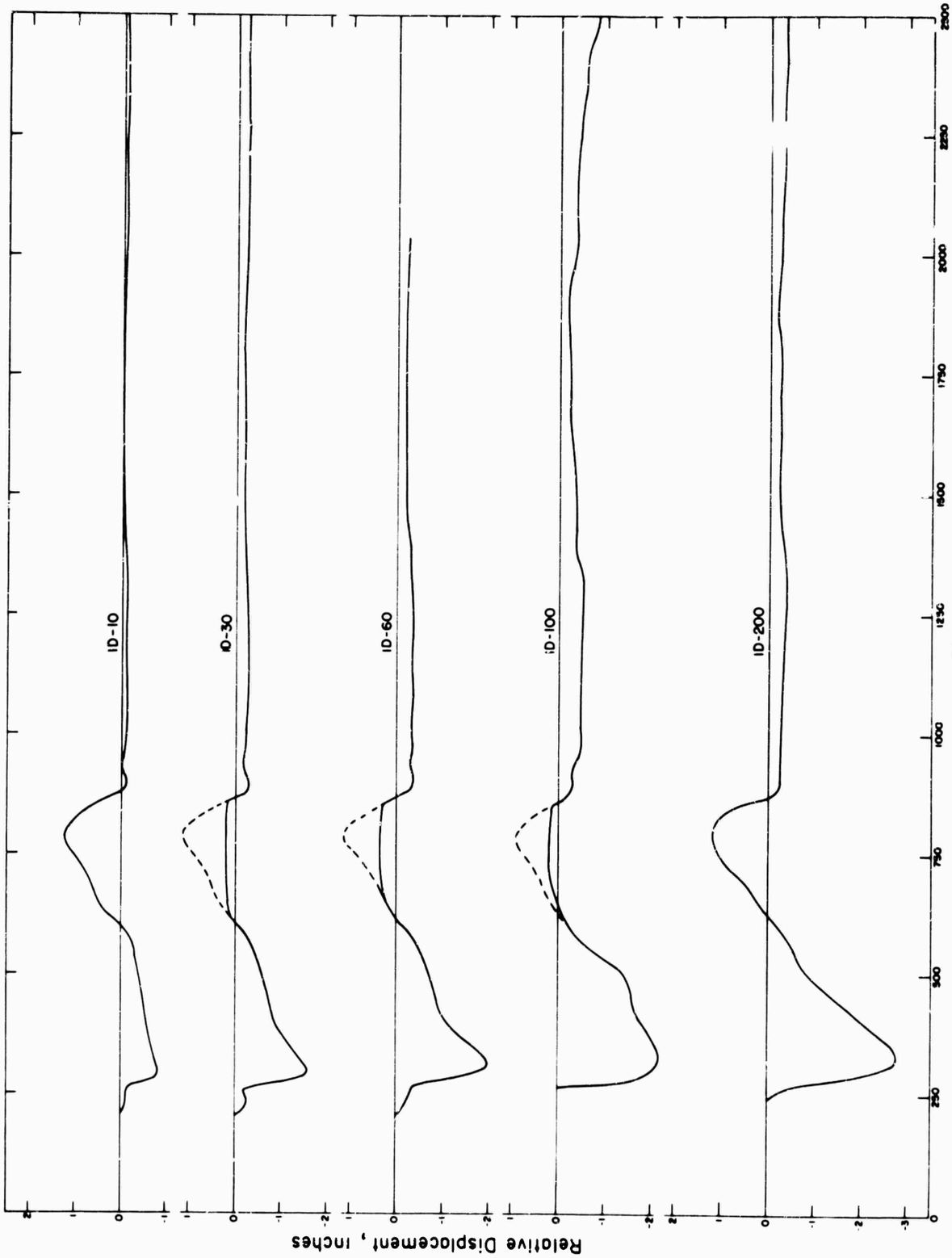

Figure 4.27 Relative displacement, Station F-1.5-9012.03.

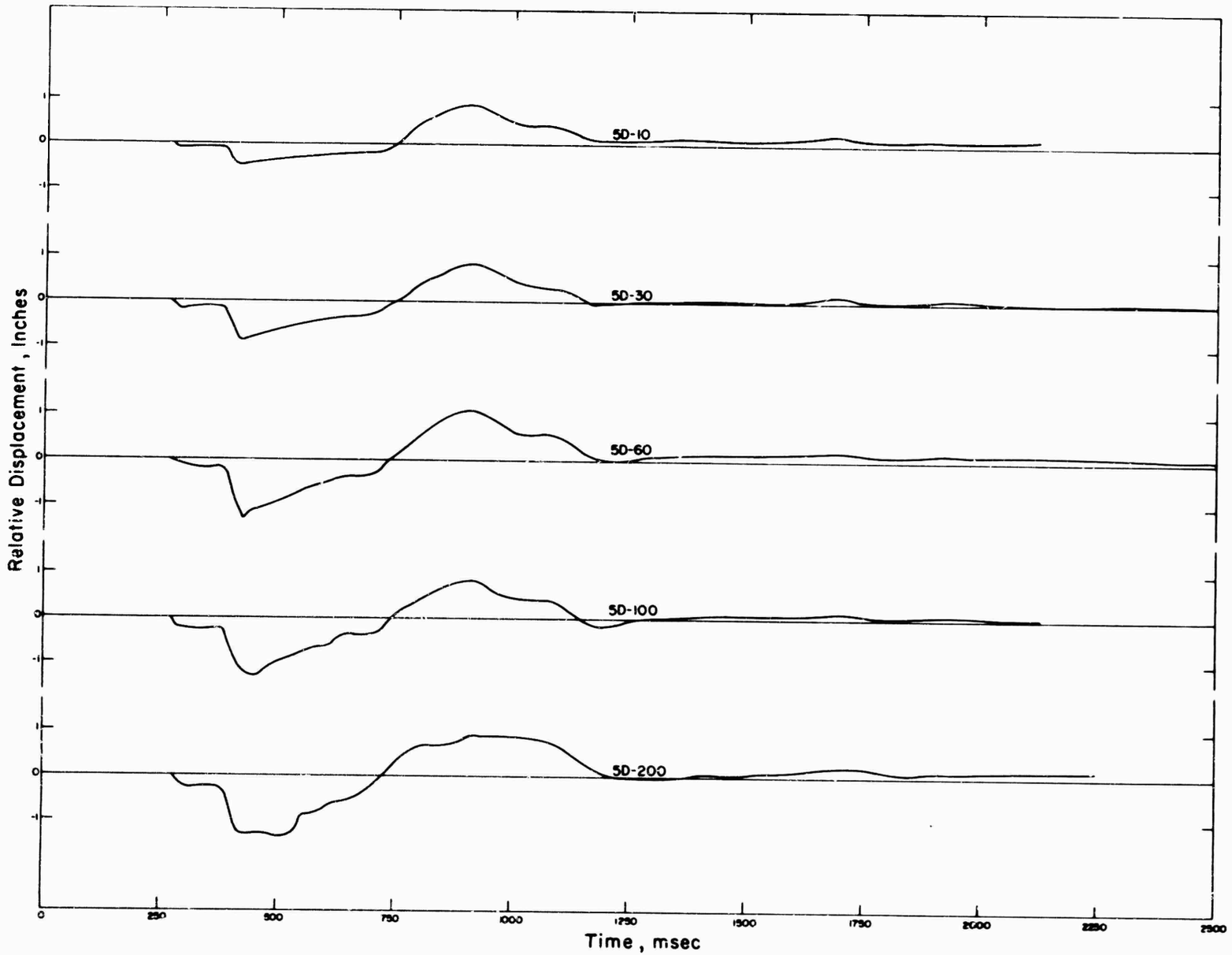

Figure 4.28 Relative displacement, Station F-1.5-9012.04.

Absolute displacements at other depths were derived by subtracting, point-for-point, the record for 10-, 30-, 60- and 100-foot-deep gages from those for the 200-foot gages. At Station F-1.5-9012, there is inconsistency between the 100-foot and 200-foot gages in that the record for the latter is more irregular and its peak is slightly less than that for the shallower gage. The

TABLE 4.5 RELATIVE DISPLACEMENTS

Gage Number	Ground Range	Span	Displacement		Set Range
			Down	Up	
	ft	ft	in	in	in
4D-10	650	0 to 10	2.81	2.41	3
4D-30	650	0 to 30	5.45	1.99	6
4D-60	650	0 to 60	7.06	0.75	7
4D-100	650	0 to 100	8.88	0.71	15
4D-200	650	0 to 200	9.93	—	24
2D-10	850	0 to 10	2.18	2.46	3
2D-30	850	0 to 30	4.00	1.93	6
2D-60	850	0 to 60	4.80	1.23	6
2D-100	850	0 to 100	6.22	1.19	21
2D-200	850	0 to 200	5.79	0.53	24
1D-10	1,050	0 to 10	0.84	1.26	1.5
1D-30	1,050	0 to 30	1.55	0.23	4.5
1D-60	1,050	0 to 60	1.98	0.32	6
1D-100	1,050	0 to 100	2.15	0.20	15
1D-200	1,050	0 to 200	2.92	1.43	24
5D-10	1,350	0 to 10	0.46	0.89	1.5
5D-30	1,350	0 to 30	0.88	0.85	3
5D-60	1,350	0 to 60	1.29	1.11	4.5
5D-100	1,350	0 to 100	1.25	0.86	9
5D-200	1,350	0 to 200	1.37	0.91	15

general nature of the records suggest that the 100-foot anchor should be assumed to be undisturbed; at this station absolute displacements extend only 60 feet deep. Curves showing absolute displacement as a function of time are compiled in Figures 4.29 through 4.32; pertinent relative displacement data are compiled in Table 4.5; and similar absolute displacement data are contained in Table 4.6.

TABLE 4.6 ABSOLUTE DISPLACEMENTS

Ground Range	Depth	Arrival Time	Displacement			Incident Overpressure	Impulse Intensity
			Down	Up	Residual		
ft	ft	msec	in	in	in	psi	psi-sec
Station F-1.5-9012.01							
650	0	138	−9.9	0.3	−3.3	270	14
	10	150	−7.7	−2.0	−2.3		
	30	163	−5.6	−1.1	−1.1		
	60	170	−3.8	0.02	−0.4		
	100	195	−2.2	0.6	0.2		
Station F-1.5-9012.02							
850	0	150	−6.2	1.2	−2.0	187	9.5
	10	160	−4.1	−0.8	−1.2		
	30	170	−2.7	−0.4	−0.9		
	60	190	−1.9	0.3	0.5		
	100*	—	0	0	0		
Station F-1.5-9012.03							
1,050	0	210	−2.8	1.2	−0.3	120	7.8
	10	225	−2.0	0.2	−0.2		
	30	240	−1.5	0.4	−0.1		
	60	250	−1.1	0.4	0.02		
	100	270	−0.6	0.6	0.2		
Station F-1.5-9012.04							
1,350	0	272	−1.4	0.9	0.17	59	6.9
	10	284	−1.0	0.2	0.05		
	30	290	−0.8	0.3	0.18		
	60	280	−0.5	0.1	0.03		
	100	340	−0.4	0.3	0.12		

* Displacement of 2D-100 anchor at 100-ft depth assumed zero

Two features of the displacement curves should be discussed here: first, extension springs of certain of the long-span gages bottomed against the rigid containing conduit and caused flat portions of the relative displacement curves. This resulted from insufficient free-run in design for the long set ranges adopted. Dashed curves above portions of the solid ones are traced sec-

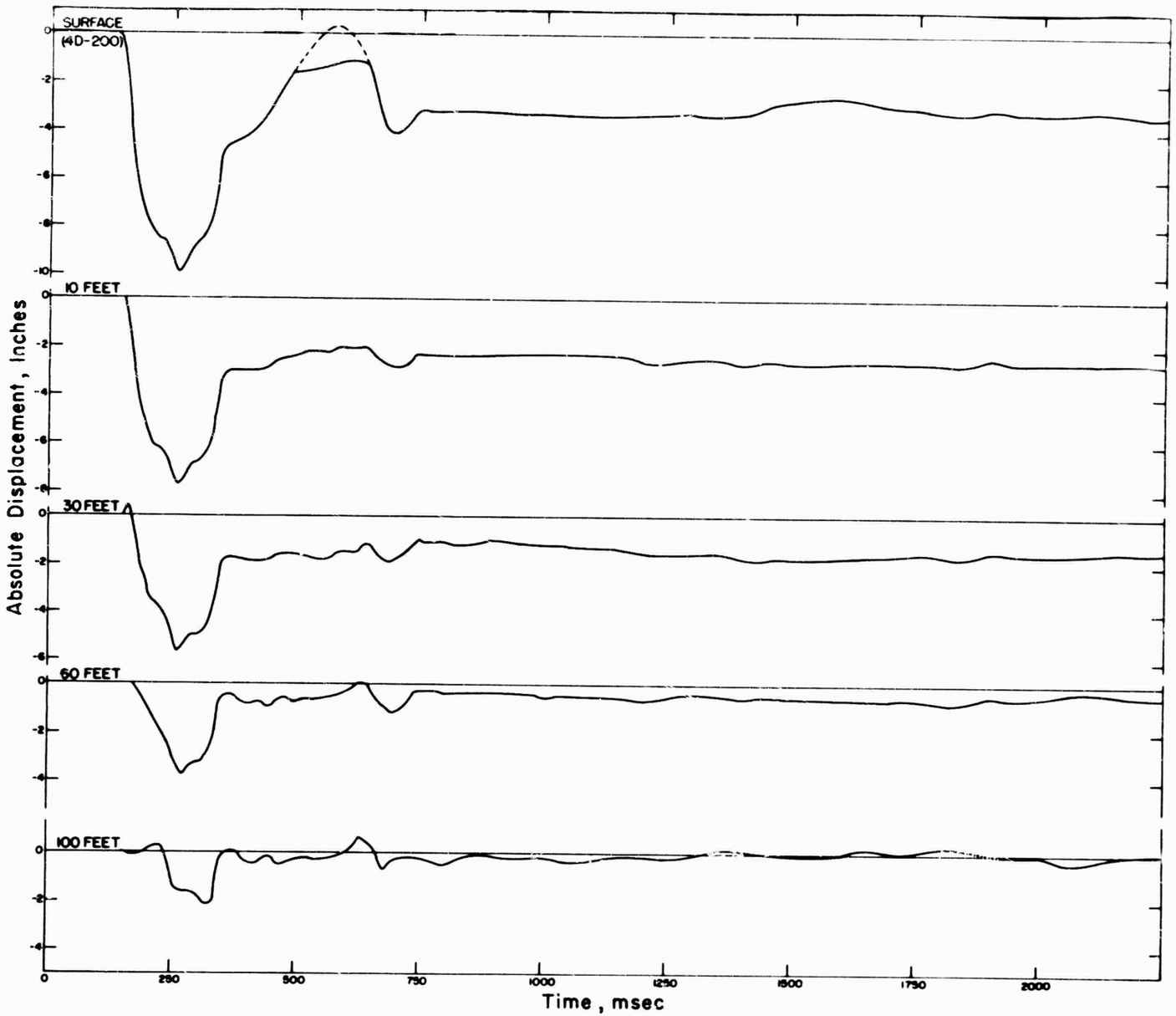

Figure 4.29 Absolute displacement, Station F-1.5-9012.01.

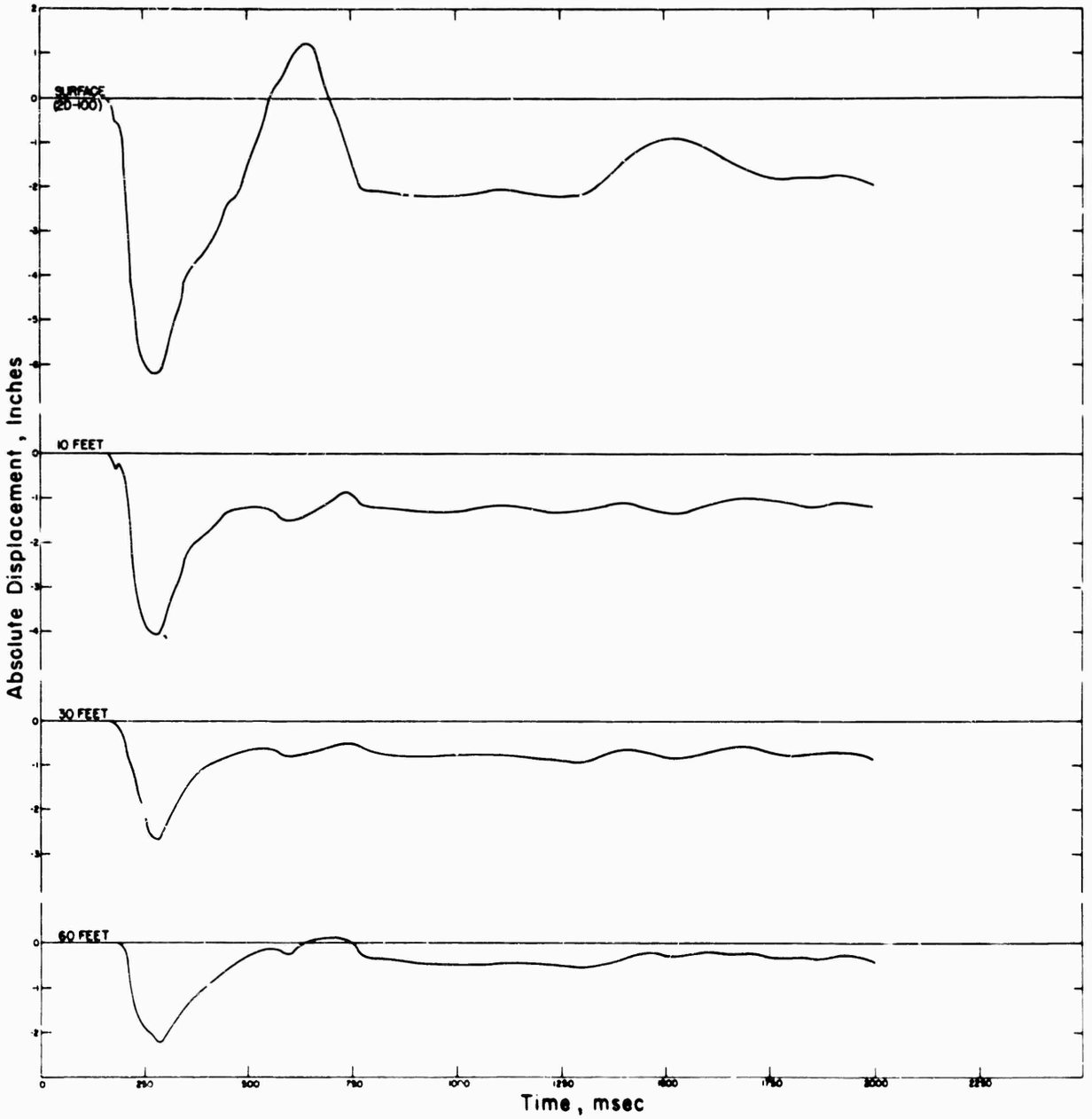

Figure 4.30 Absolute displacement, Station F-1.5-9012.02.

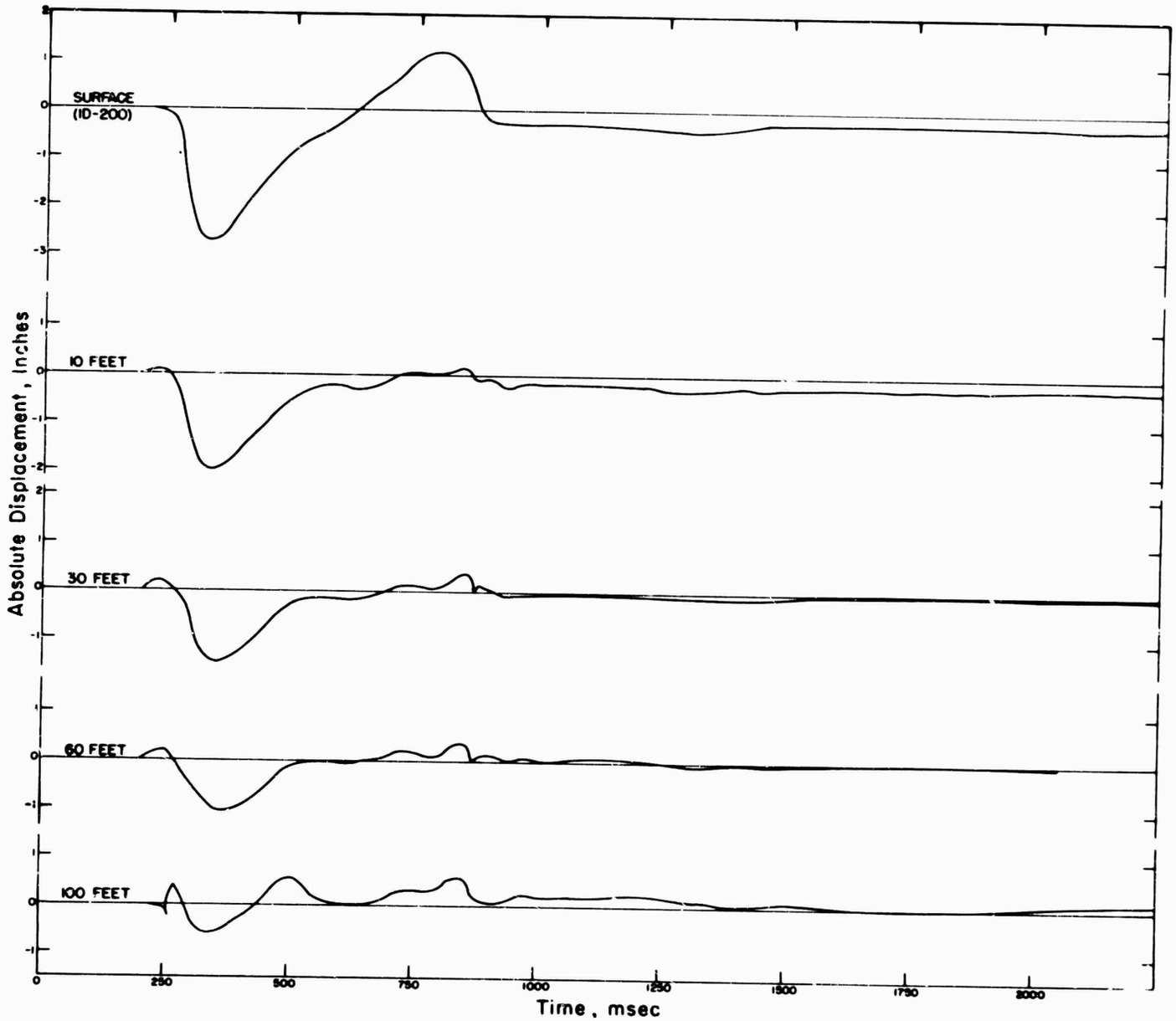

Figure 4.31 Absolute displacement, Station F-1.5-9012.03.

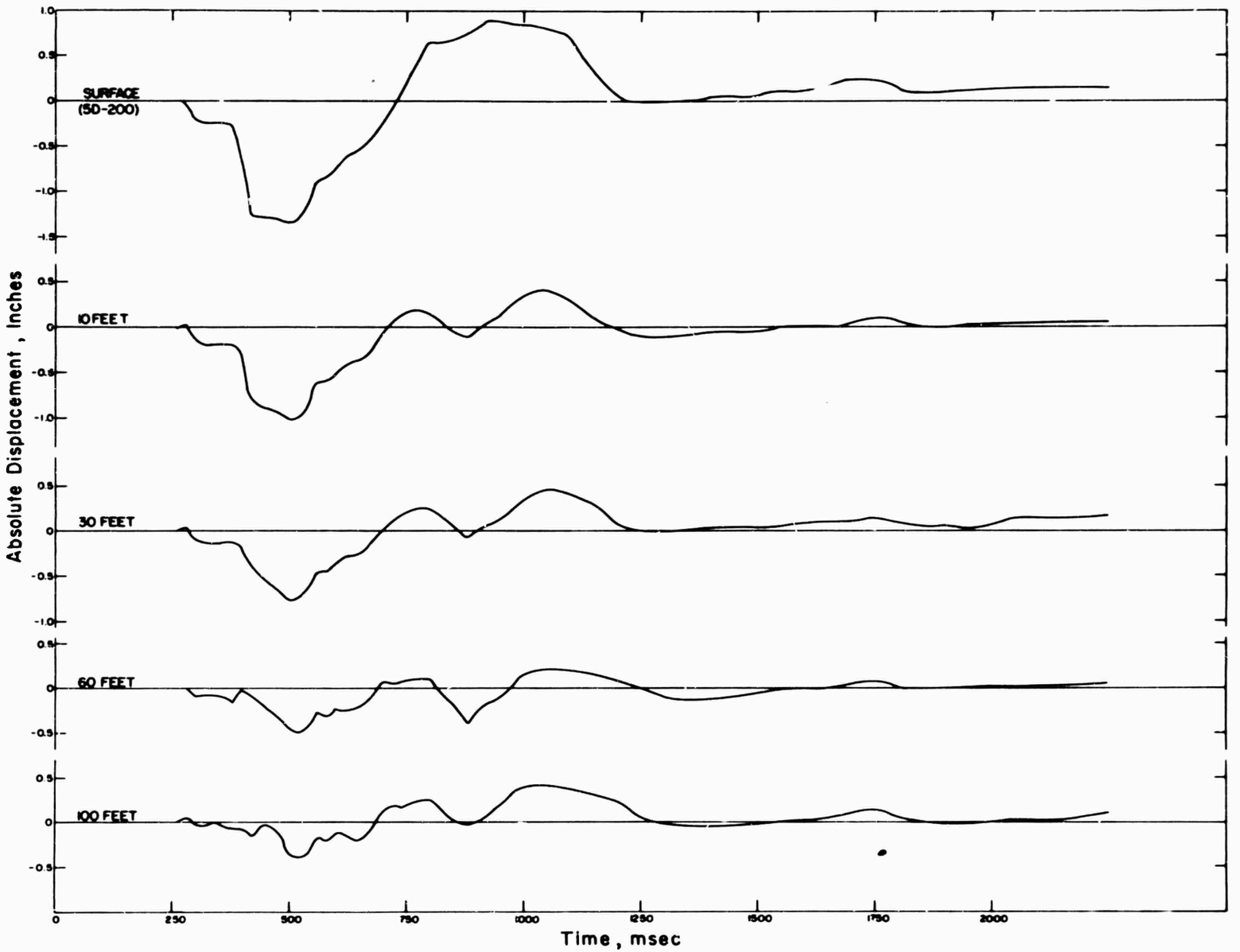

Figure 4.32 Absolute displacement, Station F-1.5-9012.04.

tions of records from other gages of the same group which operated freely. Absolute-displacement data are differences between pairs of records and, for the deeper positions, are small differences between relatively large quantities. Hence, the actual motion must have been much smoother than the curves indicate. Local discontinuities are indicative of the nature and precision of the data, not of ground motion.

TABLE 4.7 PRISCILLA PILE DATA

Gage Number	Ground Range	Depth	Arrival Time	Acceleration		Velocity		Displacement		Set Range	Maximum Signal as Percent of Set Range
				Positive	Negative	Positive	Negative	Positive	Negative		
	ft	ft	msec	g	g	ft/sec	ft/sec	in	in	g	pct
Station F-1.5-9054.01											
2AV-25-0	850	1	177	9.76	17.8	1.7	3.5	—	2.4	99	18
2AV-25-100	850	99	176	0.76	4.50	0.73	3.0	—	3.6	99	5
Stations F-1.5-9054.02 and -9054.03											
1AV-25-0	1,050	1	197	2.69	4.82	—	2.4	—	2.4	99	5
1AV-25-100	1,050	99	234	0.96	2.97	—	1.3	—	1.4	99	3
1AR-25-100	1,050	99	No Data								<0.5
1AV-50-0	1,050	1	199	3.59	5.41	—	2.2	00	2.0	99	6
1AV-50-100	1,050	99	245	1.51	1.98	0.33	1.4	—	1.4	99	2

4.6 MOTION OF CONCRETE PILES

Accelerometers at the foot and head of each pile gave legible records, with the exception of the radial gage at the foot of Station F-1.5-9054.02. Peak values from all of these channels were low, averaging less than 5 percent of set range, but only the radial gage showed no record amplitude as great as 0.5 percent of set range.

TABLE 4.8 BEFORE AND AFTER SURVEYS

Station	Ground Range	Preshot Elevation	Postshot Elevation Difference	
	ft	ft MSL	ft	in
9012.04	1,350 W			
A		3,077.790	+0.005	+0.06
B		3,077.782	+0.002	+0.02
C		3,077.781	+0.005	+0.06
9012.03	1,050 W			
A		3,077.686	−0.034	−0.41
B		3,077.682	−0.035	−0.42
C		3,077.683	−0.038	−0.46
9012.02	850 W			
A		3,077.489	−0.151	−1.81
B		3,077.490	−0.157	−1.98
C		3,077.480	−0.153	−1.84
9012.01	650 W			
A		3,077.082	−0.270	−3.24
B		3,077.083	−0.276	−3.32
C		3,077.084	−0.285	−3.42
9011.05	500 W	3,076.359	−0.452	−5.42
9011.04	400 W	3,076.990	−0.571	−6.86
9011.03	300 W	3,077.177	−0.732	−8.80
9011.02	200 W	3,077.525	−0.757	−9.09
9011.01	100 W	3,077.960	−0.700	−8.40
Ground Zero	0	3,078.080	−1.350	−16.2
9011.06	100 E	3,078.006	−0.751	−9.03
9011.07	200 E	3,078.017	−0.605	−7.26
9011.08	200 E	3,078.225	−0.229	−2.73
9011.09	400 E	3,077.665	−0.265	−3.18
9011.10	500 E	3,076.574	−0.149	−1.79
9011.10A	500 E	3,076.596	—	—
9011.11	650 E	3,077.196	−0.119	−1.43
9011.12	850 E	3,077.368	−0.091	−1.09
9011.13	1,050 E	3,077.628	−0.092	−1.10
9011.14	1,350 E	3,077.827	+0.025	+0.30

Vertical-acceleration records were integrated and corrected velocities were converted to displacement-time data. Curves for all three parameters for each station are presented in Figures 4.33 through 4.36. Data from the measured and computed results are compiled in Table 4.7.

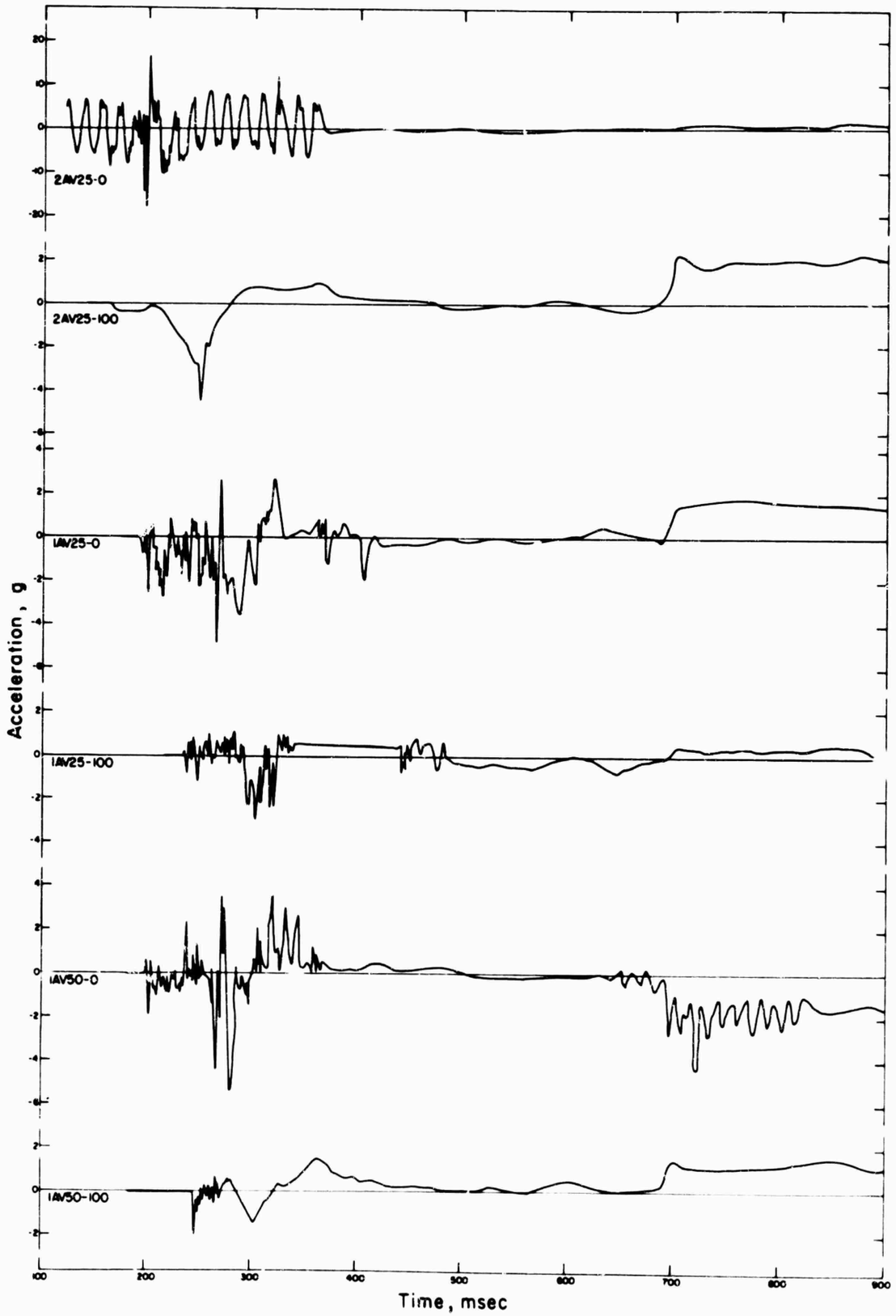

Figure 4.33 Vertical acceleration, Stations F-1.5-9054.01, .02, .03.

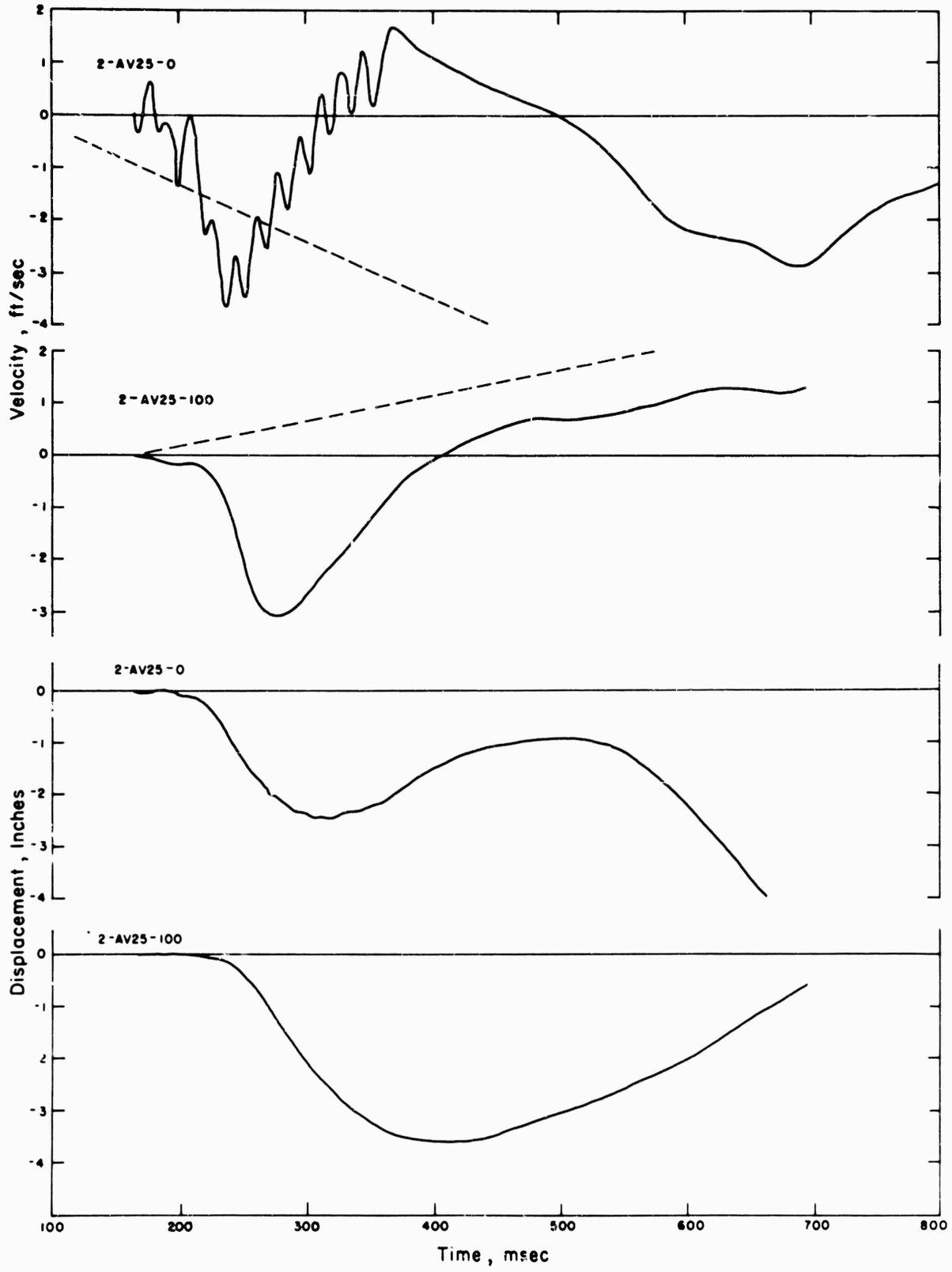

Figure 4.34 Vertical velocity and displacement, Station F-1.5-9054.01.

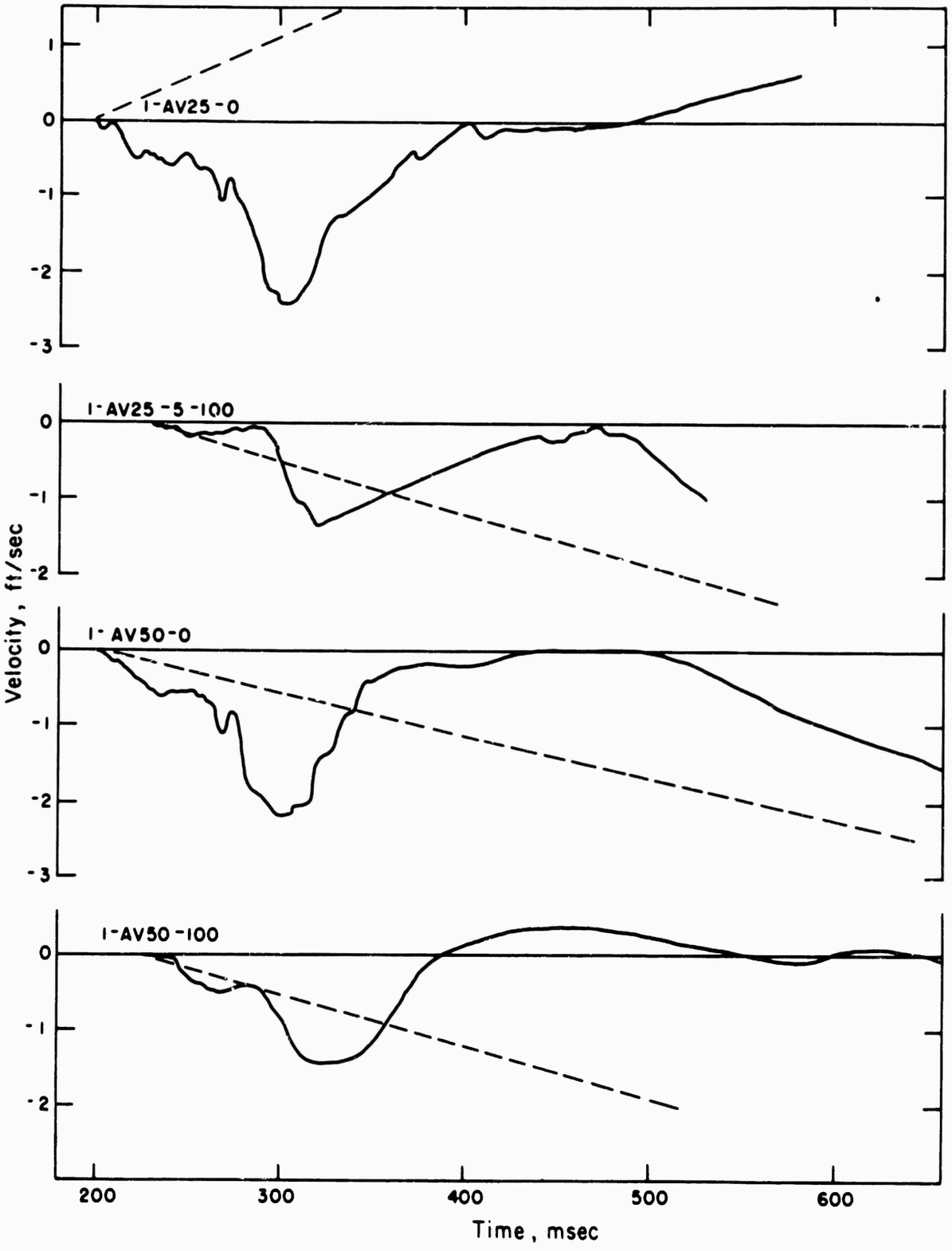

Figure 4.35 Vertical velocity, Stations F-1.5-9054.02, .03.

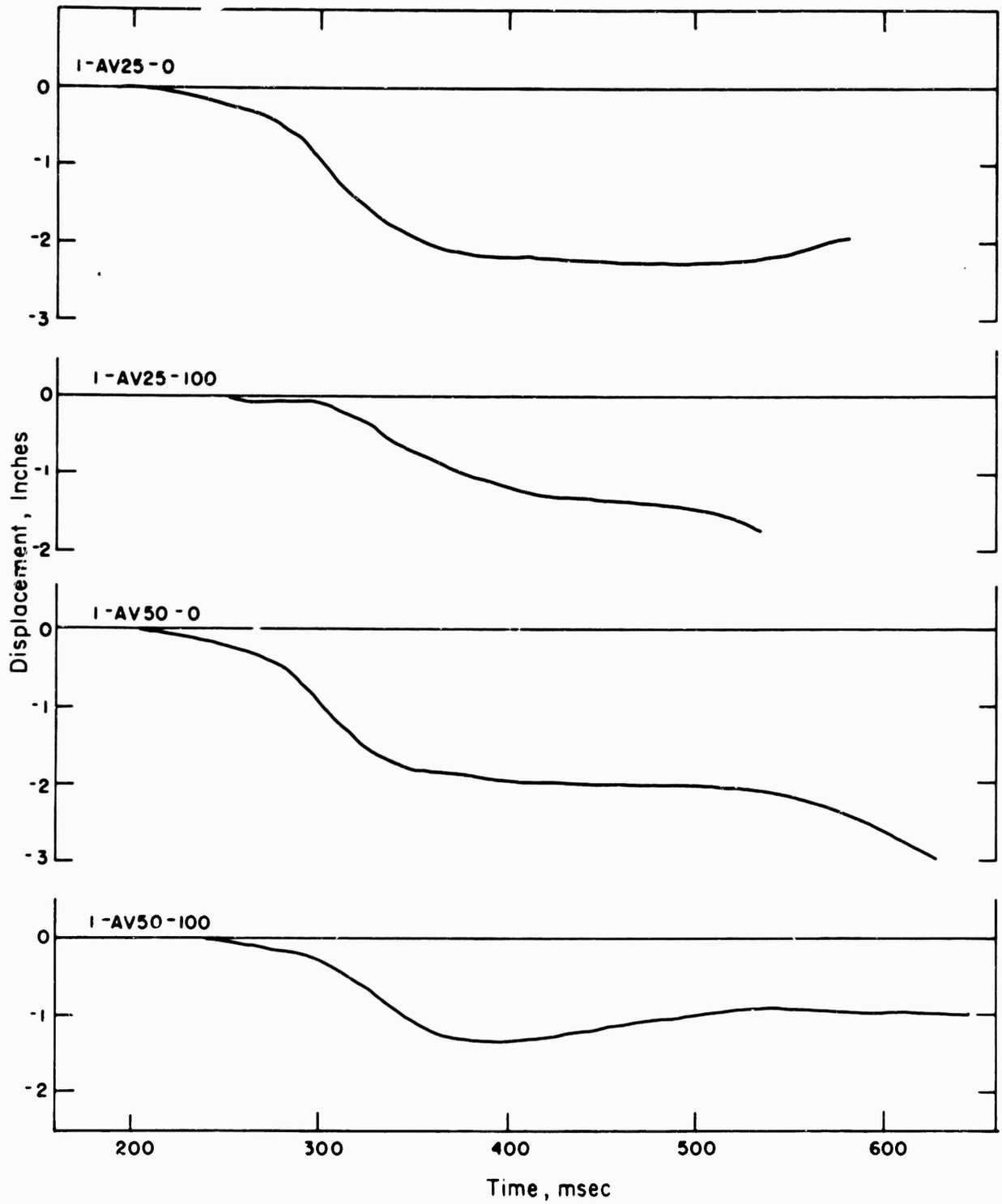

Figure 4.36 Vertical displacement, Stations F-1.5-9054.02, .03.

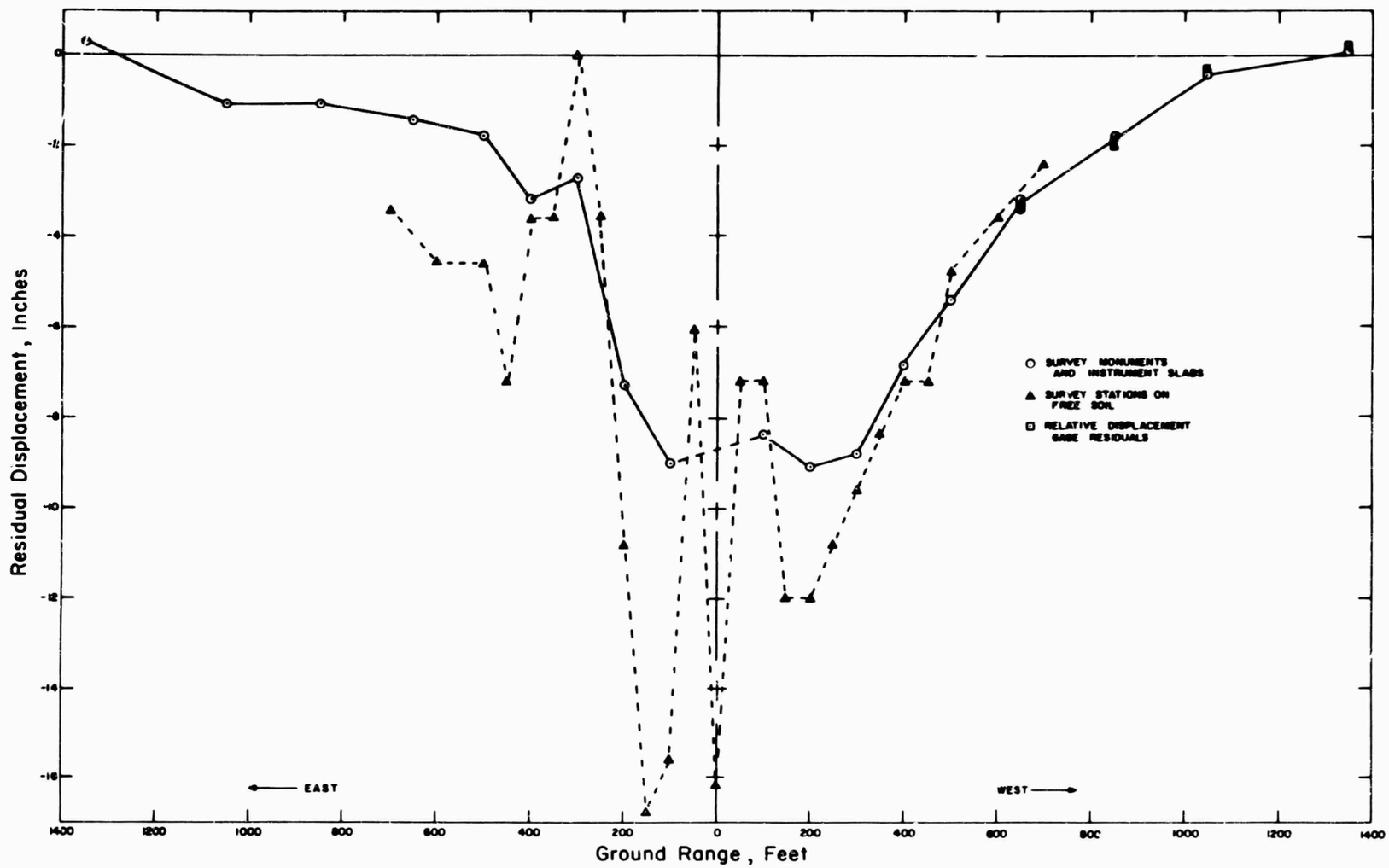

Figure 4.37 Residual displacement on range through ground zero.

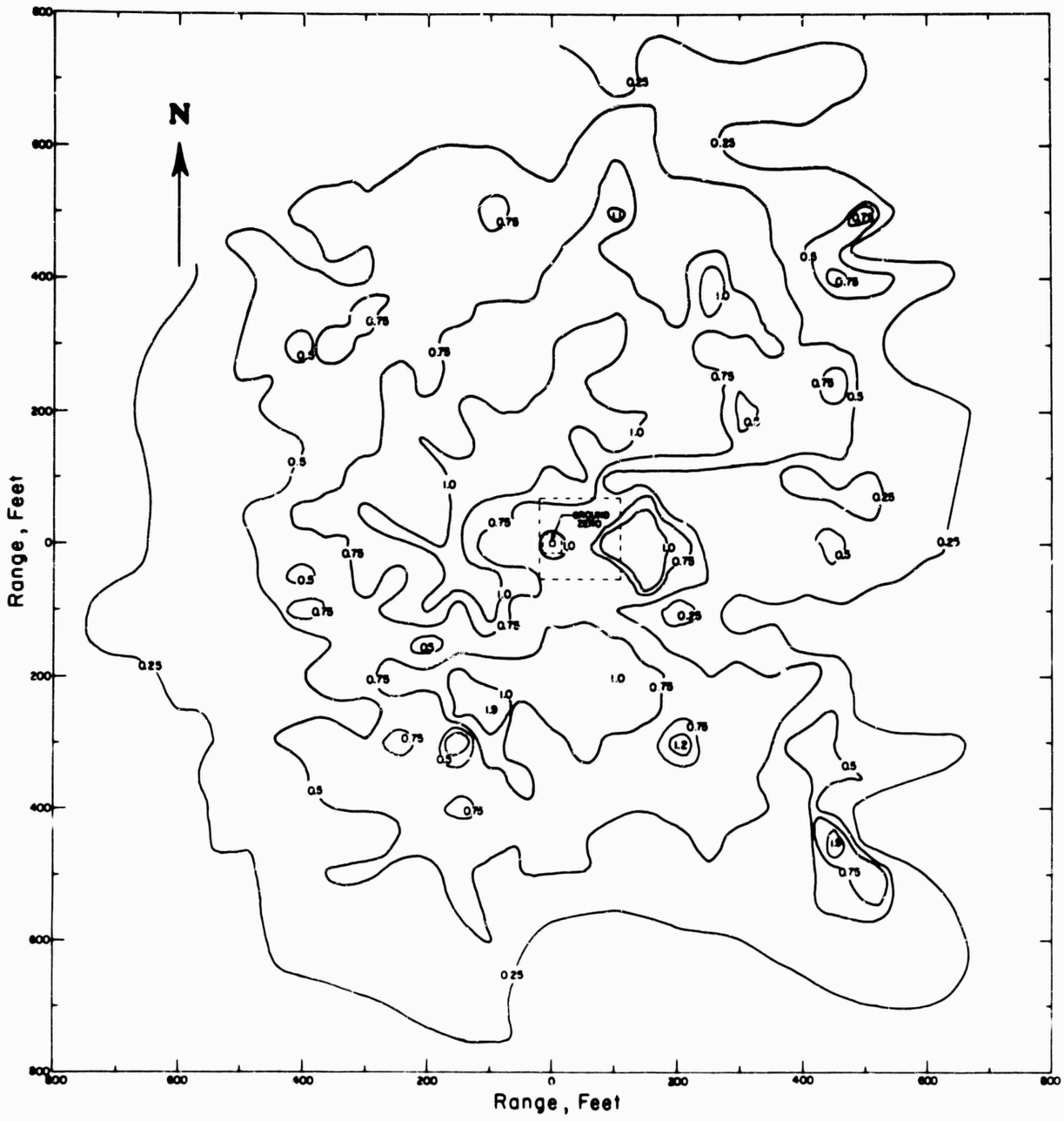

Figure 4.38 Residual displacement map, vicinity of ground zero.

The low precision of these records throws considerable doubt on the accuracy of the integrated parameters. However, the results appear reasonable and are probably valid within a factor of 2.0.

4.7 PERMANENT DISPLACEMENTS

Permanent or residual displacements determined by before and after surveys of the F-1.5-9012 slabs and F-1.5-9011 monuments are presented in Table 4.8 and Figure 4.37, in which residual displacements derived from relative displacement gages are plotted for comparison.

Results of the grid survey in the vicinity of ground zero are presented as contours on a map in Figure 4.38.

Chapter 5
ANALYSIS and DISCUSSION of RESULTS

Analysis of data from an experiment of the type undertaken by Project 1.5 should be directed toward understanding the mechanism of transmission of transient plane waves through soil. The medium, Frenchman Flat lake bed, is fairly uniform both along the blast line and in depth to the region of the deepest gages, although there is a variation of seismic velocity (Reference 10) and of density (Reference 13) with depth. This project has provided good data on absolute displacement as a function of time at four levels of incident overpressure and at five depths within the ground. It has also provided usable acceleration data at the same stations, although this is not so reliable as the displacement data. All this data should provide a reasonable basis for describing transmission of motion downward through the ground.

The analysis consists of a study of variation of peak values of observed and computed parameters with peak incident overpressure and with depth. Peak incident overpressure is chosen as the independent variable, rather than ground or slant range, since it is a characteristic of the forcing function. A nearly identical forcing function could be obtained at different ranges from other explosive energy sources of roughly similar magnitude, and similar response of the ground would be anticipated. Results of this study are also investigated briefly for general consistency with performance of a model medium.

Arrival time and peak values of all measured and computed ground-motion variables are recapitulated in Table 5.1 by stations. Computed velocities and displacements are derived from the acceleration records, and measured displacements are absolute displacements derived from the relative-displacement gages. Arrival times are taken from acceleration data except at the surface, where air-blast data was used.

5.1 FREE-FIELD ACCELERATION

A logarithmic plot of peak vertical accelerations versus depth for each station is shown in Figure 5.1. Points plotted on the 1-foot abscissa are really those observed by surface instruments. These correspond to points on the plotted straight lines at depths of 4 to 6 feet. Actually, metal liners and concrete of the surface slabs extended to depths greater than 3 feet. There is a suggestion, thus, that motion of the rigid slab and liner assembly was controlled by the soil beneath it.

At the three remote stations, the data shows degradation of acceleration peaks inversely as the $^3/_4$ power of depth. At the station subjected to the highest peak load, degradation of peak accelerations was at a rate nearly twice as great. There is no apparent explanation for this sort of change; precision of all measurements is generally lower than desirable, but is probably better than difference in slopes implies. Equations for the curves are included in Figure 5.1 beside each curve.

Examination of peak accelerations as functions of peak incident overpressures and maximum incident impulse intensities shows no consistent simple relationship, probably because peak accelerations are related closely to rates of rise of pressures. The presence of a precursor of varying amplitude and duration, as well as the shape of pressure peaks, must affect particle acceleration notably. Incident overpressure rates of rise are greater at higher pressure stations, as would be expected; but the character of the differences does not suggest the differences between slopes. Rates of rise derived from velocity curves, which can be assumed to approximate roughly rates of rise of vertical stress in the ground, vary with depth in a manner similar

to the depth variation of vertical acceleration, station by station. However, in this particular case, similarity is hardly relevant, since the velocities were derived by integration of acceleration data.

Horizontal radial acceleration data are sparse and of low precision. One complete set and two partial sets of data have been plotted in Figure 5.2. This data fits an exponential relationship reasonably. For the F-1.5-9012.02 and .03 stations an expression of the form

$$a = a_0 e^{-0.02D} \tag{5.1}$$

holds for most of the data. Here a is the peak outward acceleration along the horizontal radius, a_0 is the value of this parameter at the surface, both in g-units, and D is the depth in feet. A

TABLE 5 1 SUMMARY OF GROUND MOTION DATA

Vertical negative is downward. Radial positive is outward.

Depth	Arrival Time	Downward Vertical Components				Outward Radial Components		
		Acceleration, Measured	Velocity, Computed	Displacement, Computed	Displacement, Measured	Acceleration, Measured	Velocity, Computed	Displacement, Computed
ft	msec	g	ft/sec	in	in	g	ft/sec	in
Station F-1 5-9012.01: Overpressure 270 psi; impulse 14 psi-sec.								
0	130	—	—	—	−9.9	—	—	—
10	132	−177	−30.7	−16.8	−7.7	—	—	—
10*	141	−228	−30.4	−16.2	—	—	—	—
30	155	−34.8	−9.0	−4.2	−5.6	—	—	—
60	173	−10.6	−5.13	−3.94	−3.8	—	—	—
100	188	−10.8	−4.32	−4.03	−2.0	4.2	0.80	0.22
200	230	−2.8	−1.58	−1.45	0	—	—	—
Station F-1.5-9012.02: Overpressure 187 psi; impulse 9.5 psi-sec.								
0	163	−45.7	−13.3	−8.76	−6.2	19.9	—	—
10	170	−17.9	−8.45	−4.89	−4.1	16.4	1.28	1.78
30	190	−13.6	−4.37	−2.62	−2.7	9.3	0.63	0.02
60	199	−4.9	−2.99	−3.02	−1.9	5.6	0.92	0.20
100	214	−3.9	−2.21	−1.95	0	2.9	0.92	0.29
Station F-1.5-9012.03: Overpressure 120 psi; impulse 7.8 psi-sec.								
0	197	−27.0	−5.66	−6.13	−2.8	8.5	—	—
10	209	−8.8	−5.33	−6.55	−2.0	—	—	—
10*	210	−8.4	−5.66	−7.86	—	—	—	—
30	—	—	—	—	−1.5	—	—	—
60	233	−1.9	−3.61	−7.20	−1.1	2.73	0.85	0.44
100	246	—	—	—	−0.6	1.9	0.75	0.26
Station F-1.5-9012.04: Overpressure 59 psi; impulse 6.9 psi-sec.								
0	268	−9.1	−3.43	−3.69	−1.4	1.1	—	—
10	271	−5.4	−2.47	−2.39	−1.0	2.5	1.90	4.30
30	284	−2.2	−1.52	−2.07	−0.8	—	—	—
60	298	−1.8	−1.35	−1.97	−0.5	1.7	1.45	0.79
100	312	−1.0	−1.13	−1.54	−0.4	1.4	1.4	0.87

* Indicates duplicate gages offset 10 feet laterally from station

similar exponential equation seems to hold for data from Station F-1.5-9012.02, but the coefficient of D is about 0.008, rather than 0.02.

Again, there is no consistent relationship between radial acceleration and incident overpressures or impulses beyond the very general one that at similar depths accelerations vary directly with peak overpressures.

5.2 PARTICLE VELOCITIES

Peak velocities derived from integrated vertical acceleration data (Table 5.1) decrease with depth and with incident peak overpressure. A logarithmic plot of velocity versus depth, Figure 5.3, indicates that particle velocity falls off inversely with varying powers of the depth.

The equations shown on the curves in Figure 5.3 indicate a consistent decrease in the inverse power of depth from −1 for the high overpressure station. Data from the 120-psi station (F-1.5-9012.03) is limited, and the slope indicated is unreliable. These relationships, like all empirically derived power laws, must be applied with caution. Interpolation within the range of the

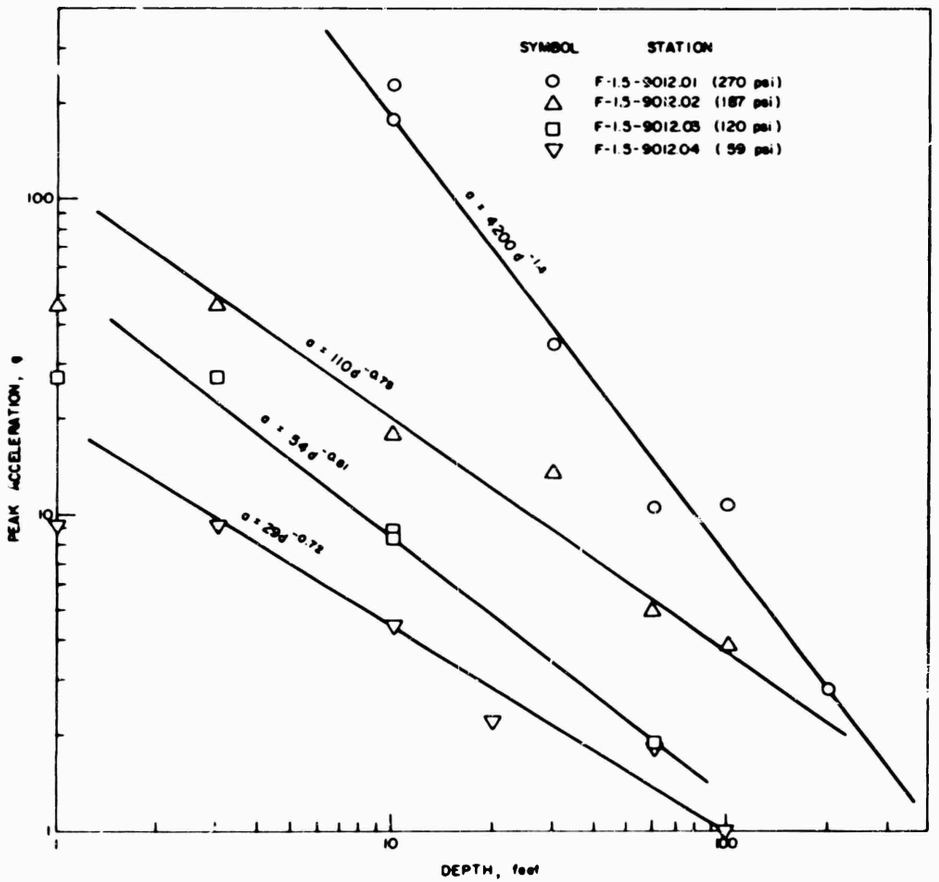

Figure 5.1 Peak vertical acceleration attenuation.

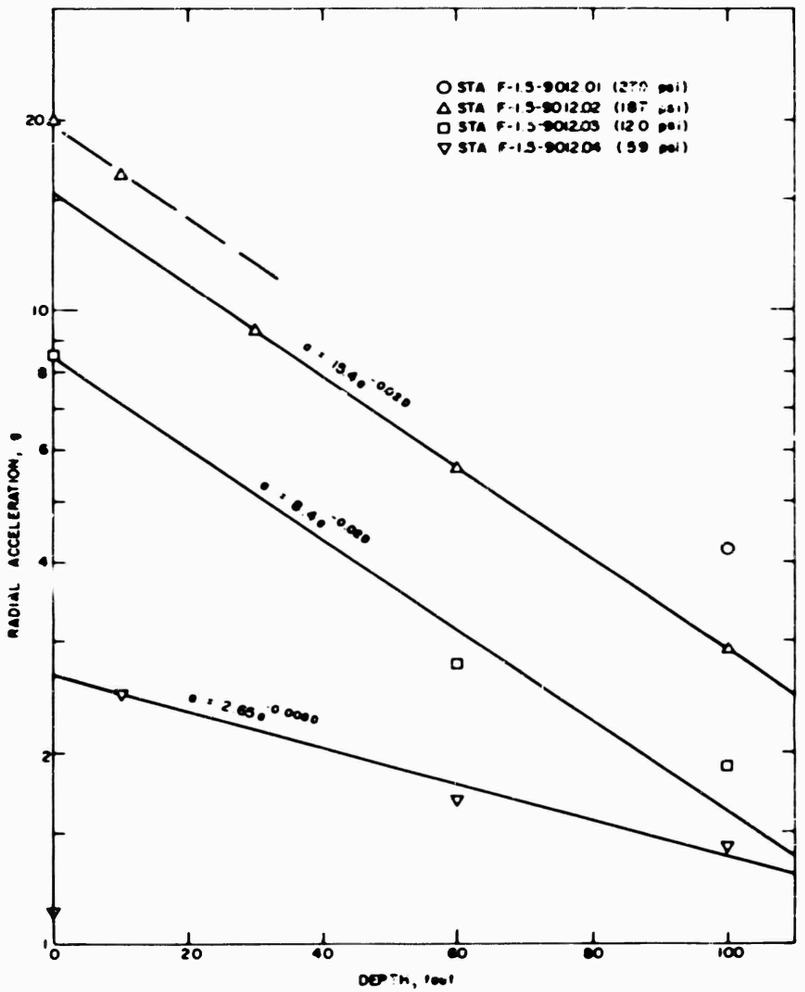

Figure 5.2 Peak radial acceleration attenuation.

data is reasonably safe; extrapolation to appreciably greater or lesser depths may be misleading. For example, it is reasonable, within the reliability of the data, to expect a peak velocity of about –5.6 ft/sec and at a depth of 20 feet where loading was similar to that at Station F-1.5-9012.02, but extrapolation to 32 ft/sec at 1 foot in depth, or 0.59 ft/sec at 1,000 feet in depth, should be regarded with considerable skepticism.

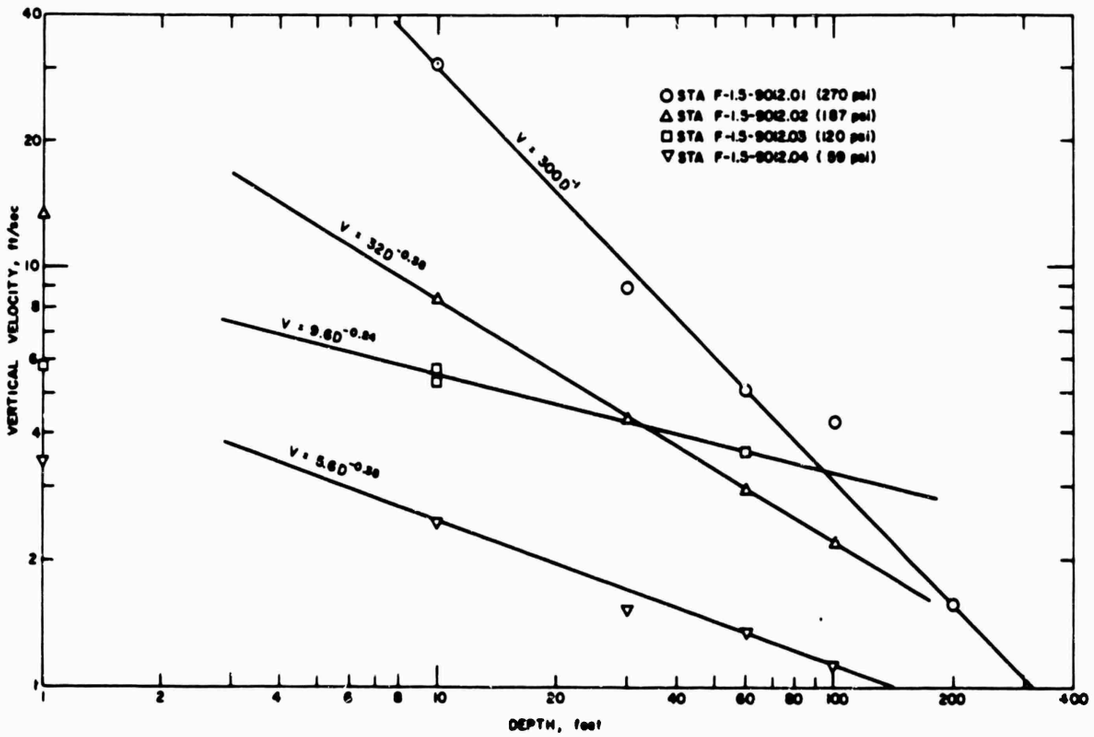

Figure 5.3 Peak vertical particle velocity attenuation.

There is a certain degree of doubt associated with velocities derived from integration of acceleration data involving appreciable time spans and corrections of zero lines. To examine reliability, a rough comparison check of peak vertical velocities derived from the Project 1.5 free-field accelerometers was made against particle velocities derived from slopes of absolute-

TABLE 5.2 DISPLACEMENT DATA, STATION F-1.5-9012.01

Depth	Peak Velocities in ft/sec		
	Integrated Acceleration	Differentiated Displacement	
		10-msec Intervals	2-msec Intervals
ft			
0	—	19.3	25
10	30.7 and 30.4	18.3	27
30	9.0	8.75	9.2

displacement curves. Displacement-curve slopes were obtained over 10-msec intervals (the data-conversion interval). Peak velocity values from displacement data were consistently lower than those from accelerations. However, three sets of displacement data were recomputed by taking slopes at 2-msec intervals by interpolation. The difference between peak velocities from acceleration and displacement became less, as indicated in Table 5.2.

It is of interest to inquire into the range of vertical earth stress suggested by particle velocity data. The nature of the driving force, incident air blast on the ground surface, and the overstress produced by the shock wave in earth, i.e., the excess of stress above the ambient

geostatic pressure, should correspond roughly to pressures derived from conservation of energy across the front in shock wave theory; that is, $\sigma = \rho_0 Vc$, where σ is stress, ρ_0 ambient density, V particle velocity, and c phase velocity of the propagating wave. The latter is not properly represented by seismic velocity, as usually determined from first arrivals, but by the phase velocity of later features of the wave such as peaks.

Peak particle velocities (Table 5.1) multiplied by approriate values of ρ_0 and c should, then, give reasonable magnitudes for peak stresses. Densities were observed for undisturbed samples of soil by Project 3.8 at various depths in a boring 200 feet deep. Density values (solid points) appropriate to accelerometer levels were chosen from these data as plotted in Figure 5.4. In the same figure a seismic velocity profile observed by Project 1.4 (Reference 10) is plotted. These are first arrival velocity data. Sufficient data from Project 1.5 was not available from which phase velocities of peaks could be directly deduced. However, nineteen observations from this project and from Project 1.4 of Operation Upshot-Knothole (Reference 4) provided a basis for deriving an average ratio, 0.524, of phase-to-seismic velocities in Frenchman Flat soil. Phase velocities at each depth appropriate to gage positions (except surface gages) were obtained by application of this ratio to propagation velocities (solid points) taken from the curve in Figure 5.4. Near the surface, where rise times are short, phase velocities will differ little from seismic velocities, which are characteristically low. Therefore, stresses for near-surface positions were computed with propagation velocity of 1,000 ft/sec.

Stresses arising from peak particle velocities are plotted in Figure 5.5 as a function of depth for each F-1.5-9012 station. Analysis of the plotted data shows attenuation of stress with depth differing only slightly from velocity attenuation, which is likely, considering the method used for deriving the stresses. The curves for two of the sets of data are obviously questionable. At Station F-1.5-9012.01 the peak incident overpressure was 270 psi; the computed vertical stress at the 10-foot depth is about 600 psi. Particle velocity here at the 10-foot depth also appears high, but no reasonable correction is apparent in derivation of the velocity data. Peak velocity found by differentiation of absolute-displacement data at 10 feet is about 0.6 of that derived from acceleration data. This would reduce the corresponding peak stress to about 350 psi.

Peak stresses were computed for the three stations for which surface acceleration records could be integrated. These results, tabulated below, compare reasonably with the observed peak overpressures.

Station	Overpressure	Computed Stress
	psi	psi
F-1.5-9012.02	187	234
F-1.5-9012.03	120	103
F-1.5-9012.04	59	60

The implication of this analysis is that within the depth range between 10 and 100 feet vertical stress induced by incident air blast of from 200 to 60 psi may be attenuated roughly proportional to the square root or cube root of the depth. Above 10 feet attenuation is much less rapid, perhaps closer to the tenth root of depth. It is, of course, not clear that fractional-power-law attenuation is a proper description of the situation, which is probably more complicated; but velocity and stress data from Project 1.5 seem to correspond more nearly to power-law attenuation than to exponential decay.

Horizontal radial velocities stemming from acceleration data are few (Table 5.1), and perhaps not very meaningful, except as they may be compared with corresponding vertical velocities. In general, the peak radial velocities are less than vertical by a factor of two to four, except at Station F-1.5-9012.04 (59 psi) where they are roughly the same or slightly greater. Radial velocities tend to decrease only slightly with depth. In a few cases (see curves of Figures 4.7, 4.12, 4.18, and 4.23) inward peaks appear to exceed outward peaks. However, the necessity for adjustments of zeros in integration makes small differences in peaks question-

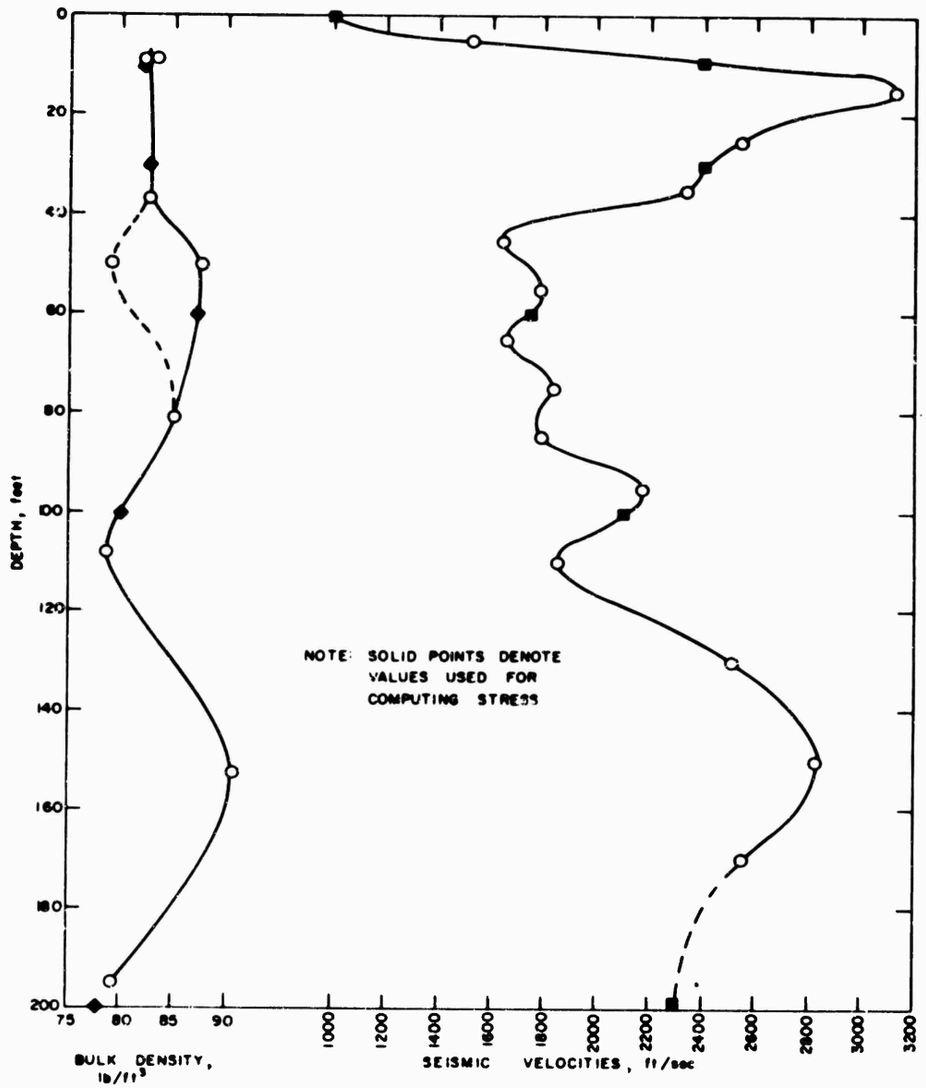

Figure 5.4 Soil density and seismic velocity profiles for Frenchman Flat.

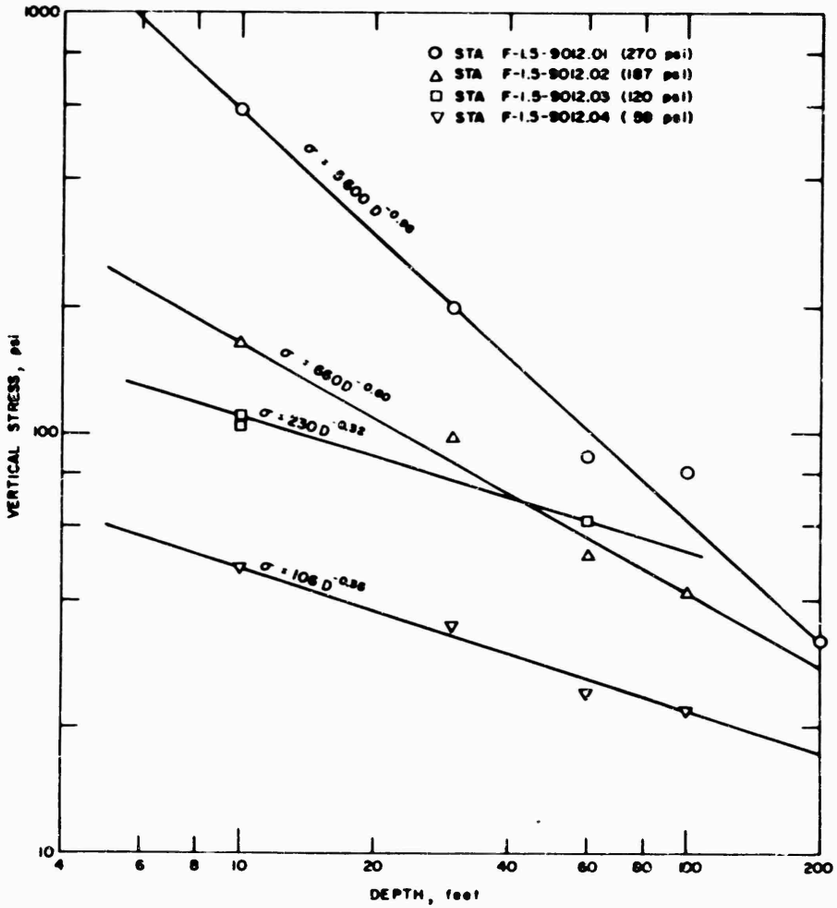

Figure 5.5 Vertical stress attenuation.

able. Perhaps only peak-to-peak magnitudes form valid data where precision of the basic acceleration records is low, as in the present case.

5.3 PARTICLE DISPLACEMENTS

"Absolute" displacements derived from differences between relative-displacement data represent particle displacements at the specified depths (sixth column of Table 5.1 and Figures 4.29 through 4.32). Data from the referenced figures were converted to families of deflection contours on maps of peak incident overpressure versus time for five depths, including the

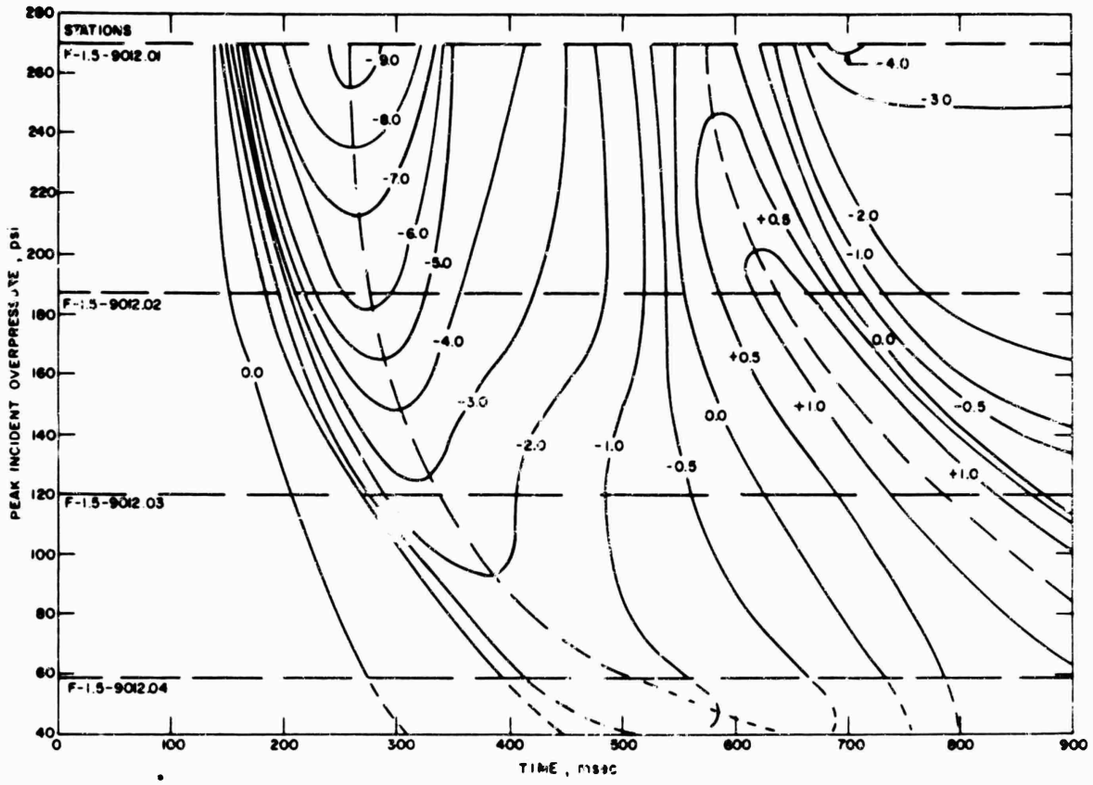

Figure 5.6 Deflection contours for incident overpressure versus time, surface.

surface, (Figures 5.6 through 5.10) and on maps of depth versus time (Figures 5.11 through 5.14) at the four F-1.5-9012 stations. These curves are useful for visualizing the manner and rate of variation of the displacement-time history of soil down to 100 feet as a function of load history. They should provide an effective means for correlating theoretical studies involving nonlinear soil models under air-blast loading.

A contour map of peak absolute displacements as a function of depth and peak overpressure is presented in Figure 5.15. The peak overpressure was again chosen as the independent variable, rather than ground range, since it is the more significant characteristic of the displacement forcing function. The contours indicate a depressed bowl, the sides of which increase in slope with decreasing peak displacements. There is evidence of a slope inversion in the 2- through 5-inch contours, which correspond roughly in depth to the region of high seismic velocity observed by Project 1.4 (Figure 5.4) between 10 and 30 feet.

Logarithms of peak absolute displacements are plotted versus depth in Figure 5.16. Data points for each station fall very close to a straight line except for the surface point, which is consistently high. All lines as plotted have equal slopes. Displacement attenuation follows an exponential law of the form

$$\delta = \delta_0 e^{-0.017D} \qquad (5.2)$$

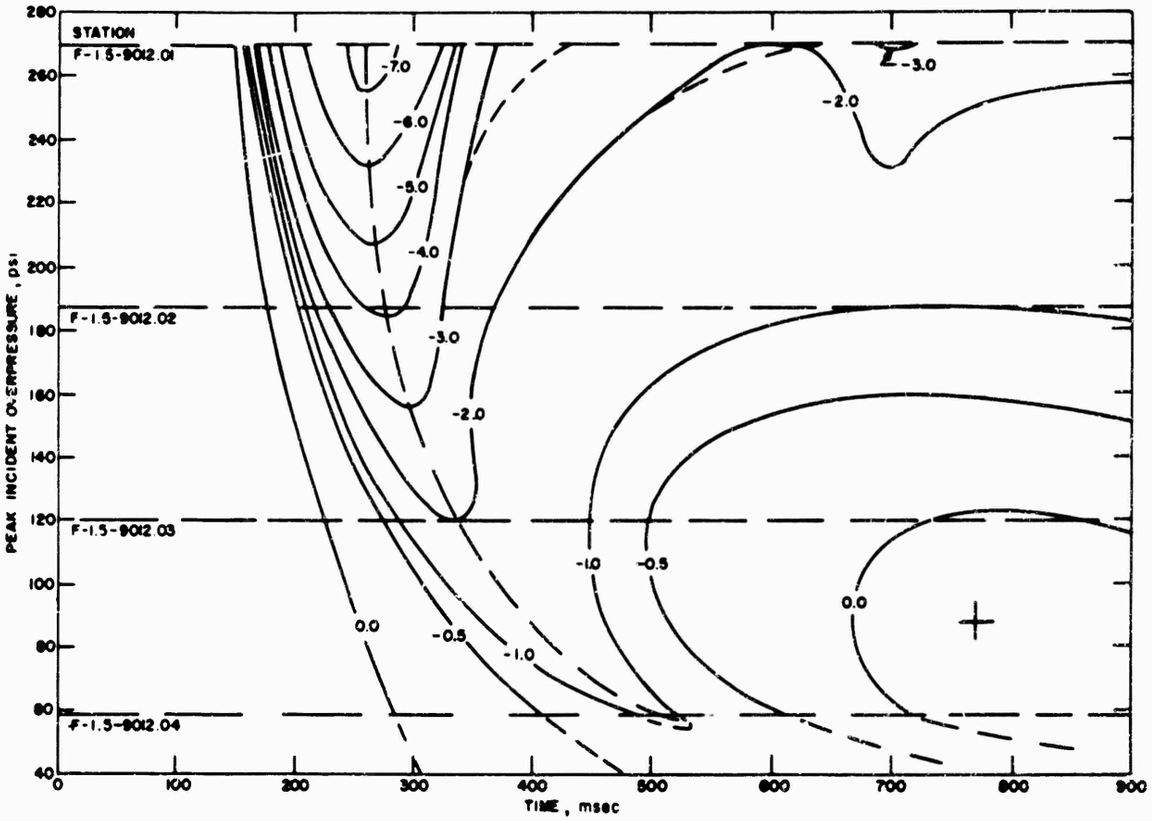

Figure 5.7 Deflection contours for incident overpressure versus time, 10-foot depth.

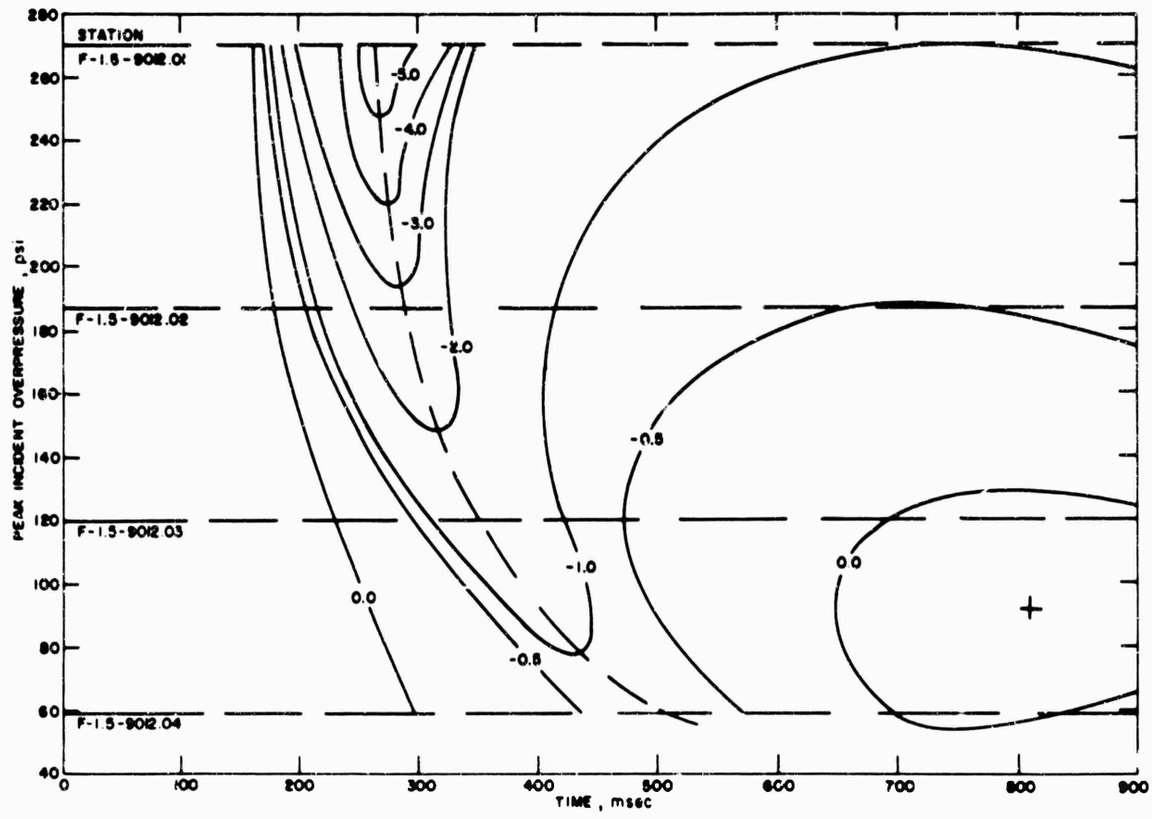

Figure 5.8 Deflection contours for incident overpressure versus time, 30-foot depth.

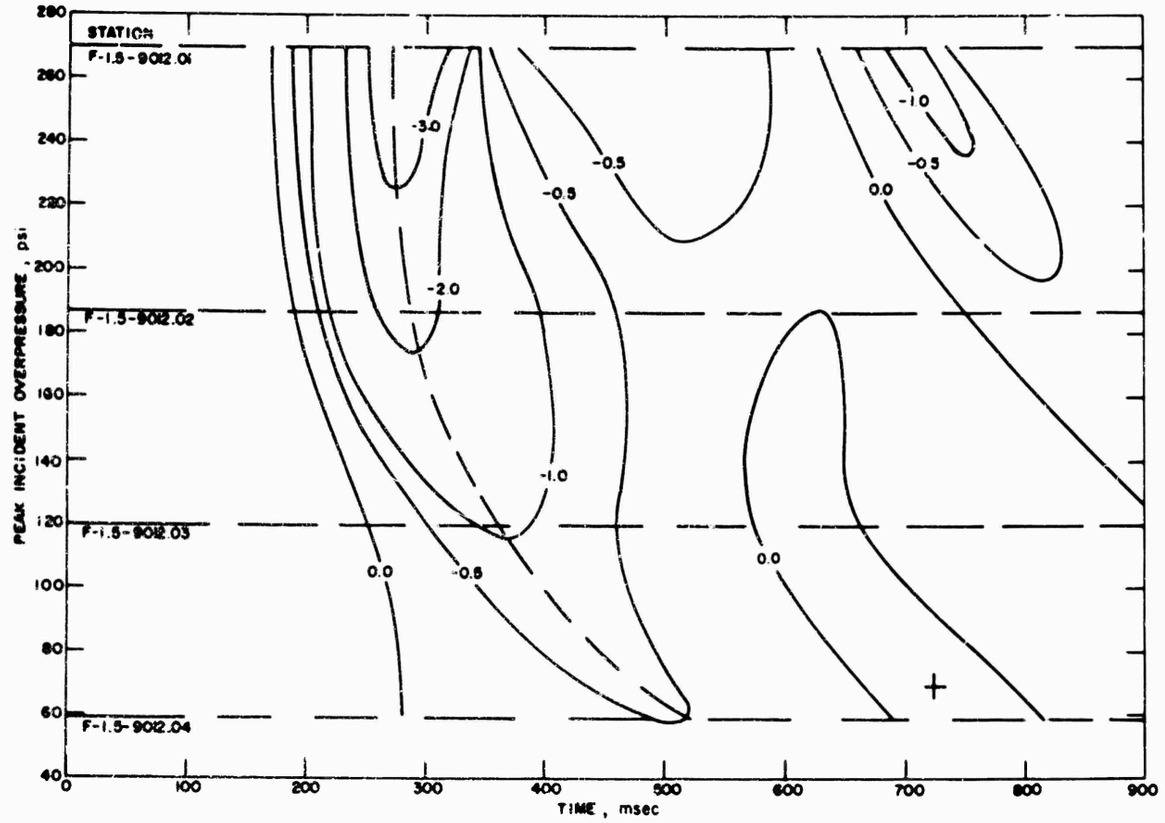

Figure 5.9 Deflection contours for incident overpressure versus time, 60-foot depth.

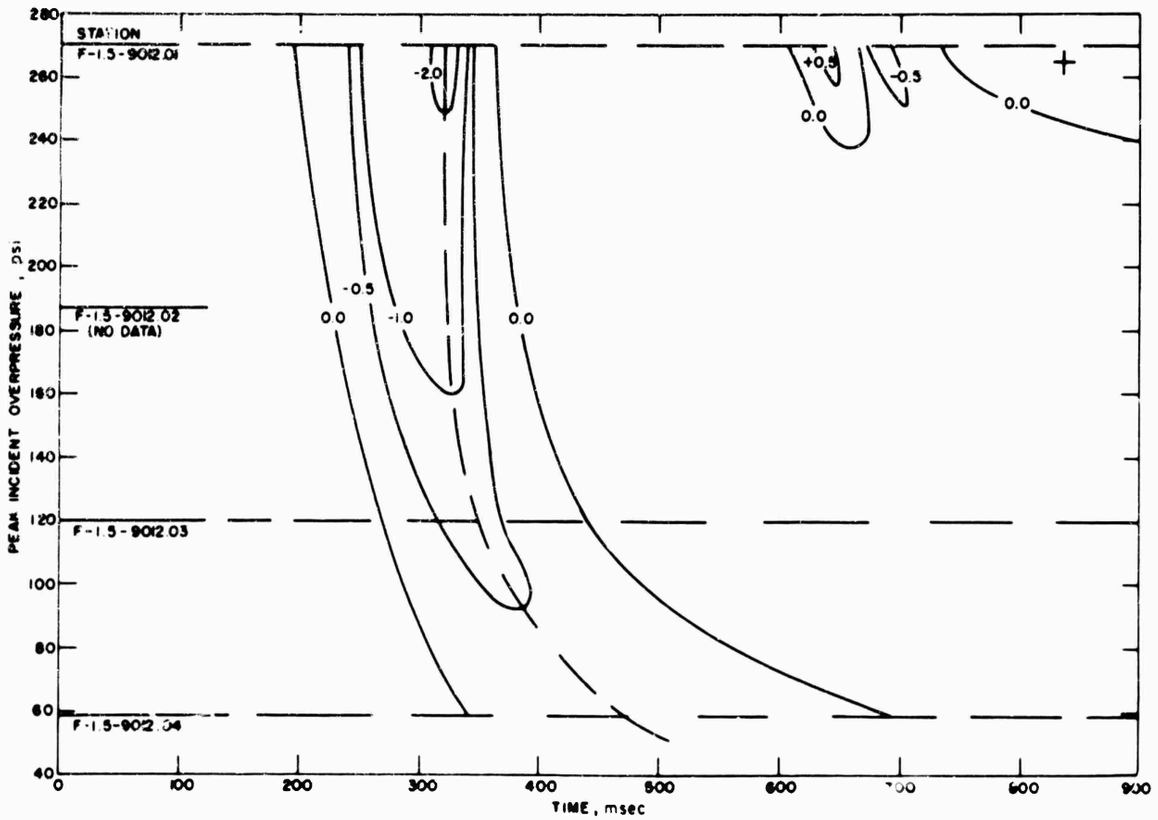

Figure 5.10 Deflection contours for incident overpressure versus time, 100-foot depth.

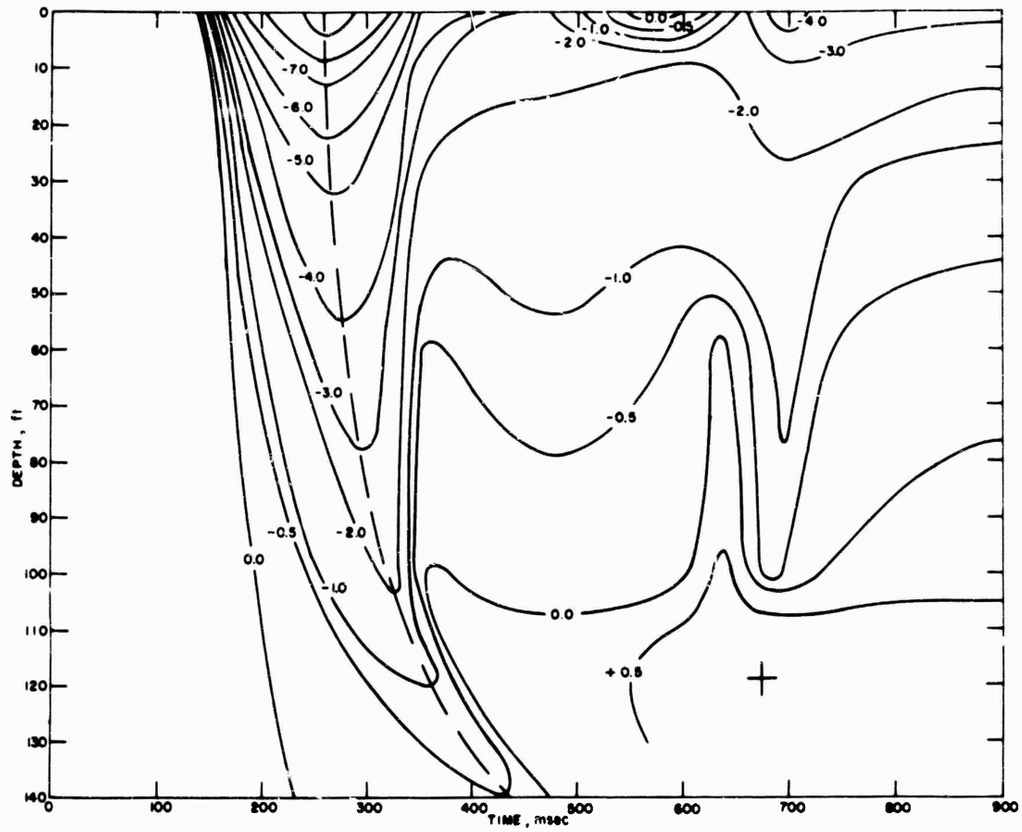

Figure 5.11 Deflection contours for depth versus time, Station F-1.5-9012.01.

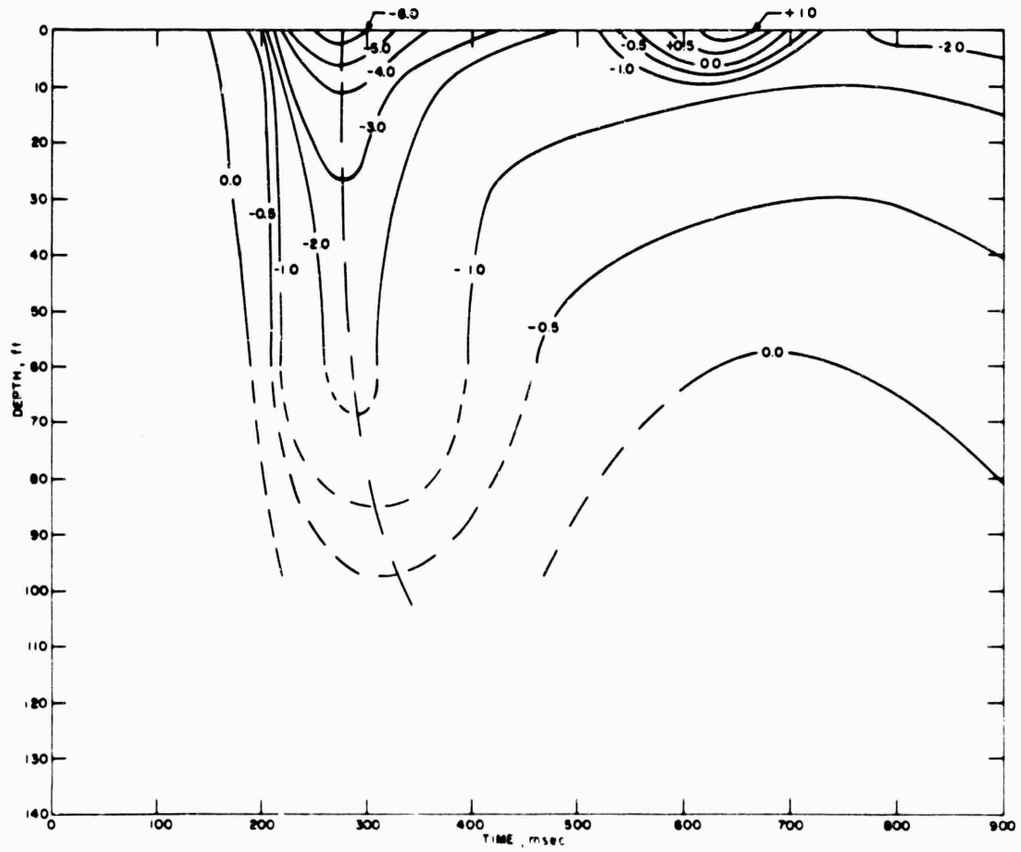

Figure 5.12 Deflection contours for depth versus time, Station F-1.5-9012.02.

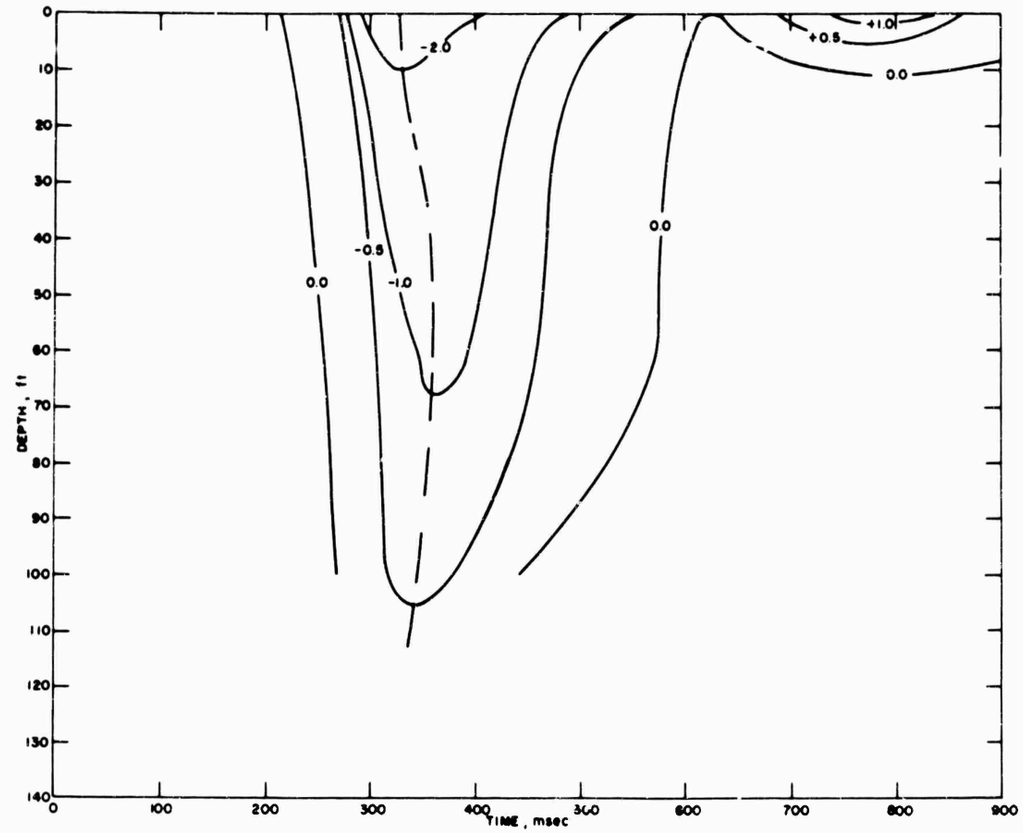

Figure 5.13 Deflection contours for depth versus time, Station F-1.5-9012.03.

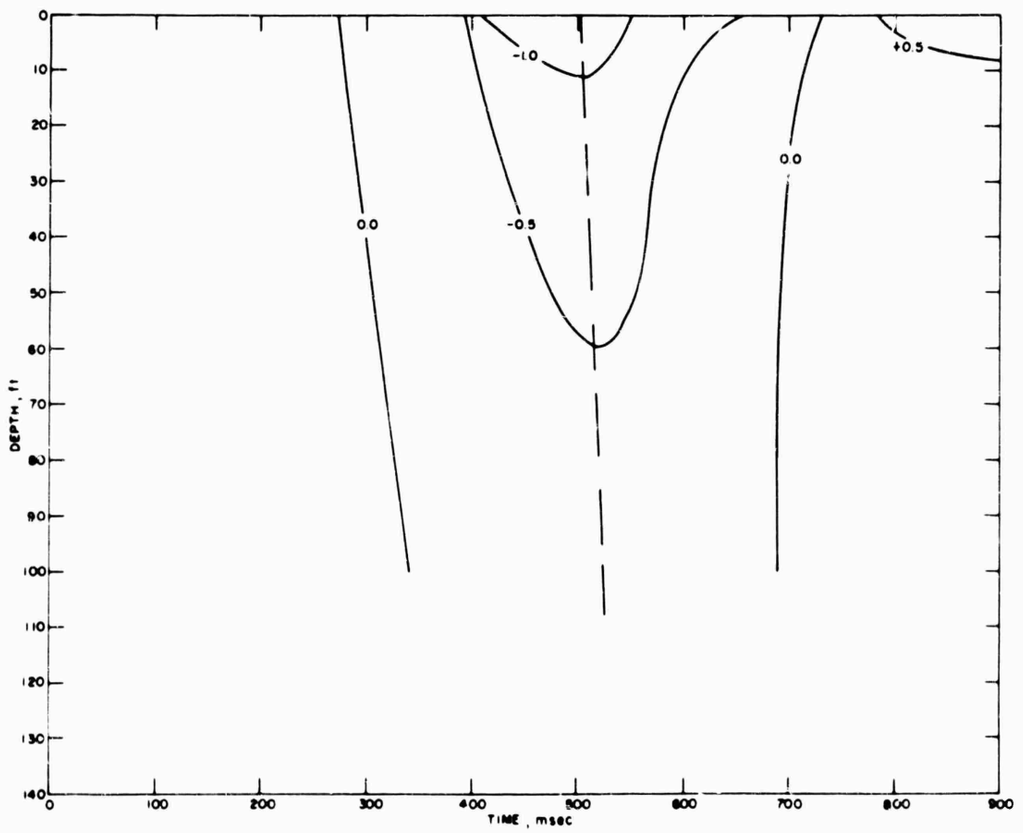

Figure 5.14 Deflection contours for depth versus time, Station F-1.5-9012.04.

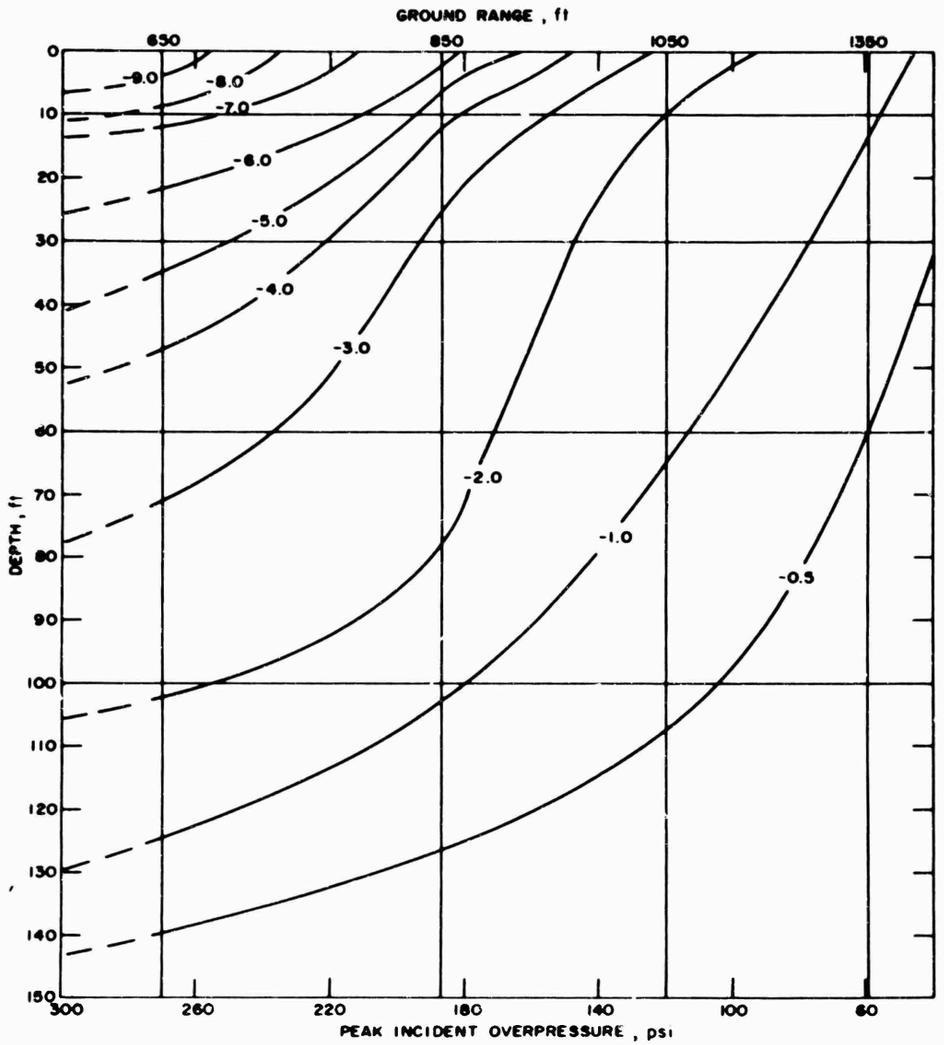

Figure 5.15 Peak displacement contours for depth versus incident overpressure.

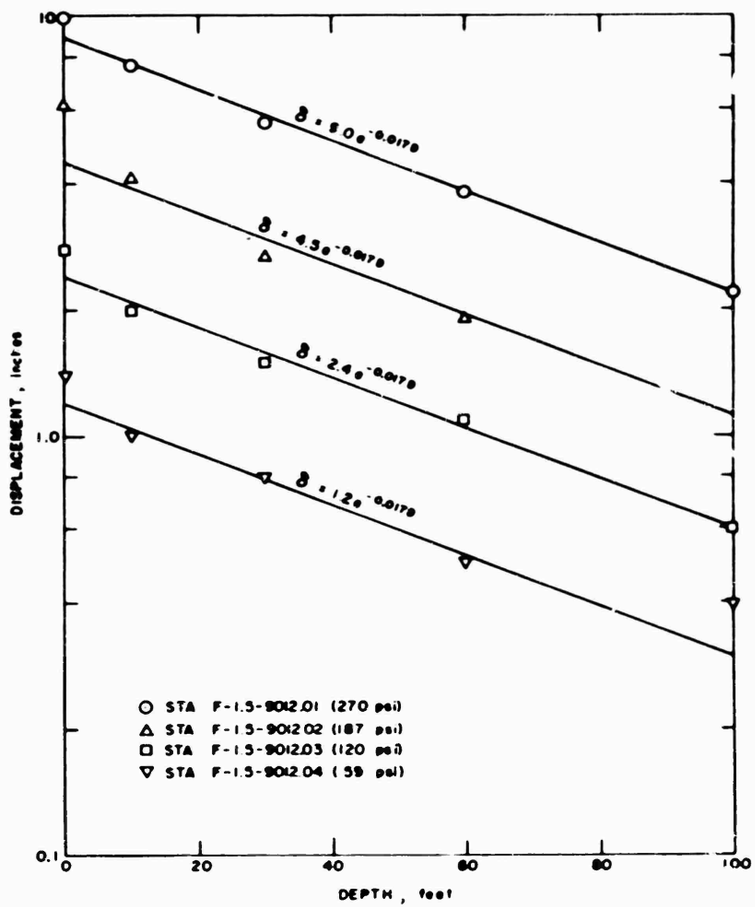

Figure 5.16 Peak displacement versus depth.

where δ is the absolute particle displacement in inches, δ_0 is the displacement at the surface (represented here by intercept of the straight line with the zero-depth axis), and D is the depth in feet. The greater observed surface displacement, as compared to the δ_0 values, results from characteristically greater compressibility of near-surface soil. The discrepancy at the surface ranges from as little as 0.2 inch to 1.6 inches. No other departure of a data point from the plotted lines exceeds 0.3 inch.

Use of displacement-depth data as a means of checking theoretical analyses should be fruitful. A few studies, based principally on linear elastic models, have been made for motion induced by incident air blast on the ground. Of these, one made by P. Chadwick of the United Kingdom Atomic Weapons Research Establishment (Reference 14) has been chosen for a very rough check. Chadwick assumes an overpressure wave, $\Delta p(t)$, of the Friedlander type passing over the ground surface at velocity v in the supersonic region where v is greater than both the compression wave propagation velocity v_p and the torsional or shear wave velocity v_s in the soil. The vertical displacement, u_y, derived from Chadwick's treatment has the form

$$u_y = -\frac{A}{v\tau} e^a \left[m_1 e^{-m_1 b} - \frac{1}{m_2} e^{-m_2 b} \right] \qquad (5.3)$$

where A is a parametric coefficient, τ the positive phase duration of Δp, and the parameters m_1, m_2, a, and b are defined by $-m_1^2 = 1 - (v^2/v_p^2)$, $-m_2^2 = 1 - (v^2/v_s^2)$, $a = x/v\tau$, $b = y/v\tau$, and the coordinates x and y are horizontal and vertical, respectively.

The portions of Chadwick's vertical displacement solution of particular interest to a rough check of data from Shot Priscilla is the exponential expression involving b. The first, $e^{-m_1 b}$, differs only slightly from $e^{-m_2 b}$, since v_s is generally about 0.6 v_p. Substitution of pertinent values for the velocities and positive-phase duration of the Priscilla environment shows that u_y, equivalent to δ of Equation 5.2, should vary approximately as $e^{-0.002y}$. But this is only about an eigth of the corresponding exponential, $e^{-0.017D}$, found experimentally. This discrepancy can be accounted for at least in part, as deviation of natural soil from the linearly elastic characteristics assumed in the theoretical approach. Whether this accounting is sufficient for the factor of eight is not presently clear, however. Dissipative phenomena (such as viscosity) that are characteristic of natural soils and irreversible changes in volume occurring in consolidation of porous media certainly could be expected to increase the coefficient of the depth coordinate in Chadwick's solution to an appreciable degree.

A more-rigorous theoretical approach (of the type suggested by Sauer and Brenner, Reference 15) should prove valuable. Results of such studies could be compared with the displacement results of Project 1.5 for verification. Significance of soil properties of the Frenchman Flat material to air-blast-induced motion and (by implication, at least) significant properties of other soils for correlation of load studies might thus be established on a firmer basis than exists at present.

5.4 MOTION OF RIGID COLUMNS

The vertical underground reinforced-concrete columns (piles) subjected to air-blast loading on the surface at 187- and 120-psi peak overpressure ranges showed accelerations that differed from free-field acceleration peaks by a factor of from three to five at the surface, but were of comparable magnitude at the lower end, which was about 100 feet deep (Tables 4.4 and 4.7). Downward velocities of the columns, on the other hand, tend to be lower than free field at the surface, but higher at the bottom (Tables 5.1 and 4.7). Differences between the top and bottom of each column is less than the precision of the data (less than a factor of two), so the columns may be considered to have moved essentially as rigid rods. Column displacements, top and bottom, (Tables 5.1 and 4.7) are also nearly the same; certainly differences are within precision of the computations. Free-field peak velocities and displacements differ by factors of three or more between the surface and 100 feet deep, but deep velocities and displacements of both columns and free-field gages are of comparable size, column data being the larger.

These results imply that a long vertical underground structure is constrained in its motion more by its reaction with the ground at its base than is a similar column of soil.

Transit times through 98 feet of rigid column derived from Table 4.7 are comparable to those through 100 feet of soil. This situation is inconsistent with the expected higher transmission velocity of concrete. However, the signal transmitted directly down the column should have been relatively weak and high set ranges of the accelerometers in the columns (99 g) could not resolve the weak direct signal. They could, however, resolve the much-stronger signal derived from energy transmitted through the surrounding soil and coupled to the lower portion of the column. Transit times for peak velocities through the concrete columns are less than half the transit times in surrounding soil and are more consistent with anticipated relative propagation conditions.

Chapter 6
CONCLUSIONS and RECOMMENDATIONS

6.1 CONCLUSIONS

Results of measurements of soil reaction to air-blast loading as a function of depth and incident overpressure are more significant than preliminary analysis suggested. Absolute displacements taken from data considered to be reliable within normal calibration and recording error are internally consistent and agree within reasonable limits with an approximate theoretical study. Particle velocities, although derived from acceleration data, regarded as much less reliable than data from relative-displacement gages, have usable precision (perhaps 25 to 40 percent) by virtue of comparison with peak velocities from the more-reliable absolute-displacement data.

Data analyzed in this report was secured from a source of specific magnitude and from gages in a specific type of soil. Transformation of the data to problems involving sources of different size or different soil media may be accomplished within certain limitations. Such conversion by scaling procedures is frequently made for air-blast phenomena and should be feasible for Project 1.5 data under proper control. Changes of source energy by factors of five, or even ten, may not make transformation by direct scaling seriously in error; however, increasing or decreasing the source energy by factors of a hundred or a thousand may well lead to spurious results. It should be recalled, for instance, that a thousand-fold increase in source energy will not only cause the same peak overpressure at a ten-fold increase in range, but the positive-phase duration of overpressure will be increased ten-fold. The latter factor will have a strong effect, since much more of the ground motion will be of a plastic nature because of longer application of load. Attenuation with depth will probably follow patterns similar to those indicated in this report, but depths must be increased probably in accord with the same sort of cube-root scaling that applies to range and duration. No real check of this hypothesis is possible from existing data, and precautions in use of such transformation must be correspondingly more restrictive.

Similarly, transformation of data to other media probably need not be considered a serious problem if the difference between the cemented silt of Frenchman Flat lake bed and another medium is not great. However, for very different materials, such as massive rock or water-filled or cohesive soils, too little is presently known concerning reaction to dynamic loads of the type applied to Project 1.5 gages to permit better than crude extrapolation of data to such materials.

Particle displacements of Frenchman Flat soil loaded by air blast of peak overpressures in the range from 300 to 60 psi decrease exponentially with depth according to the equation:

$$\delta = \delta_0 e^{-0.017D}$$

over the range of depths from D = 10 feet to D = 100 feet. At the surface, observed displacements are greater than this equation predicts because of greater compressibility of the uppermost few feet of soil. Magnitude of the incident overpressure affects δ_0, the near-surface displacement, but does not measurably affect the rate of attenuation.

Particle velocities within the range of depths from 10 to 100 feet vary inversely as fractional powers of depth. The rate of attenuation appears to decrease with decreasing peak incident overpressure or, perhaps, with increasing duration of the positive phase.

Vertical stresses, computed from particle velocities on the assumption that in the range of observations loading acts as a shock wave, follow attenuation power laws analogous to those found for velocity.

Peak particle accelerations decrease inversely with the $\frac{3}{4}$-power of depth at peak incident pressures in the range from 200 to 60 psi. At the high-pressure station, 270-psi particle acceleration and velocity appeared to be attenuated at a rate at least twice that observed at the other stations. This rate appears to be too high and probably results from an anomalously high near-surface observation.

Vertical reinforced-concrete columns placed with tops flush with the ground surface react as rigid columns. Velocities and displacements are comparable at top and bottom, but differ from corresponding free-field parameters, which are considerably greater at the surface and smaller at the bottom.

6.2 RECOMMENDATIONS

Results of observations made by Project 1.5 of Shot Priscilla are limited in usefulness primarily by the range of incident overpressures covered. Information of the type reported here for loading at peak overpressures below 60 psi, although of interest, is not so important to protective construction design as that to be acquired at very-high ranges of overpressure. Therefore, it is recommended that a study similar to Project 1.5 be undertaken to cover the range of overpressures from those incident in the immediate vicinity of ground zero downward to the 200-psi peak-overpressure region. This study should be undertaken in the Frenchman Flat area for consistency in environment and should preferably be made under yield and burst-height conditions closely approximating those of Shot Priscilla. Instrumentation should be similar to that described in this report, but depths of close-in stations should be increased to about 500 feet.

It is further recommended that a theoretical study of the type suggested by Sauer and Brenner (Reference 15) for particle displacement induced by air-blast loading be undertaken.

REFERENCES

1. D.C. Sachs, and L.M. Swift; "Small Explosion Tests"; Project Mole, AFSWP-291, December 1955; Armed Forces Special Weapons Project, Washington, D.C.

2. J.S. Fischer, and R.E. Reisler; "Ground Acceleration Measurements"; Project 1.6, Operation Tumbler-Snapper, WT-516, January 1953; Ballistic Research Laboratories, Aberdeen Proving Ground, Aberdeen, Maryland; Confidential.

3. V. Salmon, and S.R. Hornig; "Earth Acceleration versus Time and Distance"; Project 1.7, Operation Tumbler-Snapper, WT-517, February 1953; Stanford Research Institute, Stanford, California; Confidential.

4. W.R. Perret, and V.L. Gentry; "Free-Field Measurements of Earth Stress, Strain, and Ground Motion"; Project 1.4, Operation Upshot-Knothole, WT-716, February 1955; Sandia Corporation, Albuquerque, New Mexico; Secret Restricted Data.

5. W.R. Perret; "Ground Motion Studies on Operations Ivy and Castle"; WT-9002, February 1955; Sandia Corporation, Albuquerque, New Mexico; Secret Restricted Data.

6. W.R. Perret; "Ground-Motion Studies"; Project 30.2, Operation Redwing, WT-1364, June 1958; Sandia Corporation, Albuquerque, New Mexico; Confidential Restricted Data.

7. W.R. Perret; "Earth Stresses and Earth Strains"; Project 19.1, Operation Tumbler-Snapper, WT-503, September 1952; Sandia Corporation, Albuquerque, New Mexico; Unclassified.

8. R.V. Whitman, and others; "The Behavior of Soils Under Dynamic Load"; AFSWP-118, August 1954; Armed Forces Special Weapons Project, Washington, D.C.

9. L.M. Swift, D.C. Sachs, and F.M. Sauer; "Air-Blast Phenomena in the High-Pressure Region"; Project 1.3, Operation Plumbbob, ITR-1403, October 1957; Stanford Research Institute, Menlo Park, California; Confidential, Formerly Restricted Data.

10. L.M. Swift, D.C. Sachs, and F.M. Sauer; "Ground Acceleration, Stress, and Strain at High Incident Overpressures"; Project 1.4, Operation Plumbbob, ITR-1404, October 1957; Stanford Research Institute, Menlo Park, California; Confidential.

11. P.A. Northrop; "Instrumentation for Structures Program"; Annex 3.4, Part I, Operation Greenhouse, WT-1, January 1951; Sandia Corporation, Albuquerque, New Mexico; Official Use Only.

12. J.J. Meszaros, and J.I. Randall; "Structures Instrumentation"; Project 3.28.1, Operation Upshot-Knothole, WT-738, February 1955; Ballistic Research Laboratories, Aberdeen Proving Ground, Aberdeen, Maryland; Confidential Restricted Data.

13. T.B. Goode, and others; "Soil Survey and Backfill Control in Frenchman Flat"; Project 3.8, Operation Plumbbob, WT-1427, October 1959; U.S. Army Engineer Waterways Experiment Station, Vicksburg, Mississippi; Unclassified.

14. P. Chadwick, R.E. Rowe, D.E.J. Samuels, and F.J. Walford; "Blast Loading"; FWE-171, August 22, 1958; Atomic Weapons Research Establishment, Aldermaston, Berks., England; Confidential Defense Information.

15. F.M. Sauer, G.W. Evans, C.M. Ablow, and J.L. Brenner, "Ground Motion Induced by Nuclear Explosions, A Study of Fundamental Problems"; AFSWC-TN-58-23, November 5, 1958; Stanford Research Institute, Menlo Park, California; Confidential Defense Information.

SUPPLEMENTARY

INFORMATION

Defense Nuclear Agency
6801 Telegraph Road
Alexandria, Virginia 22310-3398

SSTL

ERRATA

AD-611339

14 September 1995

MEMORANDUM TO DEFENSE TECHNICAL INFORMATION CENTER
ATTN: OCD/Mr Bill Bush

SUBJECT: Change of Distribution Statement

The following documents have been downgraded to Unclassified and the distribution statement changed to Statement A:

WT-1307, AD-311926
POR-2011, AD-352684
WT-1405, AD-611229
WT-1420, AD-B001855
WT-1423, AD-460283
WT-1422, AD-615737
WT-1225, AD-460282
WT-1437, AD-311158
WT-1404, AD-491310
WT-1421, AD-691406
WT-1304, AD-357971
WT-1305, AD-361774
WT-1303, AD-339277
WT-1408, AD-344937
WT-1417, AD-360872
WT-1348, AD-362108
WT-1349, AD-361977
WT-1340, AD-357964

151208

If you have any questions, please call MS Ardith Jarrett, at 325-1034.

FOR THE DIRECTOR:

Ardith Jarrett
for JOSEPHINE WOOD
Chief
Technical Support

ERRATA